UNIVERSITAT DE BARCELONA

Role of polyreactive autoantibodies in the physiopathology of Sjögren's Syndrome

Rebeca Gutiérrez Cózar

Doctoral Program in Biomedicine

Unitat d'Immunologia

Departament de Biomedicina

Facultat de Medicina i Ciències de la Salut

Universitat de Barcelona

Role of polyreactive autoantibodies in the physiopathology of Sjögren's Syndrome

Rebeca Gutiérrez Cózar

For the award of the degree in:

Doctora per la Universitat de Barcelona

Supervisor and Tutor: **Dr. Pablo Engel Rocamora**

Rebeca Gutiérrez Cózar

Pablo Engel Rocamora

Barcelona, 2023

A mis padres,

a Miriam, a Sergio,

y a Vega.

“No pienses que no pasa nada simplemente porque no ves tu crecimiento. Las grandes cosas crecen en silencio.”

Siddhārtha Gautama

INDEX

INDEX ..... **VII**

ABBREVIATIONS ..... **XI**

THESIS SUMMARY ..... **XVIII**

I. INTRODUCTION **1**

1. Immunological tolerance **3**

1.1. T lymphocytes tolerance 3

1.2. B lymphocytes tolerance 6

2. Autoimmunity **10**

2.1. Autoimmune diseases 10

2.2. Autoantibodies: diagnosis and pathogenesis 13

3. Sjögren's syndrome **19**

3.1. Immunopathology 20

3.2. Treatment and on-going therapies 24

3.3. Mouse models 25

4. Natural antibody repertoire and polyreactive antibodies **28**

4.1. Natural antibodies and polyreactivity definition 28

4.2. Polyreactive antibodies in pathogenesis 32

4.3. B cell antibody repertoire in a mouse model of Sjögren's syndrome 35

II. HYPOTHESIS **41**

III. OBJECTIVES **45**

IV. MATERIALS & METHODS **49**

1. Hybridoma culture and subcloning **51**

1.1. Hybridoma culture and subcloning 51

1.2. Hybridoma freezing 52

2. Monoclonal antibody production **52**

2.1. Monoclonal antibody purification and dialysis 52

2.2. Antibody biotinylation 53

3. Mice **53**

3.1. Blood and plasma collection 53

3.2. MRL/lpr mice MCMV infection 54

***4. In vivo* determination of polyreactive antibodies' role in SjS pathogenesis** **54**

4.1. Polyreactive antibodies half-life assay 54

4.3. Polyreactive antibodies in vivo assay 55
4.4. Anti-Ro52 and anti-dsDNA determination in mouse sera 55
4.5. Flow cytometry 56
5. Immunohistopathological analysis 56
5.1. Lymphocytic infiltrates number and area determination 57
5.2. Immunofluorescence assay 57
5.3. Immunohistochemistry for Ro52 expression determination 58
6. Identification and characterization of autoantibodies against new autoantigens 58
6.1. Autoreactivity assay 58
6.2. Immunohistochemistry with paraffin-embedded tissue 59
6.3. Salivary gland lysate 59
6.4. Western blot 60
6.5. Antigenic microarray 61
7. Statistics 61
8. Cell Culture Medium and Buffers 62

V. RESULTS 65

1. Polyreactive antibodies reactivity 67
2. Sjögren's syndrome MCMV infection model set up 70
3. Antibodies half-life assay 73
4. H2h4.7.50 increases SjS-related autoantibodies in mouse sera 74
5. H2h4.7.50 increases salivary gland infiltration 76
5.1. H2h4.7.50 increases foci number in salivary gland 76
5.2. H2h4.7.50 induces lymphocytic infiltration in salivary gland 78
5.3. H2h4.7.50 induces infiltration by CD3 and CD8 cells in salivary gland 79
5.4. H2h4.7.50 induces Ro52 overexpression in salivary gland 81
6. Lymphocytic population analysis by flow cytometry 82
7. Potential new autoantibodies showed to be polyreactive 86

VI. DISCUSSION 97

VII. CONCLUSIONS 111

IX. REFERENCES 115

X. ACKNOWLEDGMENTS 139

Abbreviations

ADCC – Antibody dependent cellular cytotoxicity

AIDS – Acquired Immune Deficiency Syndrome

AIRE – Autoimmune Regulator

ALPS – Autoimmune lymphoproliferative syndrome

ANA – Antinuclear antibodies

ANCA – Anti-neutrophil cytoplasmic antibodies

Anti-CCP –Anti- Cyclic citrullinated peptide

Anti-TG – Anti-thyroglobulin

Anti-TPO – Anti-thyroperoxidase

APC – Antigen presenting cell

APECED – Autoimmune Polyendocrinopathy-Candidiasis-Ectodermal Dystrophy

aPL – Antiphospholipid antibodies

B6 – C57B/6

BAFF – B cell activating factor belonging to the TNF family

BCR – B cell receptor

Bim – Bcl-2-interacting mediator of cell death

bNAbs – Broadly neutralizing antibodies

BTK – B-cell lymphocyte kinase

Btk – Bruton's tyrosine kinase

Abbreviations

CD – Cluster of differentiation

CDR – Complementary determining regions

CHB – Congenital heart block

CLE – Cutaneous lupus erythematosus

CLL – Chronic lymphocytic leukemia

CMV – Cytomegalovirus

CNS – Central nervous system

CSF – Cerebrospinal fluid

CTL – Cytotoxic T lymphocytes

CTLA-4 – Cytotoxic T-lymphocyte-associated protein 4

D – Diversity

DAMPs – Danger-associated molecular patterns

DCs – Dendritic cells

dH_2O – Distilled water

DMEM – Dulbecco's Modified Eagle Medium

DNA – Deoxyribonucleic acid

dsDNA – Double stranded DNA

EBER – Epstein-Bar Early RNA

EBNA-2 – Epstein-Bar Virus Nuclear Antigen 2

EBV – Epstein-Barr virus

ELISA – Enzyme-linked immunosorbent assay

FasL – Fas ligand

FcγR – Low affinity-activating fragment crystallizable gamma receptor

FO – Follicular B cell

GBS – Guillain-Barré syndrome

GC – Germinal center

GPA – Granulomatosis with polyangiitis

GWAS – Genome-wide association studies

H&E – Hematoxylin-Eosin

H1 – Histone 1

HIV – Human Immunodeficiency Virus

HLA – Human leukocyte antigen

HTLV-1 – Human T-cell lymphotropic virus type 1

IBD – Inflammatory Bowel Disease

ICs – Immunocomplexes

IF – Immunofluorescence

IFN-I – Type I interferon

Ig – Immunoglobulin

IHC – Immunohistochemistry

IL – Interleukin

IPEX – Immune dysregulation, polyendocrinopathy, enteropathy, X-linked syndrome

J – Junction

kDa – Kilodalton

LPS – Lipopolysaccharide

Lyn – Lck/Yes novel tyrosine kinase

mAb – Monoclonal antibody

MALT – Mucosa-associated lymphoid tissue

MFI – Mean Fluorescence Intensity

MHC – Major histocompatibility complex

MS – Multiple Sclerosis

mTEC – Medullary thymic epithelial cells

MZ – Marginal zone

NAbs – Natural antibodies

NLS – Neonatal lupus syndrome

NMDAR – N-methyl-D-aspartate receptor

NOD – Non-Obese Diabetic

Nup 62 – Nuclear pore glycoprotein p62

O/N – Overnight

OVA – Ovalbumin

PBMCs – Peripheral blood mononuclear cells

PC – Plasma cell

pDC – Plasmacytoid dendritic cell

PI3K – Phosphoinositide 3-kinase

PR3 – Human proteinase 3

PTPN22 – Protein Tyrosine Phosphatase Non-Receptor Type 22

RA – Rheumatoid arthritis

RAG – Recombination-activating gene

RF – Rheumatoid factor

RNA - Ribonucleic Acid

RT – Room temperature

SGECs – Salivary gland epithelial cells

SHIP-1 – SH-2 containing inositol 5' polyphosphatase 1

SHM – Somatic hypermutation

SHP-1 – Src homology region 2 domain-containing phosphatase-1

SjS – Sjögren's Syndrome

SLE – Systemic lupus erythematous

Sn/RNP – Small nuclear ribonucleoprotein particles

SSA – Sjögren's-syndrome-related antigen A

SSB – Sjögren's-syndrome-related antigen B

ssDNA – Single stranded DNA

ssRNA – Single stranded RNA

STAT4 – Signal transducer and activator of transcription 4

T reg – T regulatory

TCR – T cell receptor

TFG – Transforming growth factor

Tfh – Follicular helper T cell

Th – T helper

TIGIT – T cell immunoreceptor with Ig and ITIM domains

TLR – Toll-like receptors

TRIM – Tripartite motif containing

UVR – Ultraviolet radiation

V – Variable

VH – Variable heavy chain

VL – Variable light chain

Thesis summary

Sjögren's syndrome (SjS) is a chronic autoimmune disease that mainly affects the exocrine glands and is characterized by the presence of antinuclear antibodies such as anti-Ro52 and anti-dsDNA. Our previous analysis of the B lymphocyte repertoire in NOD.H-2^{h4} mice, which spontaneously develop SjS-like disease, showed that these mice had a higher frequency of autoreactive/polyreactive B lymphocyte clones that increased with age compared to B6 (WT type) mice. No loss of polyreactivity due to antibody class switching to IgG or somatic mutation was observed. Furthermore, surprisingly, all anti-Ro52 IgG autoantibodies were polyreactive. Given the B-cell dysfunction in SjS and the possible involvement of Ro52 in its pathogenesis, we hypothesized that polyreactive antibodies recognizing Ro52 might be a key factor in the development of the disease. Therefore, we predict that polyreactive anti-Ro52 antibodies (H2h4.7.50 and H2h4.7.94), obtained from NOD.H-2^{h4} mice, would induce pathogenic phenomena when injected into genetically susceptible mice, whereas the polyreactive anti-Ro52 antibody (B6.2.58) obtained from the non-autoimmune B6 strain would not induce disease development. On the other hand, we considered the possibility of identifying new autoantigens by analyzing our library of monoclonal antibodies derived from the NOD.H-2^{h4} strain.

Polyreactive anti-Ro52 antibodies were injected into autoimmune MRL/lpr mice infected with murine cytomegalovirus, and evaluation of their pathogenic effect was performed by measuring serum anti-dsDNA and anti-Ro52 autoantibodies, lymphocytic infiltration in exocrine glands, and analyzing lymphocytic subpopulations in spleen and bone marrow. The H2h4.7.50 antibody induced increased serum autoantibody levels, as well as increased salivary gland infiltration, mainly by CD8 T lymphocytes, which were also increased in the spleen. The B6.2.58 antibody, however, showed no effect on disease progression. On the other hand, the antibodies selected from the library as potential new autoantibodies because of their salivary gland-specific pattern were found to be highly polyreactive. In conclusion, the observed pathogenic effects induced by H2h4.7.50 indicate the role of polyreactive anti-Ro52 IgG2 antibodies in the pathogenesis of SjS.

I. INTRODUCTION

1. Immunological tolerance

The mammalian immune system has an extraordinary capacity to recognize and respond against virtually any foreign antigen or entity that enters the organism through a huge and diverse repertoire of specific receptors. However, within this repertoire, there are receptors that can recognize self-structures, so the immune system has evolved to control this self-response by several genetic and cellular mechanisms. This ability of the immune system to avoid damaging self-structures and tissues is known as immunological tolerance. When some of these mechanisms are deficient, self-tolerance breaks down and consequently self-damage occurs, leading to autoimmunity (Goodnow et al., 2005; Brown and Rudensky, 2023).

During B and T lymphocytes development and maturation, autoreactive cells are eliminated or functionally inactivated to avoid their release to the periphery from primary lymphoid organs; thymus for T cells, and bone marrow for B cells (Goodnow et al., 2005). This process is known as central tolerance (**figure 1**). However, some autoreactive lymphocytes scape central tolerance mechanisms, achieving a mature state and reaching peripheral tissues. To avoid self-recognition and response by these autoreactive lymphocytes, peripheral tolerance mechanisms take place (Mueller, 2010; Brown and Rudensky, 2023).

1.1. T lymphocytes tolerance

1.1.1. Central tolerance mechanisms

During T lymphocytes development, medullary thymic epithelial cells (mTECs) express a broad variety of self-antigens, some of them specific from certain peripheral organs. This ectopic expression is mediated by Autoimmune Regulator (AIRE) protein, that acts as a transcription regulator activating the expression of tissue-restricted antigens. Developing T lymphocytes that recognize these self-antigens via T cell receptor (TCR) with high affinity are eliminated by a process termed negative selection, since this high avidity TCR - self-antigen interaction induces programmed cell death (apoptosis) by Bcl-2-interacting mediator of cell death (Bim) activation. Therefore, AIRE is essential for immunological tolerance establishment and maintenance. In fact, it has been described that loss-of-function mutations in AIRE gene cause a life-threatening autoimmune disease called Autoimmune Polyendocrinopathy-Candidiasis-Ectodermal

Dystrophy (APECED) (Arstila and Java, 2013; Yamada et al., 2017; Besnard et al., 2021).

However, not all the autoreactive T cells are depleted when they recognize self-antigens in the thymus. Some of the autoreactive $CD4^+$ T cells evolve into T regulatory (T reg) lymphocytes and move to peripheral tissues, where they will be participating in peripheral tolerance maintenance and autoimmunity prevention (ElTanbouly and Noelle, 2021). Besides, it has been described that a minority of self-reactive T lymphocytes have the chance to edit their TCR alpha chain to decrease their autoreactivity and continue with their maturation process (Nemazee and Hogquist, 2003).

1.1.2. Peripheral tolerance mechanisms

Autoreactive naïve T cells that scape central tolerance mechanisms, exit the thymus and migrate to peripheral tissues, where they are subjected to peripheral tolerance mechanisms (**figure 1**). These mechanisms are:

- Anergy. It is induced when the T lymphocyte specifically recognizes its antigen via TCR (signal 1), but there are no danger signals that activate innate response such as those induced by Toll-like receptors (TLR), and consequently there is no induction of the expression of co-stimulation receptors in the antigen presenting cells (APCs) membrane such as B7.1 (CD80) and B7.2 (CD86). This co-stimulation deficient signaling after antigen-specific recognition triggers anergy, which induces T cell hyporesponsiveness, limiting the T cell response to self-antigens (Baxter and Hodgkin, 2002; ElTanbouly and Noelle, 2021).

- Treg suppression. These T regulatory cells can suppress autoreactive T cells activation by suppressive cytokines production, such as IL-10 and TGFβ; decreasing the activation capacity of APCs via inhibitory receptors such as CTLA-4; or metabolic disruption by local IL-2 consumption since Treg cells present a high expression of CD25 (alpha chain of IL-2 receptor, IL-2R alpha) (Thornton and Shevach, 1998; Sakaguchi et al., 2008).

- Deletion. Programmed cell death can be activated through mitochondrial (intrinsic) or death receptor (extrinsic) pathways (Griffith and Ferguson, 2011). Within extrinsic pathways by death receptors, the best described is Fas (CD95), and its interaction with its ligand, FasL (CD178). When a T lymphocyte is repeatedly activated, FasL starts being expressed in their membrane, so it binds Fas in the same or adjacent lymphocyte surface. This Fas-FasL interaction activates a caspase-mediated signaling cascade that induces apoptosis (Krammer, 2000; Yamada et al., 2017). Interestingly, defects in Fas-mediated apoptosis cause an accumulation of autoreactive T cells, leading to autoimmune lymphoproliferative syndrome (ALPS), mainly characterized by cytopenia, splenomegaly, lymphadenopathy, autoimmune disorders, and a greatly increased lifetime risk of lymphoma (Matson and Yang, 2020).

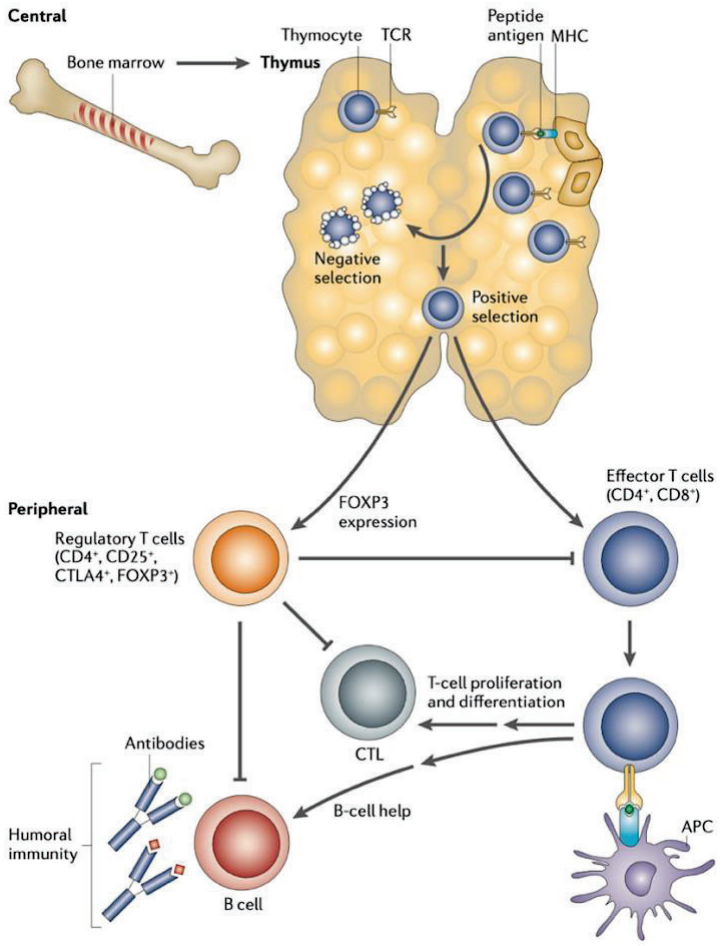

Figure 1. T lymphocytes central and peripheral tolerance. The top panel represents central tolerance mechanisms in thymus, where negative and positive selection takes place. Once cells overcome selection, the migrate to periphery as effector cells (CD4+ or CD8+), or as T regulatory cells (T regs). In periphery T cells undergo tolerance checkpoints, and autoreactive T lymphocytes will undergo anergy, suppression by Tregs or apoptosis (not shown). Figure obtained from Gregersen and Behrens, 2006.

1.2. B lymphocytes tolerance

B cell tolerance is mediated by various checkpoints. Central tolerance occurs at early stages of the B cell development in the bone marrow, when B cells express IgM but not IgD (IgM+ IgD-). Peripheral tolerance mechanisms occur when B cells co-express IgM and IgD receptors in their membrane, can be completely activated and can produce high affinity antibodies (Nemazee, 2017: Wang et al., 2020). Interestingly, almost 20% of B cells are autoreactive in the periphery of healthy and mature B cell repertoire. It has been estimated that a 75% of new-formed B lymphocytes have detectable autoreactivity. Therefore, central and peripheral tolerance mechanisms are essential to decrease this high autoreactivity level and maintain organism homeostasis (Wardemann et al., 2003; Getahun, 2022).

1.2.1. Central tolerance mechanisms

B cell central tolerance is mediated by three mechanisms: clonal deletion, receptor editing and anergy (**figure 2**). First, when an immature B lymphocyte recognizes a self-antigen that is present at high concentration in the bone marrow, B cell receptors (BCRs) get cross-linked, inducing a strong signal to the lymphocyte. This strong signal can lead to apoptosis, so this negative selection process is known as clonal deletion. Alternatively, depending on the BCR affinity, this strong signal via BCR may induce RAG enzymatic reactivation leading to a new light chain rearrangement. This process is known as receptor editing (Halverson et al., 2004). This new light chain will create a potentially non-autoreactive BCR (Nemazee, 2017).

However, if BCR recognizes self-antigens with relatively low avidity, these cells will become unresponsive or anergic, and they will migrate to the periphery. This anergic state is characterized by a desensitized BCR signaling due to chronic exposure to self-antigens, and the suppression of the differentiation into plasma cells (Verbeek et al., 2019; Pelanda et al., 2022).

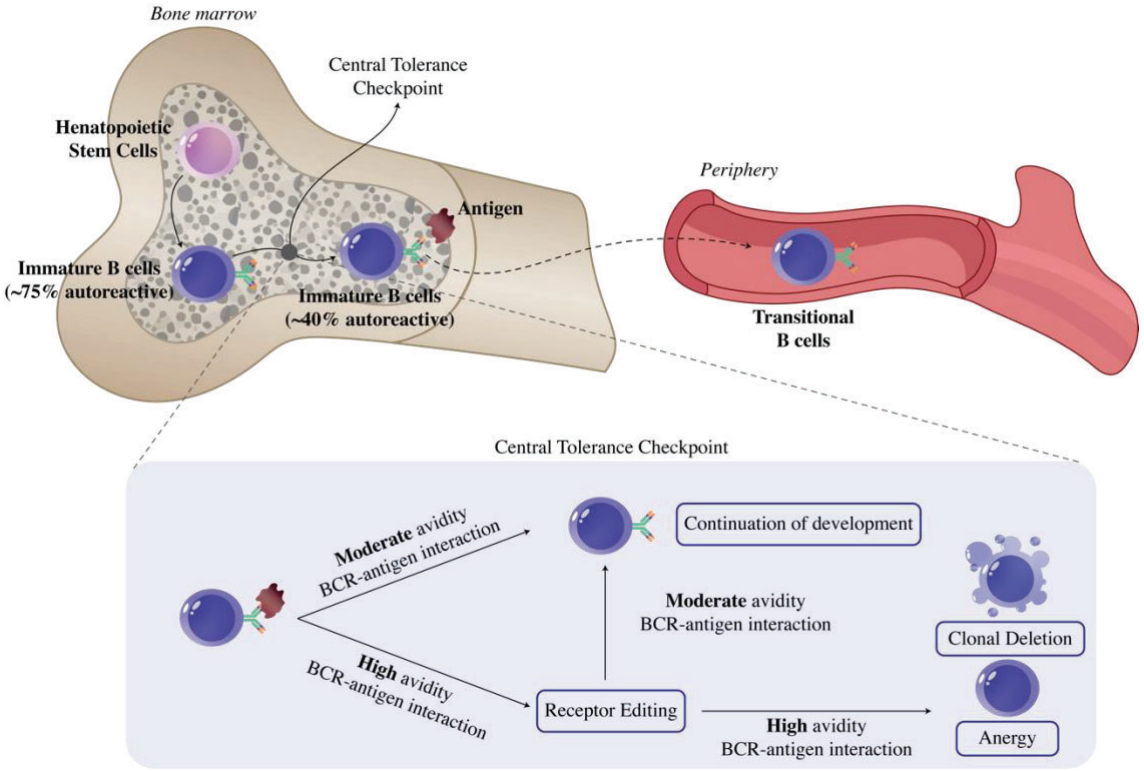

Figure 2. B lymphocytes central tolerance mechanisms. At the bone marrow, during B lymphocytes development, autoreactive B cells are reduced by central tolerance mechanisms that include clonal deletion, anergy and receptor editing. These mechanisms are based on the binding strength between self- antigens present in the bone marrow and the BCR expressed on immature cells. Figure based on Bonasia et al., 2021.

1.2.2. Peripheral tolerance mechanisms

While clonal deletion at bone marrow is an effective mechanism for preventing self-reactive B cell entering the peripheral repertoire, some B cells will only encounter their cognate antigen after migrating to periphery, so peripheral tolerance mechanisms are needed (Brink and Phan, 2018) (**figure 3**).

Once B cells reach the spleen from bone marrow, they undergo a second round of negative selection, so self-reactive transitional B cells, in the spleen, are depleted by apoptosis (Überhart and Jumaa, 2015; Yamada et al., 2017). Besides, once autoreactive B cells reach peripheral tissues, they can be found either in an ignorant or an actively suppressed state. When B autoreactive lymphocytes do not bind the self-antigen they are specific for, or the interaction avidity is not enough to induce BCR cross-linking, B cells will be maintained in an ignorant state. However, autoreactive B cells that do interact with their specific self-antigen are actively suppressed. This active suppression can be performed by intrinsic or extrinsic mechanisms, and it may lead to apoptosis via Bim, through the mitochondrial pathway (Wang et al., 2020; Getahun, 2022).

- Intrinsic mechanisms: the absence of specific T helper cell or active suppression by Tregs can induce an anergic state of autoreactive B cells. If these cells don't receive enough survival signals, they could finally undergo cell death.

- Extrinsic mechanisms: these mechanisms act limiting the signals that B cells require for their activation and are mainly based on the activation of inhibitory signaling pathways. The main pathway involved in inhibitory signaling in autoreactive B cells is the Lyn-SHP-1-SHIP-1 axis, which is essential to regulate the response amplitude via BCR. Besides, it also plays a critical role in peripheral tolerance as it prevents autoreactive B cell activation through the inhibition of the PI3K cascade, a critical signaling pathway for BCR signaling (Pauls and Marshall, 2017; Getahun, 2022).

Interestingly, B cells have a higher risk of generating peripheral self-reactivity than T cells as they can undergo somatic mutations at the immunoglobulin genes in germinal centers (GC) that change their BCR affinity for the cognate antigen. When this autoreactivity of B cells is increased after somatic hypermutation (SHM), these self-reactive cells are eliminated in the GC through Fas-FasL interaction (expressed on activated B cell surface and on helper T cell membrane respectively). Another essential regulatory mechanism here is the expression of FcγRIIb; the co-engagement of BCR and FcγRIIb by immunocomplexes (ICs) can, under specific conditions, induce the apoptosis of autoreactive B cells in the GC (Verbeek et al., 2019; Wang et al., 2020).

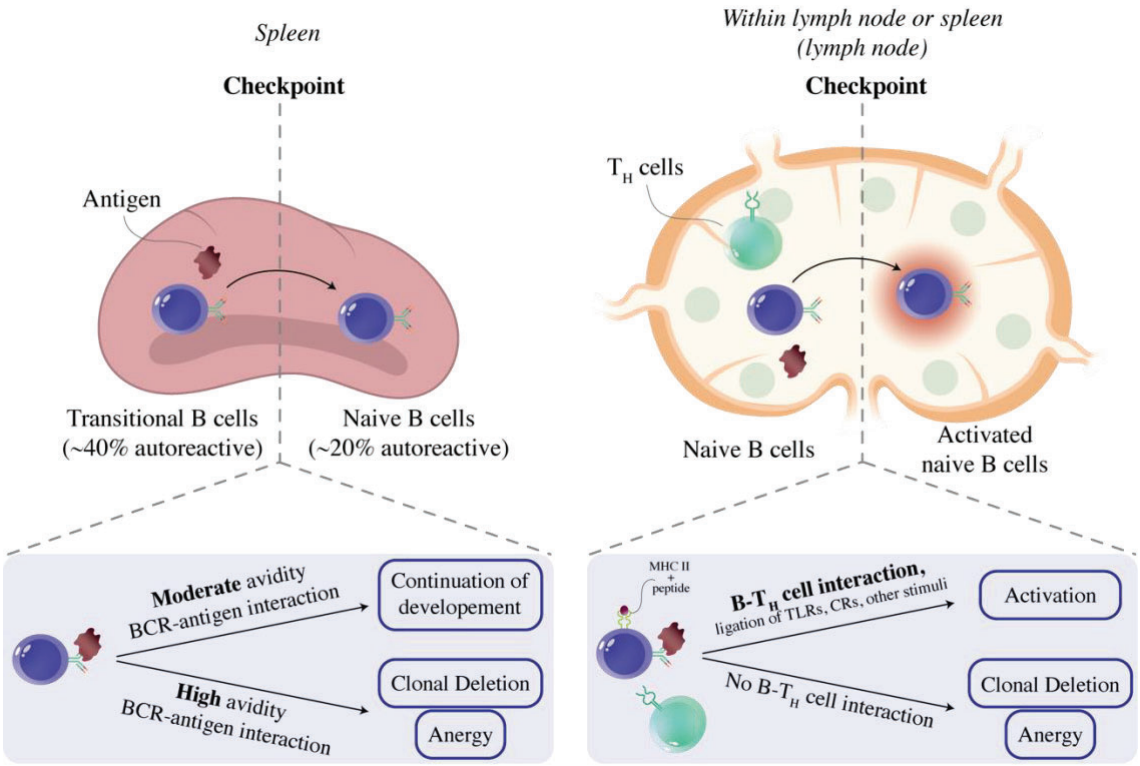

Figure 3. B lymphocytes peripheral tolerance mechanisms. In the spleen, transitional B cells that strongly bind self-antigens undergo clonal deletion or anergy, while transitional B cells that moderately bind self-antigens mature into naïve B cells. Besides, naïve B cells that do not interact with $CD4^+$ T_H cells undergo clonal deletion or anergy. Figure based on Bonasia et al., 2021.

2. Autoimmunity

At the beginning of the twentieth century, Paul Ehrlich coined the term "*horror autotoxicus*", that included all those processes in which there is a harmful immune response against "self". Nowadays, it is known as autoimmunity, and it occurs when the delicate balance of immune tolerance mechanisms is disrupted, so autoreactive lymphocytes are not eliminated or their activation is not suppressed, leading to autoimmune diseases.

2.1. Autoimmune diseases

Autoimmune diseases affect 3 - 8% of the global population, and it has been estimated that around 80% of them are women. This sex difference has been related to female hormones, and the immune challenges that women go through during their life, for instance during pregnancy. It has been also related to certain X chromosome linked genes that are involved in the immune response, such as X-linked gene TLR7, coding for Toll like receptor 7, implicated in systemic lupus erythematous (SLE) development. Some of the most frequent autoimmune diseases are SLE, rheumatoid arthritis (RA), type I diabetes, Crohn's disease, psoriasis, myasthenia gravis, or Sjögren's Syndrome (SjS) (Wilkinson et al., 2022; Brown et al., 2022, Miller, 2023).

Autoimmune diseases can be classified as systemic (e.g., SLE) or organ-specific (e.g., type I diabetes), depending on the cognate self-antigen/s distribution. They can also be classified depending on the effector mechanism: B cell-mediated disease if the main effector mechanisms are circulating autoantibodies, or T cell-mediated disease if the effector autoreactive T cells are the cells carrying out the tissue damage. Autoimmune diseases tend to be chronic and progressive, and tissue damage together with the consequent cell apoptosis leads to epitope spreading, inducing autoantigens exposure and disease perpetuation. Besides, it is common that once patients develop an autoimmune disease, more autoimmune diseases appear. These associations make obvious the common genetic underlying mechanisms between certain autoimmune diseases (Voight and Cotsapas, 2012; Samuels et at., 2022).

Autoimmunity is the result of a complex interaction and combination of different factors, such as genetic predisposition, environmental influences, and abnormal immune response, for example during viral infections or after a tissue injury or trauma (Xiao et al., 2021). Related to genetic factors (**table 1**), most autoimmune diseases present polygenetic and complex genetic profiles. It has been well described the common association between different autoimmune diseases with certain human leukocyte antigen (HLA) alleles, that determine the haplotype and make individuals prone to develop these diseases. For instance, this underlying genetic pathogenesis associated with HLA alleles has been evidenced by the high disease concordance found between identical twins. More recently, human genome sequencing technology advances have allowed the understanding and analysis of how certain haplotypes are overrepresented in different diseases populations. This has led to the elucidation that autoimmune diseases present a high degree of heritability (Bogdanos et al., 2012; Harroud and Hafler, 2023). Some common and well-described HLA-disease associations are HLA-B27 alleles and ankylosing spondylitis, HLA-DRB1*01/04*/10* and RA, and HLA-DRB1*0301*/0401* and pemphigus vulgaris. These are HLA-DR or HLA-DQ alleles, that code for major histocompatibility complex (MHC) class II molecules, which are essential for $CD4^+$ T cell activation and their role in humoral and cellular response, as well as in the immune response regulation (Dendrou et al., 2018).

Apart from HLA genes, there are also certain genes polymorphisms associated to autoimmunity. For instance, PTPN22 gene, that codes for tyrosine phosphatase N22, has been linked with SLE, RA and type I diabetes; polymorphisms in NOD2 gene, which codes for a cytoplasmic microbial sensor, have been related to Crohn's disease. Besides, alterations in FCGRIIB gene, which codes for FcγRIIb, have been related with SLE (Sidiq et al., 2016; Vang et al., 2018; Verbeek et al., 2019).

However, autoimmunity is not always caused by multiple genetic factors, but there are some rare autoimmune diseases caused by monogenic mutations on AIRE, FAS, or CTLA-4 genes, among others, all of them crucial for immune tolerance maintenance (Staels et al., 2021).

Table 1. HLA alleles, non-HLA polymorphisms, and monogenic mutations association with autoimmune diseases predisposition and/or development.

Gene/s	Associated autoimmune disease/s
HLA allele/s	
HLA-DRB1*01/04*/10*	RA
DRB1*0301*/0401*	Pemphigus Vulgaris
DRB1*0301 and DQA1*0501	Type I diabetes
DRB1^0301 and BRB1*1501	SLE
Non-HLA polymorphisms	
PTPN22	AR, type I diabetes
BLK	SLE, RA
IL10	SLE, type I diabetes
Monogenic mutations	
AIRE	APECED
FAS/FASL	ALPS
FOXP3	Immune dysregulation, polyendocrinopathy, enteropathy, X-linked syndrome (IPEX)
C4	SLE

Regarding environmental factors, tolerance breakdown can be induced by tissue anatomic alterations, due to inflammation after infections, or an injury that leads to self-antigens exposure that are typically hidden from the immune system in immune-privileged organs such as testicles or eyes. Others like lifestyle, exposure to certain chemicals, for instance due to pollution or smoking, are also risk factors (Xiao et al., 2021). Regarding infections, pathogens can induce autoimmunity by two main mechanisms:

- Infections induce innate immune responses, for instance binding TLRs, that lead APCs activation. This activated APCs start expressing co-stimulatory receptors and secreting cytokines that can activate autoreactive T cells in the periphery, breaking tolerance. This activation is performed in an antigen-independent manner since the activated autoreactive lymphocytes don’t need to be specific for any antigen in the infectious agent. This process is known as bystander activation (Pacheco et al., 2019). Microbes that bind TLRs on APCs membrane can also bind these innate receptors on autoreactive B cell’s membrane, inducing their activation, so this will induce autoantibodies production. In fact, TLR7 and other innate virus-sensing pathways such as cGAS-STING play an essential role in B cell systemic autoimmune diseases' development (Vinuesa et al., 2023).

- During infections, pathogen-specific T and B cell clones are expanded. The infectious agents present foreign antigens that can have structural similarities with self-antigens naturally present in the organism. Thus, in genetically susceptible individuals, an infection can favor autoreactive B and T cells activation, since they cross-react with self-antigens, leading to autoimmunity. This mechanism is known as molecular mimicry, and it has been related to Epstein-Barr virus (EBV) and its role in Multiple Sclerosis (MS) or SjS, *Campylobacter jejuni* and Guillain-Barré syndrome (GBS) development, or anaerobic microbiota dysbiosis and Inflammatory Bowel Disease (IBD) induction. The potential role of cytomegalovirus (CMV) in the induction of SjS in susceptible individuals has been also proposed (Rojas et al., 2018, Liu and Chu, 2021; English et al., 2023; Soldan and Lieberman, 2023).

2.2. Autoantibodies: diagnosis and pathogenesis

Lymphocyte tolerance mechanisms breakdown leads to the presence of autoreactive B cells in periphery that differentiate into antibody-secreting plasma cells and produce autoantibodies, immunoglobulins that recognize self-antigens. These autoantibodies producing B cells can be originated during B cell development in bone marrow, where the recombination of variable (V), diversity (D) and junction (J) immunoglobulin genes are recombined resulting on an autoreactive BCR; or during SHM of the BCR during immune response in GCs, where randomly introduced point mutations in V(D)J genes can induce or increase the BCR affinity against a certain self-antigen. The role of SHM in autoreactivity induction has been demonstrated for several autoantibodies when these points mutations were reverted to germline sequence, showing no detectable affinity for the self-antigens (Reed, 2022). Besides SMH, anergic and ignorant autoreactive B cells that scaped central tolerance mechanism can be also recruited to GCs, so peripheral tolerance is crucial to avoid the activation of these autoreactive B cells. In fact, it has been suggested that ignorant self-reactive B cells may be essential for SLE development (Ludwig et al., 2017; Brink and Phan, 2018).

Human case reports and passive transfer experiments in animal models have allowed to confirm that several autoantibodies play a key pathogenic role on certain autoimmune diseases pathogenesis, causing severe disease manifestations. Besides, several autoantibodies are crucial for disease diagnosis, so they are used as very useful

biomarkers. However, healthy individuals or asymptomatic patients also have autoantibodies in their sera, so it is not always clear whether the presence of an autoantibody is causally related to disease pathogenesis. Interestingly, it has been described that initially non-pathogenic autoantibodies, after sequence modifications during to SHM, could become insoluble so they induce coprecipitation and cause tissue damage for instance in kidney or skin, becoming pathogenic (Reed, 2022).

2.2.1. Autoantibodies in diagnosis

The detection of autoantibodies is a basic diagnostic tool for autoimmune diseases. Several autoantibodies can be detected years before the onset of disease symptoms appear. This may indicate that autoimmune diseases are developed in stages, so before the clinical manifestations appear, there is a "benign" phase characterized by the presence of autoantibodies in serum in the absence of pathology (Reed, 2022).

The main autoantibodies groups used for the diagnosis of systemic autoimmune diseases are the following:

- Antinuclear antibodies (ANA): are the most common type, and they are directed against nuclear components such as histone, DNA, RNA or complexes as SSA/Ro and SSB/La among others. ANAs are commonly used for diagnosis of several autoimmune diseases such as SLE, SjS, scleroderma, and mixed connective tissue disease. It should be noted that these autoantibodies can also be found at lower levels in healthy individuals, as well as in neoplastic patients or infectious diseases patients (Bossuyt et al., 2020).
- Anti-neutrophil cytoplasmic antibodies (ANCA): are directed against neutrophils and monocytes cytoplasmic proteins; the two major target antigens are myeloperoxidase (MPO) and proteinase 3 (PR3). These autoantibodies are mainly associated with vasculitic diseases, such as ANCA-associated vasculitis or granulomatosis with polyangiitis (GPA) (Nakazawa et al., 2019).
- Anti-CCP (cyclic citrullinated peptide) antibodies: these antibodies are directed against citrullinated peptides present in joints. They are useful for the diagnosis of rheumatoid arthritis (Rönnelid et al., 2021).

- Anti-thyroglobulin (anti-TG) and anti-thyroperoxidase (anti-TPO) antibodies: these are directed against thyroglobulin and thyroperoxidase, respectively, and they are used in the diagnosis of autoimmune thyroid diseases, such as Hashimoto's thyroiditis and Graves' disease (Fröhlich and Wahl, 2017).
- Antiphospholipid antibodies (aPL): these antibodies are directed against phospholipids and phospholipid-bound proteins. They are associated with antiphospholipid syndrome, which can cause abnormal blood clotting and pregnancy complications (Schreiber, 2018).

2.2.2. Role of autoantibodies in pathogenesis

The fact that an autoantibody is used as a biomarker for a certain autoimmune disease diagnosis, doesn't mean that it plays a role in disease pathogenesis. The transition between the "benign" phase, where autoantibodies can be found in sera before disease manifestations appear, to the "pathogenic" phase, has been correlated with an increase of autoantibodies titer in serum and the accumulation of autoantibody specificities. The latter is related to epitope spreading, that can be intramolecular (if autoantibodies against different epitopes of the same molecules are generated), or intermolecular (if autoantibodies are generated against different molecules that are usually physically linked to the initial autoantigen). This epitope spreading induces disease perpetuation, and two clinically relevant cases are anti-Sm antibodies in SLE, or anti-Ro/SSA and anti-La/SSB antibodies in SjS patients (Reed, 2022).

To elucidate whether an autoantibody is participating in disease pathogenesis or not, three rules were established (Bona, 1991):

- Disease association: exclusive detection in patients with the disease or significantly higher proportion in patients' sera than in healthy population.
- In vivo pathogenicity: passive transfer in animal models and/or placental transfer to neonate induces equivalent pathology.
- In vitro pathogenicity: it initiates cellular damage and/or inflammation in functional assays.

Autoantibodies that meet these three rules are usually responsible for organ-specific diseases, where autoantibodies recognize molecules expressed on cell-surface, for instance anti-acetylcholine antibodies in myasthenia gravis. On the other hand, autoantibodies found in systemic autoimmune diseases such as SLE or SS, commonly bind ubiquitous antigens such as nucleic acids or ribonucleoproteins, that are usually released due to cellular apoptosis and necrosis (Xiao et al., 2021).

The pathogenic mechanisms of autoantibodies are diverse and depend on the antibody features, for instance the isotype, and the autoantigen, or even the epitope they recognize in this autoantigen. The main pathogenic mechanisms are direct cell lysis (autoimmune idiopathic thrombocytopenia), immunocomplexes deposition and consequent inflammation by complement cascade activation (SLE), neutrophil activation (granulomatosis with polyangiitis), cell signaling alteration (pemphigus), inflammation induction at the binding site (RA), mimicry of receptor stimulation by hormones (Graves' disease), or blockade of neuronal transmission (myasthenia gravis) (Ludwig et al., 2017) (**figure 4**).

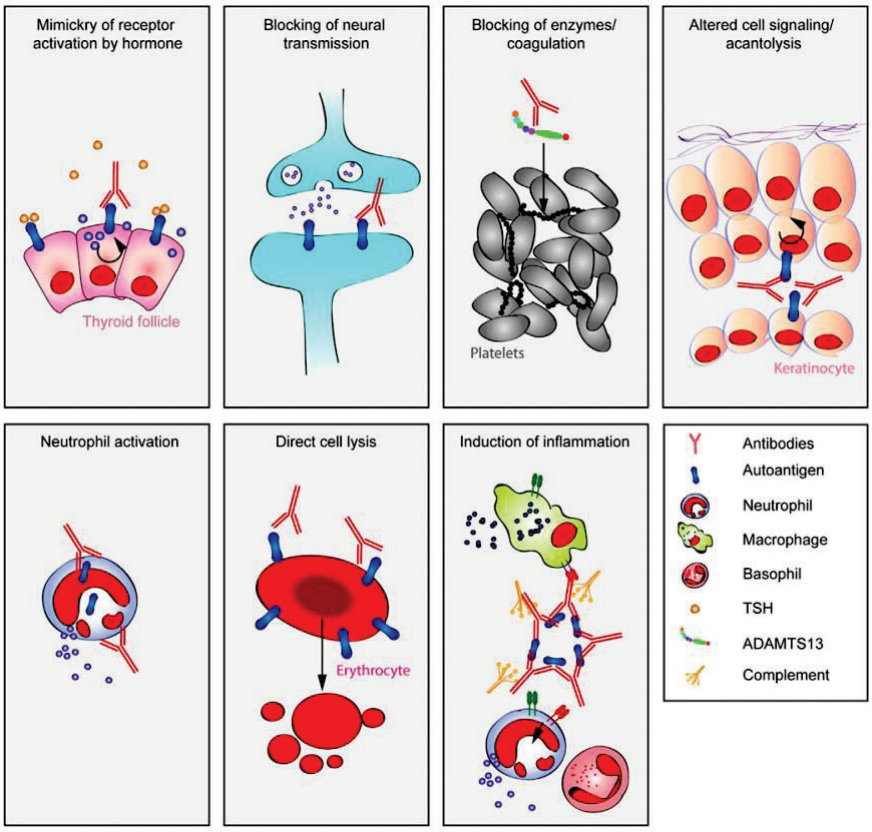

Figure 4. Pathogenic mechanisms of autoantibodies. Autoantibodies can induce pathogenesis through different mechanisms: mimicry of receptor activation by hormones, blocking neuronal transmission, altered cell signaling, neutrophil activation, direct cell lysis and inflammation induction in the binding site. Figure obtained from Ludwig et al., 2017.

Furthermore, several IgG autoantibodies play a pathogenic role when they are transferred across the placenta from maternal bloodstream to the fetus, causing neonatal syndromes. Some of the most common maternal autoantibodies-associated neonatal diseases are myasthenia gravis (anti-acetylcholine receptor autoantibodies placental transfer induces muscle weakness), pemphigus vulgaris (anti-desmoglein 3 autoantibodies transfer induces epidermis damage), and Graves' disease (anti-TSH autoantibodies transfer causes hyperthyroidism) (Lleo et al., 2010). Moreover, anti-thyroid antibodies have been directly related to recurrent pregnancy loss in humans (D'Ippolito et al., 2020), and it has been also demonstrated in animal models, as the injection of anti-TPO IgG autoantibodies derived from Hashimoto's thyroiditis patients induced fetal loss in naïve female mice (Borodina et al., 2021).

However, the most well-described and studied autoimmune neonatal disease is neonatal lupus syndrome (NLS). NLS is a disease observed in neonates born to ANAs seropositive mothers, who can have been previously diagnosed for the autoimmune disease or be asymptomatic. It has been demonstrated that the autoantibodies that play the key role in disease pathogenesis are anti-Ro and anti-La antibodies, since these induce a pro-inflammatory cascade once in the fetus that can induce reversible damage, such as skin lesions, or severe and irreversible lesions in cardiac tissue than can finally lead to congenital heart block (CHB) in the neonate by causing fibrosis of the fetal atrioventricular node (Gryka-Marton et al., 2021). Indeed, it was stablished that around 95% of mothers that gave birth neonates with autoantibody associated CHB were positive for anti-Ro52 autoantibodies (Salomonsson et al., 2011). These evidence were also demonstrated and enforced by animal models experiments. First, it was described that when serum with anti-Ro and anti-La autoantibodies from mothers of children with congenital heart block was injected in rats, it caused abnormalities in rat electrocardiograms (Mazel et al., 1999). More recently, in a rat model in which maternal auto-Ro52 were transferred to pups, a 100% of them developed first-degree atrioventricular block. Interestingly, these anti-Ro52 autoantibodies were directed against a specific region of Ro52, p200-239 (Ambrosi et al. 2012).

2.2.3. Ro52 and anti-Ro52 autoantibodies in autoimmunity

Ro52, also known as TRIM21, is a multifunctional cytoplasmic protein that acts as a E3 ubiquitin ligase and belongs to TRIM protein family. It presents essential roles in immune host defense and signal transduction, and it has been also related to cell cycle regulation. In cell signaling and host immune defense, Ro52 plays a key role in the regulation of type I interferon (IFN-I) pathway (crucial for antiviral immune response) since it contributes to the activation of IFN-I-inducible genes. Regarding cell cycle regulation, it was described that the overexpression of Ro52 results on decreased cell proliferation but an increased cell sensitivity to activation-induced cell death (Espinosa et al., 2006; Oke and Wahren-Herlenius, 2012). Its ubiquitin ligase activity makes Ro52 relevant in the degradation of damaged proteins inside the cell. Interestingly, as it can also act as an intracellular IgG receptor (FcR), it binds antibody-pathogen complexes once these are internalized, and it induces the degradation of pathogen's proteins inside the cell through the proteasome system, contributing to cellular homeostasis and intracellular pathogens elimination (Lee, 2017; Caddy et al., 2021). The role of Ro52 in antiviral response has also been demonstrated *in vivo* using Ro52 deficient mice for viral infectious models (Vaysburd et al., 2013).

Historically, the term "anti-Ro/SSA" included both anti-Ro60 and anti-Ro52 autoantibodies, but later it was identified that Ro52 and Ro60 were different proteins and that these were non-homologous; indeed, direct interactions between them have not been established. Anti-Ro52 autoantibodies appear in various autoimmune diseases, but the most common Ro52-associated diseases are SjS and SLE, where around 67% and 33% of patients present these autoantibodies in serum respectively. In fact, the presence of anti-Ro52 antibodies in serum is one of the main diagnostic criteria in SjS. Beyond these two autoimmune diseases, anti-Ro52 autoantibodies have been also found in the serum of patients with autoimmune myositis, autoimmune hepatitis type I, primary biliary cirrhosis and CHB (Martín-Nares and Hernández-Molina, 2019; Jones et al., 2021).

3. Sjögren's syndrome

Sjögren's syndrome (SjS) is a common and chronic systemic autoimmune disease characterized by lymphocytic infiltration in the exocrine glands and B-cell hyperreactivity. SjS is the second most common systemic autoimmune disease, and it affects from 0.1 to 4.8% population depending on the geographic area. As other autoimmune diseases, SjS presents a high female to male ratio (from 9:1 to 16:1), similar to SLE. In contrast to SLE, it mainly affects 40-50 aged women (Vivino, 2017; Yao et al., 2020).

Lymphocytic infiltration especially affects the salivary and lacrimal glands, and it induces secretory dysfunction causing dryness of mucosal surfaces, mainly in eyes and mouth, known as xerophthalmia and xerostomia respectively. However, this secretory dysfunction also takes place in nose, upper respiratory tract, and vagina. These manifestations are known as sicca symptoms. Interestingly, 25% of SjS patients present lymphoid infiltrates organized into structures similar to the GCs of secondary lymphoid organs, known as GC-like structures. These structures, that include B and T cells aggregates, follicular DCs and activated endothelial cells, provide the suitable environment for B cell proliferation, somatic hypermutation and antibody class switching, leading to disease progression (Mielle et al., 2021; Blinova et al., 2023).

Besides sicca symptoms, SjS patients also present heterogeneous extraglandular manifestations. Some patients develop cutaneous complications, arthralgias and join pain, pulmonary manifestations such as chronic obstructive lung disease, cardiovascular manifestations as Raynaud phenomenon, central and peripheral nervous system complications, and in obstetrics it can induce autoimmune CHB. Although approximately a 90% of patients don't undergo a severe course of the disease, 5-10% of patients develop non-Hodgkin's B cell lymphoma, with a high mortality rate (Goules and Tzioufas, 2019). Additionally, SjS overlap with other systemic autoimmune diseases is highly frequent, especially with SLE and RA, and some patients can also develop organ-specific autoimmune diseases such as autoimmune thyroiditis or autoimmune hepatitis. Given this heterogenicity of patients' clinical picture, the detection of autoantibodies and histological analysis of biopsies are the main diagnostic strategies nowadays (Brito-Zerón et al., 2016; Mavragani and Moutsopoulos, 2020).

These patients present B cell hyperreactivity that translates into hypergammaglobulinemia together with high levels of autoantibodies. ANAs are present on the sera of 59-85% of patients, although antibodies against Ro/SSA and La/SSB (parts of ribonucleoprotein-RNA complexes) are the major autoantibodies in SjS. Anti-Ro52 (prevalence: 66,7%) and anti-La autoantibodies (prevalence: 49%) are used as diagnostic serological markers, and they have been also associated with a higher prevalence of extraglandular manifestations and hypergammaglobulinemia. SjS patients also present anti-Ro60 (prevalence: 52,1%), anti-RF (prevalence: 36-74%) and anti-CCP autoantibodies (prevalence: 3-10%), and more recently new SjS autoantigens have been identified, such as proteins within aquaporin family. The presence of anti-aquaporin proteins autoantibodies has been related to lower resting salivary flow and more severe xerophthalmia and xerostomia. (Kyriakidis et al., 2014; Martín-Nares and Hernández-Molina, 2019). In addition to the presence of these autoantibodies, individuals with SjS exhibit significant alterations in the distribution of several B lymphocyte subsets, both in blood and the affected exocrine glands (Roberts et al., 2014; Mielle et al., 2021).

3.1. Immunopathology

The mechanisms underlying SjS development and pathogenesis remain unknown, but, as SjS is a multifactorial disease, the identification and connection between genetic, environmental, and immune system-related factors are helping to elucidate its etiology.

First, the role of genetic predisposition in the development of SjS has been evidenced. Several HLA and non-HLA susceptibility genes have been identified through large-scale or genome-wide association studies (GWAS), such as HLA-DQ and HLA-DR genes (MHC class II genes), IRF5 (involved in TLR downstream signaling and type I IFN pathway, and STAT4, involved in the production of IFN). MicroRNAs (miRNAs) have been also described as a potential susceptibility factor in SjS pathogenesis, since altered levels of certain miRNAs were described in SjS patients' PBMCs. In addition, epigenetic modifications, such as DNA methylation and histone modification, have been also related to SjS pathogenesis. Specifically, researchers identified an elevated expression of type-I IFN regulated genes on SjS patients' blood and salivary glands, and more recently it has been described that SjS patients present DNA hypomethylation at these genes, what leads to their overexpression. These altered methylation levels have

been also related to HLA genes such as HLA-DQA1 and HLA-DQB1. Thus, there is high evidence that alterations on TLR signaling, and interferon pathways are implicated on SjS pathogenesis (Imgenberg-Kreuz et al., 2021; Thorlacius et al., 2023).

Regarding environmental factors, infections may play a key role in several autoimmune diseases' development. Viral infections have been described as a potential risk factor for SjS as they can alter epithelial cells' biology, leading to overexpression of type I IFN genes, causing inflammation and tissue damage (Tian et al., 2021). First, EBV has been related to SjS development, as increased levels of EBV DNA have been found in PBMCs, salivary and lacrimal gland biopsies, and in tear specimens from SjS patients compared to SLE or RA patients, or healthy controls. Interestingly, EBV EBNA-2 protein shares 5-6 consecutive amino acid residues with Ro60 antigen, and sequence similarities have been also found between EBER-1 and EBER-2 EBV proteins and La antigen, so EBV could increase the risk and the autoimmune response, taking part in SjS development (Liu and Chu, 2021). Human T-cell lymphotropic virus type 1 (HTLV-1) has been also related to SjS pathogenesis, as increased seroprevalence was identified in SjS patients compared to healthy blood donors (23% against 3%). Besides, HTLV-1 can infect T and B cells, leading to cell activation and proliferation, and HTLV-1 patients present salivary gland lymphocytic infiltration and develop similar symptoms to SjS patients (Lima et al., 2016; Liu and Chu, 2021). Other viruses that have also been related to SjS pathogenesis are CMV, human herpesvirus type 8, and hepatitis C virus (Sandhya et al., 2017).

One of the major players on SjS development are salivary gland epithelial cells (SGECs), as abnormal exocrine gland homeostasis is considered the initial step of SjS development. These cells, which are the main target of the disease, are involved in one the most accepted theories about SjS pathogenesis, termed "autoimmune epithelitis". This theory claims that SGECs act as atypical APCs, as they can express CD80 and CD86 on their membrane, activating T cells and inducing their differentiation into T follicular helper cells (Tfh). Besides, SGECs can produce proinflammatory cytokines, inducing immune cells infiltration on exocrine glands. Interestingly, TLRs are also expressed on SGECs membrane, specially TLR7 and TLR8, which activation induces type I IFN pathway, and their importance on local and systematic SjS manifestations has been also evidenced by animal models. However, how these cells get activated is still unclear, although it has been related to epigenetic changes and latent viral

infections, and autocrine effect of BAFF secretion (Brito-Zerón et al., 2016; Kapsogeorgou and Tzioufas, 2020; Zhang et al., 2021). Besides, it has been suggested that the interactions between SGECs and B cells may induce SjS pathogenesis by multiple mechanisms, driving B cell activation, differentiation, and survival directly by cytokines production such as BAFF, or indirectly by the induction of Tfh differentiation. Indeed, it has been described that co-cultures of B cells and SGECs induce B cell differentiation to mature B cell phenotypes and increase B cell survival rate. These results highlight the critical role of SGECs and B cells crosstalk in SjS pathogenesis (Nocturne and Mariette, 2018; Du et al., 2021).

B cells can be involved in autoimmune diseases pathogenesis via various mechanisms: as cytokine producers, antigen-presenting cells, or autoantibody secretors. B cells hyperreactivity is one of the most important features of SjS, and this overreaction is the results of a multistep process, as environmental triggers, together with genetic dysregulation induces the stimulation and activation of specific B cell subsets, specifically marginal zone (MZ) B cells, memory B cells and plasma cells (Nocturne and Mariette, 2018). Regarding MZ B cells, these cells are found to be accumulated in SjS patients' salivary glands, where they contribute to tissue damage by autoantibody production, frequently in a T-independent manner (Daridon et al., 2006). MZ B cells role in SjS pathogenesis has been well described in mouse models, in which specific MZ B cells elimination induced normal saliva secretions and reduced glandular lymphocytic infiltration in salivary glands, as well as decreased autoantibody levels in serum **(**Shen et al 2016; Puñet-Ortiz et al., 2018). Moreover, the role of MZ B cells in SjS is crucial since these cells are frequently involved in the most severe complication of the disease, non-Hodgkin's B-cell lymphoma development (Demaria et al., 2019). On the other hand, memory B cells are also accumulated in the salivary glands of SjS patients, and they are involved in the ectopic germinal center-like structures formation in the exocrine glands of SjS patients, since they highly express chemokine receptors that facilitate infiltration via chemokines produced by SGECs. MZ B cells are also found in ectopic GC-like structures; indeed, the presence of these ectopic structures has been related to the risk of developing lymphoma (Sène et al., 2018). Besides, the number of IgG producing plasma cells in salivary glands has been positively correlated with lymphocytic infiltration and serum ANA titers in SjS patients (Szyszko et al., 2011; Du et al., 2021). Therefore, B cells play a crucial role in SjS pathogenesis,

infiltrating exocrine glands, leading to GC-like structures, and producing autoantibodies that induce tissue damage and disease progression.

T cells are also involved in SjS pathogenesis, as they drive disease progression by infiltration, pro-inflammatory cytokines production, damage to epithelium by cytotoxic functions, and modulating B cell functions. $CD4^+$ T helper (Th) cells are decreased in peripheral blood of individuals with SjS compared to healthy donors, probably caused by the $CD4^+$ Th cells migration to exocrine glands, since they represent the majority of infiltrating lymphocytes in SjS patients' salivary gland at early disease phase. In fact, several genetic studies associate MHC class II alleles and SjS susceptibility, highlighting the importance of autoantigens presentation to T cells, and therefore the key role of $CD4^+$ Th cells in disease pathogenesis (Verstappen et al., 2021; An et al., 2022). Both Th1 and Th17 T cells subsets have been related to SjS pathogenesis, and interestingly both present restricted clonal diversities with TCR recognizing characteristic SjS autoantigens (Ríos-Ríos et al., 2020). Th17 cells are increased in patients' SjS, and higher levels of IL-17 have been detected in saliva, tears and serum of patients compared to healthy controls. These results have been also supported by animal models, in which Th17 cells depletion ameliorated disease progression, while Th17 cells adoptive transfer restored disease phenotypes. Besides, IL-17 detection in peripheral blood has been also related to expanded γδ T cells (Fasano et al., 2020). Regarding $CD8^+$ T cells, also known as cytotoxic T lymphocytes (CTLs), these are considered as key players in SjS pathogenesis. $CD8^+$ T cells are increased in SjS patients' blood and salivary gland, and this is correlated with severity of tissue lesions (Li et al., 2023). These cells, especially tissue-resident memory $CD8^+$ T cells, secrete high levels of IFN-γ, show an hyperreactive state and proliferate abnormally, and they induce apoptosis and lysis of acinar epithelial cells in exocrine glands of SjS patients. Indeed, in mouse models $CD8^+$ cells are increased both in spleen and salivary gland, especially in advanced SjS. In fact, these mouse models studies showed that CTLs can alter tight junction integrity and function in epithelial cells of exocrine glands, leading to cell death (Barr et al., 2017; Gao et al., 2019; Zhou et al., 2021).

3.1.1. Ro52 in Sjögren's syndrome pathogenesis

The presence of autoantibodies targeting Ro52 in serum is one of the items with the highest weight in the SjS classification criteria (Shiboski et al., 2017). However, no direct pathogenic role has been attributed to anti-Ro52 autoantibodies, except in CHB disease (Nocturne and Mariette, 2018). Although it has not been elucidated yet whether Ro52 is a key autoantigen inducing autoimmune pathogenesis, it has been found to be overexpressed both in SjS patients' peripheral blood mononuclear cells (PBMCs) and salivary gland ductal epithelial cells. Indeed, Ro52 higher expression was directly correlated with inflammation and lymphocytic infiltration in patients' salivary glands, and anti-Ro52 autoantibodies titers are positively correlated with disease severity. (Zintzaras et al., 2005; Aqrawi et al., 2014; Jones et al., 2021).

Before, it was believed that Ro52 was only exposed by apoptotic cells release, so whether it could be key in SjS pathogenesis was not clear. However, it has been demonstrated that oxidative stress, which has been described in SjS patients' salivary glands, induces Ro52 exposure in SGECs' membrane (Jones et al., 2021). Besides, Ro52 have been also described to be presented by SGECs via MHC class I after TLR7 stimulation *in vitro* (Nishihata et al., 2023). Moreover, it has been also found that APCs on SjS patients' blood express Ro52, and it can be also exposed by SGECs exosomes release. Therefore, these findings suggest that Ro52 is crucial in disease pathogenesis and further research is needed to demonstrate its role (Kyriakidis et al., 2014; Hillen et al., 2020).

3.2. Treatment and on-going therapies

SjS therapy is based on symptomatic treatment. Mouth and eyes dryness are treated with oral mucolytic agents and tear substitution therapy respectively. Patients also receive secretagogues, muscarinic receptor agonists with systemic effect that ameliorate secretory dysfunction in exocrine glands. Besides, extraglandular manifestations are treated with conventional immunosuppressive drugs such as glucocorticoids (Brito-Zerón et al., 2016; Mavragani and Moutsopoulos; 2020).

However, based on SjS immunopathology findings, several therapies have been developed targeting different elements and immune processes. Given the key role of B cells in SjS pathogenesis, the most promising findings have been obtained targeting B

cells, using Rituximab (anti-CD20) and Tirabrutinib (Btk inhibitor) (Fox et al., 2019; Gandolfo and De Vita, 2019). However, despite promising results with Rituximab in the first two small trials, the following two larger randomized controlled studies failed to demonstrate its efficacy in SjS treatment. Therefore, the major challenge in B cell targeted therapy is to achieve specific reduction of disease-related B cell subsets instead of total depletion. Regarding T cells, there are also ongoing trials targeting T cells, mainly CD80 or CD86, CTLA-4/CD28 and TIGIT/CD226, since these axes have been proposed to be crucial in negative immune regulation in SjS patients, leading to T cell activation (Nocturne and Mariette, 2018; Ríos-Ríos et al., 2020).

3.3. Mouse models

SjS pathogenesis has been extensively studied using mouse models, elucidating roles of different cell subsets such as B and T cells and identifying genetic and environmental factors that can induce similar symptoms than in human disease. These mouse models can be classified in spontaneous, induced models by immunization or infection, and transgenic. Although the ideal mouse model for Sjögren's syndrome doesn't exist, some replicate human disease more closely, including clinical features like dry mouth and eyes, histopathological features such as lymphocytic infiltration, serological features such as characteristic autoantibodies'' presence, extraglandular manifestations or genetic alterations found in humans (Gao et al., 2020; Abughanam et al., 2021).

Related to spontaneous mouse models, NOD (Non-Obese Diabetic) derivatives are the most commonly used models, especially NOD.H-2^{h4} mice. This strain is characterized by spontaneous development of autoimmune thyroiditis and SjS, and it was obtained crossing NOD mice with B10.A (4R) strain. These mice don't develop diabetes, although they present relatively high incidence of mild insulitis. Their H-2K haplotype predisposes them to spontaneously develop SjS more frequently in females, maintaining sex ratios similar to human disease. Approximately 50% of 12-16 weeks old NOD.H-2^{h4} females exhibit lymphocytic infiltration in salivary glands, and this percentage increases to 100% in females aged 20-24 weeks (Karnell et al., 2014). This salivary gland infiltration leads to GC-like structures, similar to human structures. These mice also exhibit SjS characteristic autoantibodies in serum such as anti-Ro52, anti-La and anti-dsDNA. Interestingly, these autoantibodies precede the development of ectopic

GC-like structures in salivary glands (Bralley-Mullen and Yu, 2015; Puñet-Ortiz et al., 2018).

Another common and well-described spontaneous mouse model is MRL/lpr, which carries a spontaneous mutation in the gene encoding for Fas. This mutation leads to the development of a lymphoproliferative syndrome, being an appropriate model for SLE and SjS research. This model also replicates the sex ratio as in humans, and exocrine glands' infiltration can be found at 9 weeks old females, primarily in submandibular gland. It is also characterized by inflammation of multiple tissues such as skin, joints, or kidneys, that progress in an age-dependent manner. Unlike NOD.H-2^{h4}, this model does not exhibit GC-like structures, and they don't present anti-Ro52 autoantibodies, while autoantibodies recognizing ssDNA and dsDNA among other nuclear antigens are present in mice sera (Yamada et al., 2017; Li et al., 2018; Gao et al., 2020).

Regarding immunization-induced mouse models, it has been reported that immunization with Ro60 peptides induces SjS-like disease in wild-type mice. After repeated injections with an adjuvant, mice developed infiltrates in salivary gland composed by B and T cells. This was accompanied by a significant decrease of salivary flow and the presence of both anti-Ro60 and anti-La autoantibodies in serum, suggesting intermolecular epitope spreading between these two autoantigens (Scofield et al., 2005; Zheng et al., 2017; Abughanam et al., 2021).

On the other hand, infection-induced mouse models have been developed using murine CMV (MCMV), involving several mouse strains including wild type C57B/6 or autoimmunity-prone strains such as B6-lpr/lpr (deficient for Fas) or NZM2328. It is important to note that in humans, CMV mainly attacks ductal epithelial cells within salivary glands, while in mice, this virus replicates primarily within acinar epithelial cells of the submandibular gland. At 28 days post-infection, mice showed salivary gland lymphocytic infiltration and autoantibodies recognizing Ro52, La and rheumatic factor (RF) in serum. Interestingly, these disease manifestations persisted 100 days after infection in autoimmunity-prone mice but not in wild-type mice. This virus-induced SjS-like disease in mice provides an opportunity to study SjS pathogenesis and the involvement of CMV as environmental trigger. However, it can only be induced in autoimmune-prone stains, limiting its utility (Fleck et al., 1998; Ohyama et al., 2006; Gao et al., 2020).

Finally, several transgenic mouse models have been developed, since they allow studying the role of specific elements in SjS pathogenesis. Some of the most significant findings have been obtained using BAFF transgenic mice, which develop autoimmune symptoms with B-cell hyperactivation, lacrimal gland infiltration, and high levels of autoantibodies in serum, including anti-Ro52, anti-La, anti-dsDNA, and anti-RF. Moreover, SjS-like disease has been also induced in other transgenic mouse models such as HTLV-1, IL-6, IL-10, or IL-12 transgenic mice, among others (Groom et al., 2002; Gao et al., 2020).

4. Natural antibody repertoire and polyreactive antibodies

4.1. Natural antibodies and polyreactivity definition

The humoral adaptive immune response has always been associated with the generation of high-affinity and monospecific antibodies that usually undergo SHM and affinity maturation, leading to a more efficient response over subsequent encounters with a specific pathogen. However, in 1983 natural antibodies (NAbs) were first described as antibodies capable of binding antigens without prior antigenic exposure, since antimicrobial activity was found in sera of humans and animal models that had never been exposed or immunized with specific pathogens. Therefore, NAbs represent an initial defense recognizing a variety of common and conserved antigens, for instance, on microbial surfaces, being the most well-characterized epitopes phospholipids, oxidized lipids, glycolipids, and glycoproteins. NAbs can be found in blood and other biological fluids such as saliva, colostrum, or cerebrospinal fluid. NAbs are produced by B-1 and MZ B cells. B-1 cells are localized in the peritoneal cavity, bone marrow and spleen, and they often produce low-affinity polyreactive antibodies against a broad range of antigens, including self-antigens and microbial components. MZ B cells also contribute to the production of natural antibodies, particularly in response to blood-borne pathogens, since their localization in the marginal zone of the spleen allow them to rapidly act against pathogens that enter the bloodstream, leading to immune early response (Avrameas et al., 2007; Holodick et al., 2017).

Interestingly, it has been described that a high proportion of NAbs are able to bind structurally different antigens. This ability to interact with more than one antigen is termed as polyreactivity, and therefore these antibodies are known as polyreactive antibodies, also termed multispecific, degenerated or promiscuous antibodies. Generally, an antibody is considered as polyreactive when it binds at least 3 or 4 antigens from a small panel of antigens using an enzyme-linked immunosorbent assay (ELISA). These antibodies can simultaneously bind to unrelated antigen as different as DNA, lipopolysaccharide (LPS), albumin and insulin. However, when antibodies are screened using antigen microarrays that include a broad variety of antigens, it is accepted that an antibody that bind two structurally different antigens can be considered as polyreactive (Avrameas, 2016).

At first, polyreactive antibodies were believed to have lower affinity for antigens, but recent studies have confirmed that polyreactive antibodies can also exhibit high-affinity properties. In terms of their nucleotide sequences, they mostly resemble germ-line sequences with no mutations, although polyreactive antibodies with a low number of mutations in their nucleotide sequences can also be found. Initially, NAbs were thought to be unmutated and not subject to affinity maturation processes through SHM. It was believed that their presence contributed to diversifying an individual's antibody repertoire and that after encountering an antigen, B lymphocytes producing polyreactive antibodies undergo affinity maturation, increasing their affinity while losing their polyreactivity. Nevertheless, it has been demonstrated that the presence of mutations doesn't necessarily result in the loss of polyreactivity. In fact, it has been suggested that these mutations could potentially enhance the flexibility of the antigen-binding site, indicating that polyreactivity may not depend on maturation status, but rather on the inherent capacity of a paratope to adopt various structural conformations (Dimitrov et al., 2013; Holodick et al., 2017).

Although NAbs repertoires from one individual to another can differ, it has been described that the NAbs repertoire within one individual is stable with aging both in children and adults. Moreover, IgM is the most frequent isotype among polyreactive antibodies, although IgG, IgA and IgE can be also found. These NAbs repertoires also depend on environmental stimuli, since it was described that in mice housed under germ-free conditions, the levels of IgG, IgA and IgE NAbs is decreased compared to mice housed under conventional conditions, while IgM levels were maintained. Thus, it has been suggested that IgG, IgA and IgE NAbs need an exogenous antigenic contact, while IgM NAbs production is independent from this external stimulation. On the other hand, in healthy individuals, after B cell negative selection during maturation, approximately a 4% of naïve B cell present polyreactive BCRs; however, a 23% of IgG^+ memory B cells and 25% of IgA^+ intestinal cells produce polyreactive antibodies, while in newborns this percentage has been estimated to reach 50% of the B cell repertoire (Zhou and Notkins, 2004; Dimitrov et al., 2013).

4.1.1. Polyreactive antibodies molecular and structural mechanism

How polyreactive antibodies are able to bind structurally different antigens has been broadly studied from their nucleotide sequence to their structural conformations. Sequencing studies have confirmed that there is no correlation between variable heavy chain (VH) and variable light chain (VL) gene segments usage and polyreactivity. However, mutagenesis studies described the importance of CDR3 of the VH region, although other regions including CDR1, CDR2, frameworks and distant Ig regions should be also considered to contribute to polyreactivity. Indeed, it has been suggested that longer CDR3 region and aminoacidic sequence containing more hydrophilic residues could be key for polyreactivity, although no concluding results have been obtained (Torres and Casadevall, 2008; Boughter et al., 2020).

Experimental findings have indicated that polyreactive antibodies might employ distinct molecular mechanisms to bind structurally different antigens (**figure 5**). First, polyreactive antibodies might adopt a new configuration depending on the specific target antigen. This mechanism of binding is known as induced-fit model, which is also the proposed model for substrate-enzyme interactions (**figure 5A**). In contrast to the induced-fit model, the conformational isomerism model hinges on an equilibrium among all potential conformations of the polyreactive antibody. Consequently, the antibody shows diverse structural isoforms as it interacts with different target antigens (**figure 5B**). Furthermore, in addition to hypotheses centered around antibody binding site flexibility, the interaction model is based on experimental evidence that demonstrated that an antigen could bind not only to the antigen binding site but also to alternative sites on the antibody, leading to polyreactivity (**figure 5C**) (Dimitrov et al., 2013).

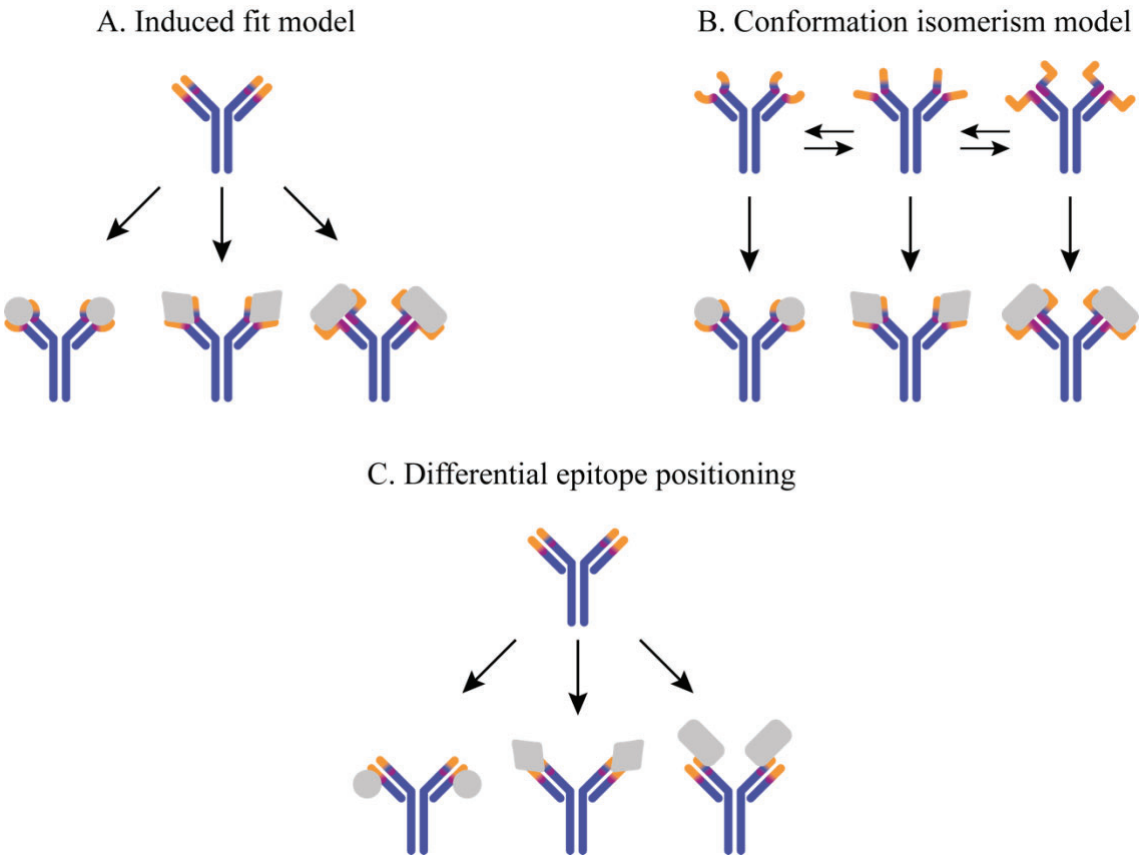

Figure 5. Antibody polyreactivity proposed molecular mechanisms. Three distinct molecular mechanisms have been suggested to elucidate how polyreactive antibodies interact with antigens that vary in structure. These mechanisms include the induced fit model (A), conformation isomerism model (B), and differential epitope positioning (C). Figure based on Dimitrov et al., 2013.

4.1.2. Physiological functions of natural antibodies

The main requirements for an antibody to be consider as a natural antibody are (1) the capacity to perform a protective, regulatory, or some other form of biological function, and (2) to have been produced previously to antigen exposure. Regarding biological functions, NAbs contribute to interconnecting both innate and adaptive immune response (Panda and Ding, 2015), and they play an important role defending the organism against bacterial, viral, and fungal infections such as *S. pneumoniae*, sepsis, *Borrelia hermsii*, or influenza virus among others. In fact, polyreactive antibodies delay pathogens propagation acting as a first barrier, increasing pathogen destruction by complement cascade activation or phagocytosis induction by macrophages. Importantly, the major protective function of NAbs is the active clearance of tissue and cell debris that follow degradation and apoptosis, leading to the control of inflammation and thus to tissue regeneration. Moreover, NAbs take part in B cell development, regulation and

repertoire selection, allergic suppression, and protection from cancer among other diseases. In fact, it has been proposed that NAbs can act as a buffer when the levels of endogenous molecules such as cytokines, anaphylatoxins, hormones, or danger-associated molecular patterns (DAMPs) abruptly change, preventing autoimmune diseases (Lutz et al., 2009; Avrameas and Selmi, 2013; Holodick et al., 2017).

Therefore, NAbs play an essential role in key functions that maintain organism homeostasis (**figure 6**). Interestingly, these protective functions of NAbs have been related to their glycosylation pattern, that differs from conventional mono-specific antibodies (Panda and Ding, 2015).

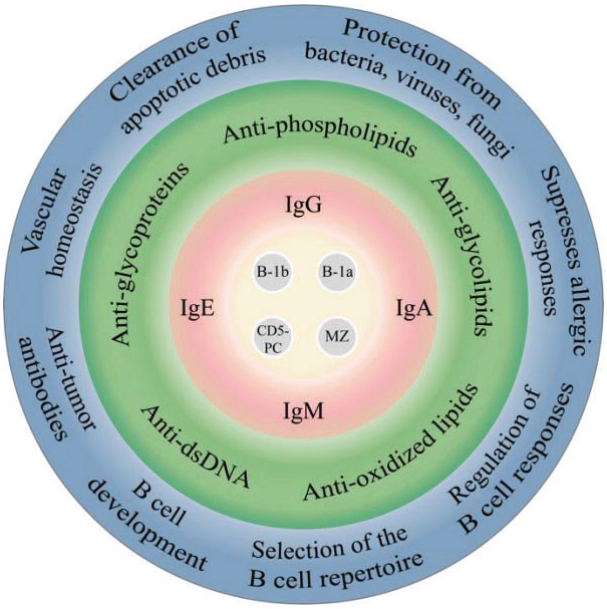

Figure 6. Natural antibodies characteristics graphical scheme. The outer circle (in green) represents the diversity of Nabs' functions, the inner circle (in blue) depicts the epitope recognition by Nabs, the inner circle (in purple) displays the possible isotypes of Nabs, and the central circle (in light orange) highlights the cells known to produce Nabs. This scheme is based on the work by Holodick et al. in 2017 (Holodick et al., 2017).

4.2. Polyreactive antibodies in pathogenesis

Polyreactive antibodies have been related to several infectious, inflammatory, and autoimmune diseases. However, it is still not clear whether these antibodies are produced only as a result of B cell dysregulation induced by disease, or if they are constitutively produced and performing biological and immunoregulatory functions participating in disease pathogenesis (Avrameas et al., 2018).

The protective role of polyreactive antibodies in infectious diseases have been broadly studied, and it has been also demonstrated using different infection mouse models. For instance, it was described that monobacterial and polymicrobial sepsis induction in Cd6 -/- mice results in lower survival rates, increases bacterial loads and pro-inflammatory cytokine levels. These results were explained based on the decrease of B-1a and MZ B cells and the subsequent decrease of natural polyreactive antibodies in these mice. Interestingly, when adoptive transfer with wild-type mouse sera or the injection of a

polyreactive monoclonal antibody improved Cd6 -/- survival rates post-sepsis (Català et al., 2022). Moreover, these protective results were also confirmed in a fungal infection mouse model using *Cryptococcus neoformans*, in which the injection of polyreactive IgM improved phagocytosis and mice survival (Subramaniam et al., 2010; Nguyen et al., 2015). Moreover, infections by Influenza, Hepatitis C, Dengue or Human Immunodeficiency Virus (HIV) viruses have been shown to induce the production of polyreactive antibodies that recognize different viral structures. Importantly, elevated levels of polyreactive antibodies have been described in HIV-infected individuals compared to healthy individuals, although how and why these antibodies are produced is still not clear.

Within the antibody repertoire of HIV-infected individual, broadly neutralizing antibodies (bNAbs) can be found, defined as those capable of neutralize the wide viral diversity. These bNAbs exhibit at least one of the following three defining features: high frequency of SHM, an elongated CDR3 region in heavy chain, or notable levels of poly- or autoreactivity (Finney and Kelsoe, 2018). Importantly, these polyreactive antibodies are highly mutated, what indicates that B cells that produced them have been positively selected (David et al., 2018); these mutations are accumulated in both variable and framework regions, contributing to thermodynamic stability and increased flexibility (Klein et al., 2013; Avrameas, 2016). Moreover, it has been hypothesized that HIV and NAbs repertoire co-evolve, as HIV has a high mutation rate (Doria-Rose and Landais, 2019). Indeed, various antibodies recognizing a highly conserved region of the Env gp41 viral protein were characterized as polyreactive, inducing virus neutralization (Molinos-Albert et al., 2017; Prigent et al., 2018).

However, polyreactive antibodies binding to viral particles is not always translated in neutralization. Despite the well described protective role of natural antibodies in HIV infection, it has been described that in certain cases, polyreactive antibodies may activate antibody dependent cellular cytotoxicity (ADCC) against CD4+ T lymphocytes, contributing to Acquired Immune Deficiency Syndrome (AIDS) (Wang et al., 1999). Moreover, in other infections such as Dengue, polyreactive antibodies binding induces virion entry to cell, thus promoting disease progression (Warter et al., 2012).

On the other hand, in B cell malignancies such as chronic lymphocytic leukemia (CLL), Mucosa-Associated Lymphoid tissue (MALT) lymphoma or splenic MZ lymphoma, polyreactive BCRs play a critical role in pathogenesis as they act inducing continuous stimulation and transmission of survival signals to the transformed B cells clones. Indeed, a more aggressive disease progression was described in CLL patients with higher levels of polyreactive BCR (Kölher et al., 2008; Lobo, 2016).

Polyreactive antibodies have been also related to autoimmune disorders. For instance, a high prevalence of B cells with polyreactive BCRs has been described in SLE and RA patients, that may be induced by B cell tolerance checkpoints disruption and dysregulation. Polyreactive antibodies in autoimmune diseases may participate in pathogenesis binding several autoantigens and inducing pro-inflammatory responses. However, differences between protective or detrimental polyreactive antibodies have still not been elucidated, but it may be related to changes in affinity, isotype, and specificity for disease-associated antigens. It has been proposed that ineffective clearance of apoptotic cells by polyreactive antibodies could lead to autoimmune diseases development, and infections by bacteria or viruses could play a key role in the dysregulation of NAbs producing B cells, leading to immunopathological state in which polyreactive antibodies participate (Sethi et al., 2006; Dimitrov et al., 2013; Panda and Ding, 2015). Interestingly, it was demonstrated that human polyreactive antibodies isolated from SLE patients are able to bind mouse glomeruli and their administration to mice brain resulted in neurologic damage, revealing their potential pathogenic role (Herzog and Jumaa, 2012).

Finally, polyreactive antibodies also contribute to allergic responses, since polyreactive IgE antibodies may continuously promote survival, cytokine secretion, and degranulation of mast cells, inducing pathogenesis (Kashiwakura et al., 2012).

In conclusion, a complete and healthy B cell repertoire consist of both monospecific and polyreactive antibodies. The former will provide fidelity and establish an efficient memory response, while polyreactive antibodies will provide adaptability and evolvability, establishing a physiological balance between protective and detrimental antibodies in order to avoid pathogenic effects (Dimitrov, 2020) (**figure 7**).

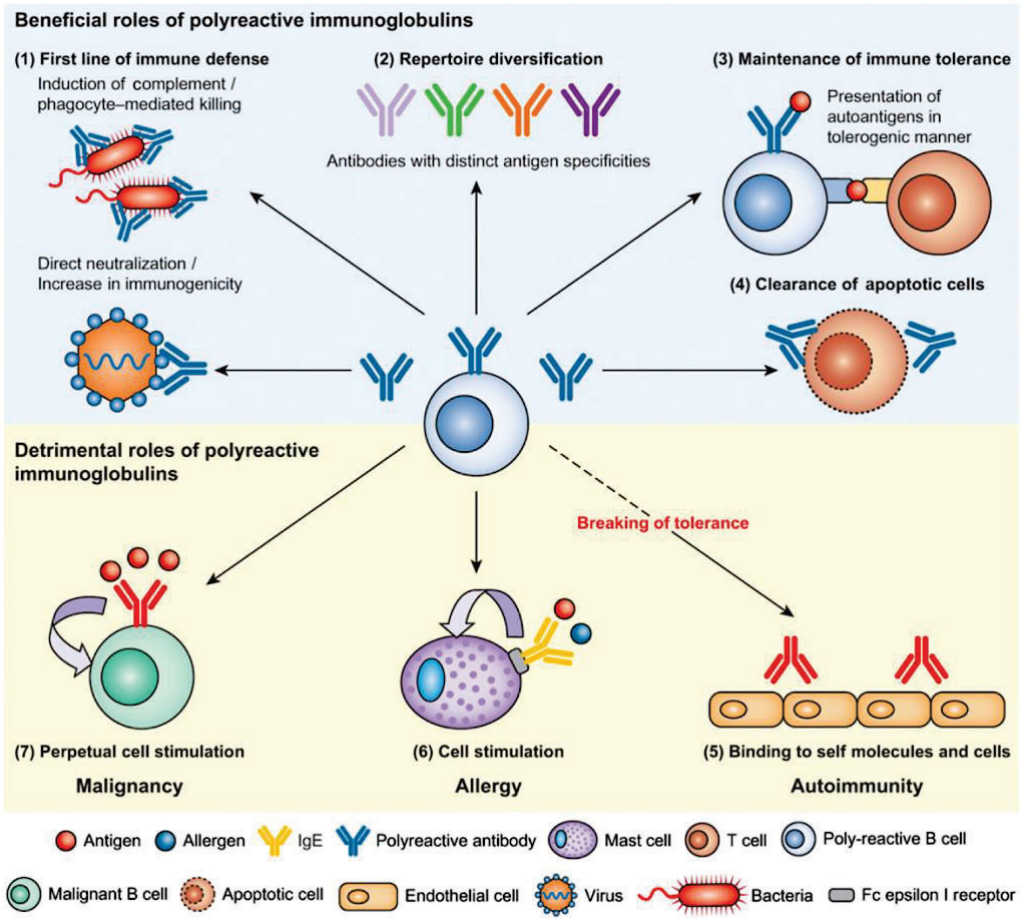

Figure 7. Beneficial and detrimental role of polyreactive antibodies. Beneficial roles of polyreactive antibodies include that these act as a first line of defense, repertoire diversification, immune tolerance maintenance, and apoptotic cells clearance. Detrimental roles of polyreactive antibodies include perpetual cell stimulation, cell stimulation that can induce allergy responses, and tolerance breakdown through self-molecules and cells binding. Figure obtained from Dimitrov et al., 2013.

4.3. B cell antibody repertoire in a mouse model of Sjögren's syndrome

B cell hyperactivity, one of the hallmarks of SjS, is a consequence of chronic antigenic stimulation, which starts polyclonally but can progress to monoclonal B cell lymphoproliferation, leading to B cell lymphoma development (Goules and Tzioufas, 2019). In susceptible individuals, chronic B cell stimulation leads to autoreactive B cell clones' expansion by a deficient negative selection that might lead to an increase in the generation of polyreactive antibodies. In the context of SjS, there exists a limited comprehension of the underlying mechanisms that contribute to the progression and emergence of autoreactivity within B cells. However, chronic pro-inflammatory stimulation by activated epithelium and SGECs apoptosis may induce the expansion of already present natural autoreactive lymphocytic clones, producing polyreactive antibodies that may participate in the pro-inflammatory response (Moutsopoulos, 2014).

In our lab, we performed a B cell antibody repertoire analysis in the spontaneous mouse model of SjS NOD.H-2^{h4}. We hypothesized that within aged SjS mice, there would be an elevated occurrence of self-reactive B cells, reflecting impaired tolerance checkpoints. Besides, under chronic antigen exposure, B cell clones producing polyreactive and autoreactive IgM antibodies might switch to IgG, changing their specificity and becoming high affinity and monospecific. Furthermore, we predicted that B cells in SjS mice could evolve to oligoclonality progressively using a more restricted V gen segments. We generated a library of 168 hybridomas from 28, 47 and 66-week old NOD.H-2^{h4} females and tested the reactivity of the secreted monoclonal antibodies and determined the gene usage of heavy and light chains variable gene segments. Additionally, we also generated a collection of 186 hybridomas from C57BL/6J (thereafter named B6) females as non-autoimmune control strain (Sáez et al., 2021).

First, our results showed elevated frequency of polyreactive B cell clones in SjS mice that increased with age (**figure 8**). The frequency of both IgM and IgG autoreactive antibodies was significantly increased in SjS mice compared to B6 wild-type mice. Within SjS mice, a significant increase was observed in the frequency of autoreactive IgG antibodies, reaching a 61% of total IgG antibodies in 66 weeks old mice. These date showed that autoreactive B cells dominate the B cell repertoire of NOD.H-2^{h4} mice.

Giving the importance of Ro52 in SjS diagnosis and pathogenesis, we also determined the frequency of anti-Ro52 antibodies within NOD.H-2^{h4} antibody repertoire. B cells from old SjS mice (over 40 weeks) showed a higher frequency of anti-Ro52 antibodies compared to B6 mice for both IgM and IgG antibodies, and the percentage of anti-Ro52 IgGs increased with age reaching a 50% of the antibody repertoire in 66 week old mice. Additionally, we also determined polyreactivity by ELISA using a panel of six structurally unrelated molecules including dsDNA, histone 1 (H1), Ro52, LPS, insulin and ovalbumin (OVA). Interestingly, a higher frequency of polyreactive antibodies was obtained for both IgM and IgG in SjS mice compared to B6 at all ages. Moreover, it was observed that this polyreactivity frequency increased with age, reaching more than 50% in 66 week old mice. These results demonstrated that, in SjS old mice, most of the autoreactivity corresponds to polyreactive antibodies.

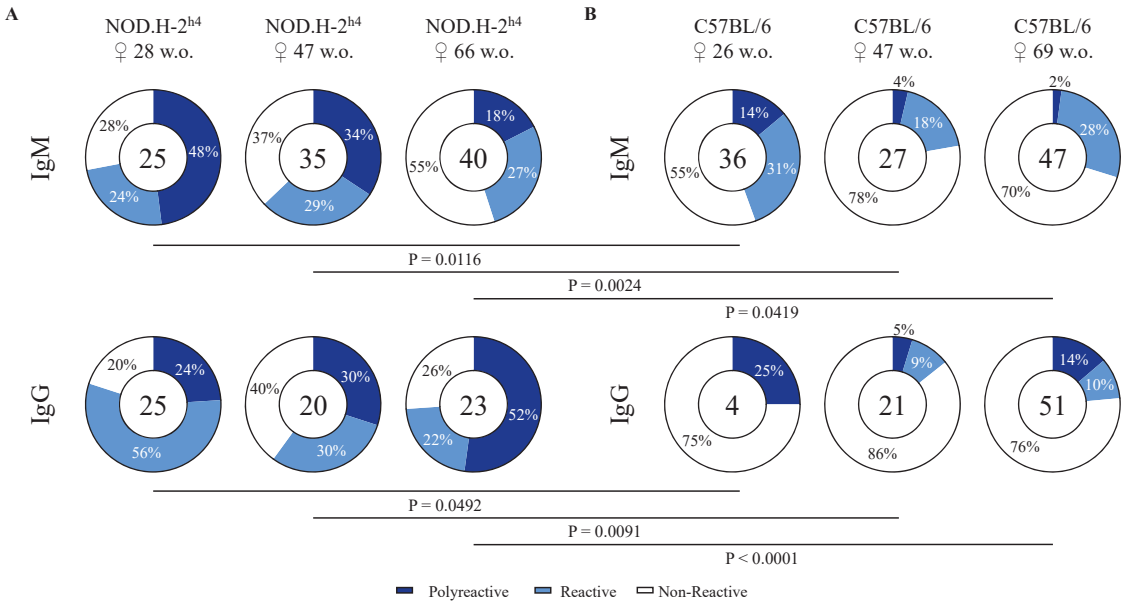

Figure 8. **Frequency of polyreactive antibodies derived from NOD.H-2^{h4} and C57BL/6J mice.** Antibody reactivity against dsDNA, H1, Ro52, LPS, Insulin, and OVA was assessed by ELISA. Pie charts illustrate the distribution of antibodies based on their reactivity: polyreactive (reactivity with ≥ 3 antigens) antibodies are represented in dark blue, reactive (reactivity with one or two antigens) antibodies in light blue, and non-reactive antibodies in white. The data are presented for each age group (NOD.H-2^{h4}: 28, 47, and 66 weeks old in panel A; C57BL/6J: 26, 47, and 69 weeks old in panel B) and for both IgM and IgG isotypes. The number of antibodies tested is indicated at the center of each pie chart. Figure obtained from Sáez et al., 2021.

In order to characterize antibody polyreactivity, we performed a semiquantitative reactivity analysis of the polyreactive antibodies with the antigens included in our panel (**figure 9**). Importantly, we observed an increase in the antigen binding reactivity of the IgG antibodies from aged SjS mice, while this was not observed for IgM antibodies and IgG antibodies from B6 mice. Surprisingly, one of our most relevant observations was that all antibodies reactive with Ro52 were polyreactive.

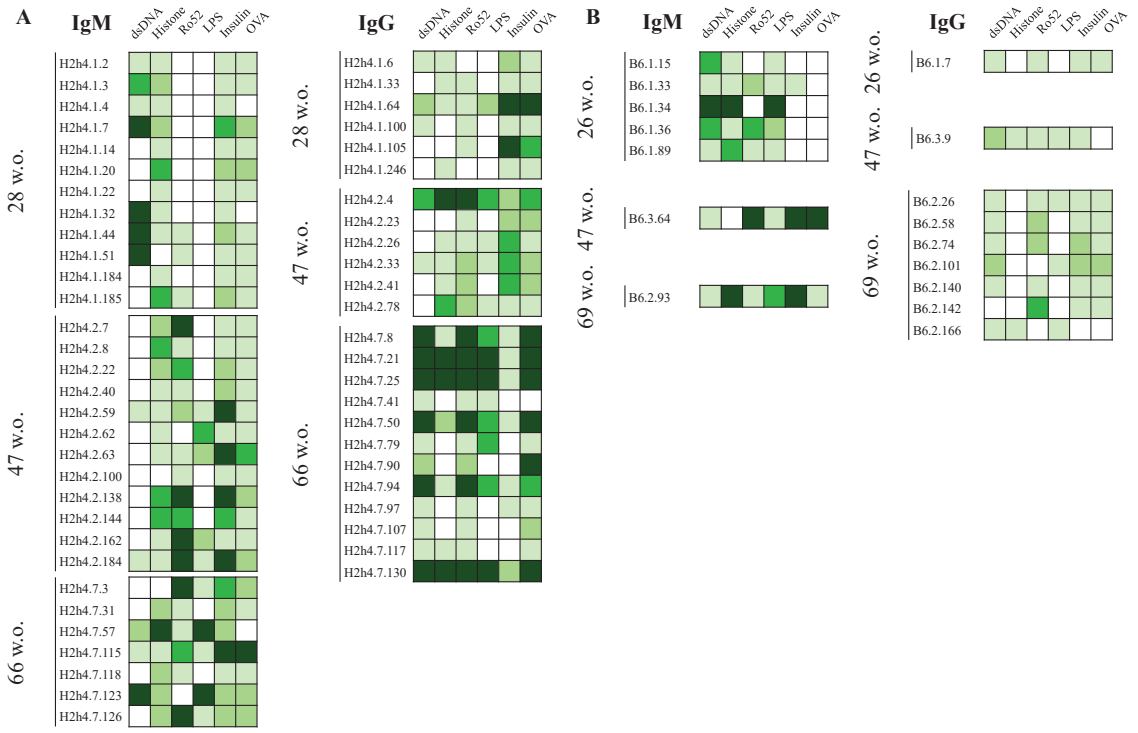

Figure 9. Polyreactivity profile of antibodies derived from NOD.H-2^{h4} and C57BL/6J mice. Heat maps depict the antibody binding patterns to a set of chosen antigens, including dsDNA, H1, Ro52, LPS, Insulin, and OVA. The data are derived from hybridomas originating from two different mouse strains, NOD.H-2^{h4} (panel A) and C57BL/6J (panel B). Color intensity within the heat maps corresponds to the level of reactivity as measured by ELISA, with darker shades of green indicating strong binding, moderate binding represented by lighter green, and low or no binding indicated by white. Figure obtained from Sáez et al., 2021.

Besides, we also analyzed repertoire oligoclonality by VH and VL gene segments sequencing. We observed that, for both NOD.H-2^{h4} and B6 strains, the variable gene segments repertoire was very heterogeneous, the CDR3 length was between standard ranges and that most IgM antibodies presented nearly germline encoded sequences. Interestingly, the majority of polyreactive IgG antibodies were IgG2b subclass in NOD.H-2^{h4} mice, whereas most of B6 polyreactive antibodies corresponded to IgG3 (**figure 10**).

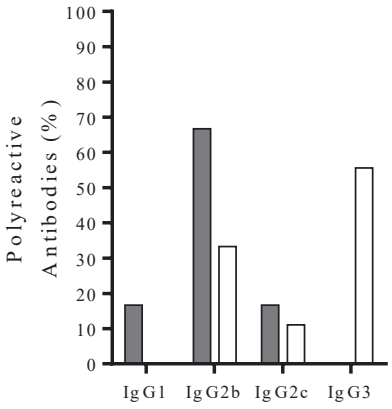

Figure 10. Frequency of polyreactive IgG subclasses in NOD.H-2^{h4} and C57BL/6J mice. Figure obtained from Sáez et al., 2021.

In 66 week old SjS mice, we observed two sets of identical sequences from IgG antibodies. First, H2h4.7.21 and H2h4.7.25 antibodies had the same variable sequence and gene segment usage, with multiple R amino acids in their heavy chain CDR3 regions, which have been related to polyreactivity. In addition, H2h4.7.8, and

H2h4.7.50 shared the same sequence, while H2h4.7.94, which uses the same variable gene segments both in heavy and light chains, presented three and two extra mutations in the heavy and light chain respectively compared with the other two related clones (**figure 11**). Therefore, these results indicated a high level of oligoclonality in these mice. Indeed, when antigen reactivity strength of these five polyreactive antibodies that correspond to the two expanded clones (H2h4.7.21 and H2h4.7.25; H2h4.7.8, H2h4.7.50 and H2h4.7.94) was tested, we observed that H2h4.7.94 antibody presented an important increase in its reactivity strength compared to its two clonally related antibodies H2h4.7.8 and H2h4.7.50. Besides, H2h4.7.94 showed a stronger cytoplasmic staining when tested against HEp-2 cells by immunofluorescence. Therefore, these data showed that antigen driven somatic mutation is able to increase the affinity of autoreactive clones maintaining the levels of polyreactivity.

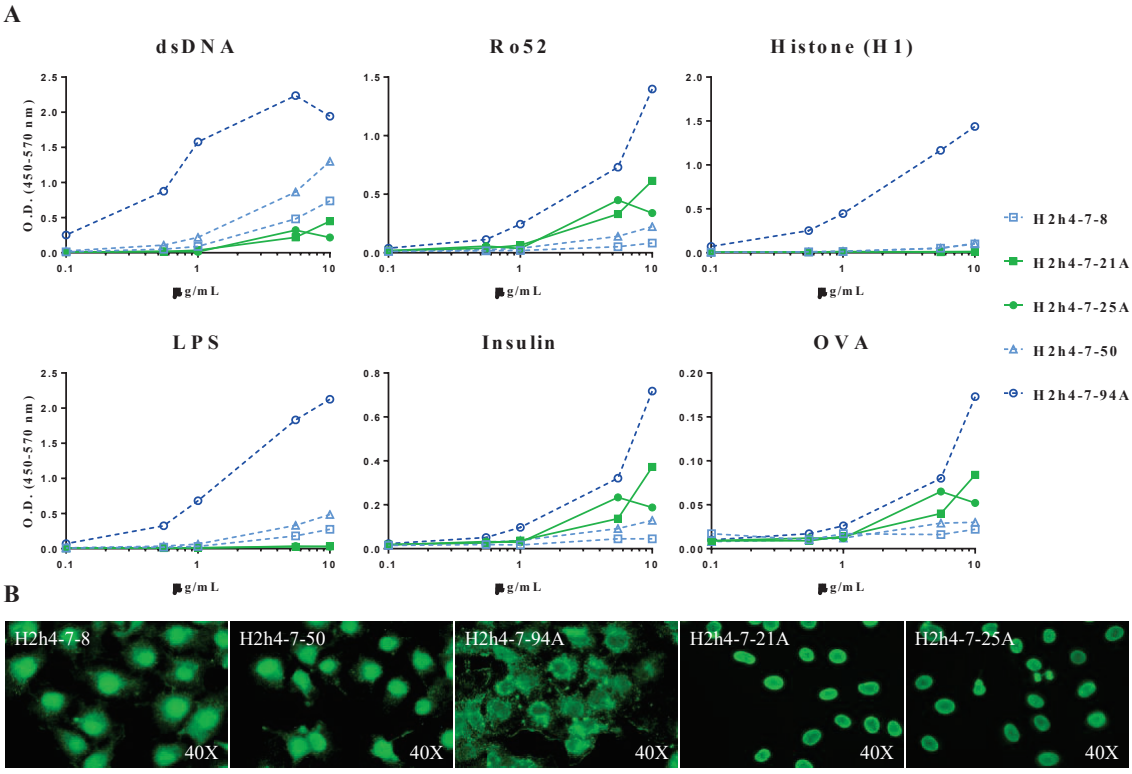

Figure 11. Affinity of polyreactive antibodies. Affinity determination of polyreactive antibodies (H2h4-7-8, H2h4-7-21A, H2h4-7-25A, H2h4-7-50, and H2h4-7-94A) for dsDNA, H1, Ro52, LPS, Insulin, and OVA by ELISA (A). Antibodies sharing identical IGHV and IGKV sequences are represented in either blue or orange, while H2h4-7-94A, shown in dark blue, carries additional mutations compared to H2h4-7-8 and H2h4-7-50, depicted in light blue. Additionally, representative immunocytochemistry images of HEp-2 cells are provided, illustrating the cellular patterns associated with each antibody (B). Figure obtained from Sáez et al., 2021.

In conclusion, the results from the B cell antibody repertoire analysis revealed that the majority of IgG+ B cells are polyreactive and maintain sequences near germline. Furthermore, there is an expansion of these polyreactive IgG B cells, probably following an unknown antigen-driven positive selection process. Consequently, studying the possible pathogenicity of these IgG2 polyreactive antibodies that recognize Ro52 could provide deeper insights into the mechanisms underlying SjS pathogenesis.

II. HYPOTHESIS

The main hypothesis of this project is that polyreactive antibodies that recognize autoantigens could lead to Sjögren's syndrome development. Giving the B cell dysfunction in SjS and the potential role of Ro52 in its pathogenesis, we hypothesize that polyreactive antibodies that recognize Ro52 might be a key factor for disease development. Thus, we predict that anti-Ro52 polyreactive antibodies (H2h4.7.50 and H2h4.7.94), obtained by monoclonal antibody generation technology from autoimmune NOD.H-2^{h4} mice, will induce an increase of SjS characteristic autoantibodies in mice sera and higher infiltration rate in exocrine glands, as well as extraglandular manifestations such as kidney tissue damage and alterations in lymphocytic subpopulations in spleen and bone marrow, when tested *in vivo* in autoimmune prone mice. In contrast, anti-Ro52 polyreactive antibodies (B6.2.58) obtained from a non-autoimmune mouse strain, will not induce disease development. In addition, we also hypothesize that new autoantigens remain to be discovered and they could be identified using our library of monoclonal antibodies obtained from NOD.H-2^{h4}.

III. OBJECTIVES

The overall aim of this project is to uncover the pathogenic mechanisms underlying the B cell dysfunction in SjS. The objectives of this project are:

1. Study the pathogenic role of polyreactive autoantibodies that recognize Ro52 using monoclonal antibody generation technology.

2. Optimize an infection mouse model of SjS using the autoimmune prone strain MRL/lpr infected with murine cytomegalovirus (MCMV) to study the pathogenic role of polyreactive antibodies *in vivo*.

3. Determine disease development by anti-Ro52 and anti-dsDNA autoantibodies measurement in mouse sera.

4. Examine histopathological effects of anti-Ro52 polyreactive antibodies measuring lymphocytic infiltration in exocrine glands and tissue damage in extraglandular tissues.

5. Examine the effects of anti-Ro52 polyreactive antibodies analyzing potential alterations in lymphocytic subpopulations in spleen and bone marrow.

6. Identification and characterization of autoantibodies against new autoantigens.

IV. MATERIALS & METHODS

1. Hybridoma culture and subcloning

1.1. Hybridoma culture and subcloning

Selected hybridoma clones were thawed and cultured in T25 flasks (SPL Life Sciences) in 8 mL of HAT+HFCS selective medium. In order to ensure monoclonal but not polyclonal antibodies production, hybridoma subcloning was performed. Once hybridomas were approximately 80% confluent, cells were counted, and 800 cells were placed in a 50 mL tube with 20 mL of HAT+HFCS selective medium. (see **table 2**) A 1/2 serial dilution was performed three times in 20 mL final volume of HAT+HFCS medium, so a final dilution of 1/8 containing 100 cells was obtained. Dilutions (800, 400, 200 and 100) were plated to a half 96 well plate (200 µL/well) and plates were incubated in a humidified incubator at 37ºC in 5% CO_2. Wells were followed to ensure that only one hybridoma clone was expanding in the 100 cell dilution; when clones were expanded enough, supernatants were tested for IgG production by ELISA.

96 well microplate for EIA/RIA (Corning®) were coated with Goat anti-mouse IgG (Sigma) at 3 µg/ml at 4ºC overnight (O/N). After incubation, plates were washed twice with PBS 1X (200 µL/well) and blocked with PBS-BSA 2% (150 µL/well) for one hour at 37ºC. Then, three washes with PBS-Tween 0'001% (200 µL/well) were performed, and hybridoma clones' supernatants were plated at 1/20 dilution in PBS-BSA 2% (100 µL/well). After one hour incubation at room temperature (RT), plates were washed three times with PBS-Tween 0'001% and Horseradish Peroxidase (HRP)-conjugated goat anti-mouse IgG (Sigma) was added (100 µL/well) as secondary antibody for 30 minutes at RT. ELISA plates were washed three times PBS-Tween 0'001% and twice with PBS 1X. Finally, microplates were developed using TMB (BD Bioscience) and reaction was stopped with 2M H_2SO_4. Microplates were read with an EPOCH Microplate Spectrophotometer (BioTek) at 450-570 nm.

Once IgG production and reactivity was confirmed, clones were selected and then expanded to a 24 well plate and then cultured in T25 flasks with HAT+HFCS medium. In order to obtain enough antibody quantity to perform the *in vitro* and/or *in vivo* assays, hybridomas were expanded to T125 flask, and cultures were left in the incubator for weeks in order to obtain enriched supernatants.

1.2. Hybridoma freezing

For hybridoma cryopreservation, cell suspension was placed into 15 mL tubes and then centrifuged for 5 minutes at 1500 rpm at room temperature (RT). After centrifugation, supernatants were carefully discarded, and pellets were resuspended by gentle tapping. Throughout the freezing process, all cryopreservation reagents were kept on ice. Cells were resuspended in 0,5 mL of previously filtered fetal bovine serum (FBS) from PAN^{TM} Biotech and transferred to a cryotube (ClearLine). Then, 0,5 mL of FBS + 20% dimethyl sulfoxide (DMSO) from Panreac AppliChem was added drop by drop and pipette up and down as carried out to ensure proper mixing. Generally, 10.10^6 cells were frozen and placed at -80ºC freezer or liquid nitrogen tanks for long-term preservation.

2. Monoclonal antibody production

2.1. Monoclonal antibody purification and dialysis

For antibody purification, hybridoma cultures were transferred into 50 mL tubes and centrifuged for 20 minutes at 2000 rpm. Supernatants were collected and antibodies were purified using the Affi-Gel Protein A MAPS II Kit (BioRad) following the manufacturer's protocol.

Once purified, antibodies were dialyzed using Slide-A-Lyzer™ dialysis cassettes. Antibody solution was injected in the dialysis cassette using a 19G needle and 10 mL syringe, and the cassette was introduced in sterile PBS 1X (Sigma) and incubated O/N in gentle agitation at 4ºC. After O/N incubation, PBS 1X was replaced under sterile conditions using the laminar flow cabin; this process of O/N incubation and PBS 1X replacement was repeated twice. Finally, PBS was discarded, and antibody solution was collected from the dialysis cassette and placed into a 15 mL sterile tube. Next, antibody solutions were tested for Endotoxin using ToxinSensor™ Gel Clot Endotoxin Assay Kit (Genscript), and antibodies were quantified using Pierce™ BCA Protein Assay Kits (Thermo Fisher Scientific) following the manufacturer's protocol.

2.2. Antibody biotinylation

For antibody biotinylation, antibodies at 0,5 mg/ml were incubated with biotinylation buffer (see **table 2**) and Biotin (Sigma) for 4 hours at RT in gentle agitation using a rotation wheel, protected from light. Then, biotinylated antibody solution was dialyzed in PBS 1X-Azide 1% solution in gentle agitation O/N at RT. Then, two more O/N incubations at 4ºC were performed using PBS 1X (Sigma). Finally, antibody solution was collected from the cassette, quantified using Pierce™ BCA Protein Assay Kits (Thermo Fisher Scientific) following the manufacturer's protocol, and stored at 4ºC until use.

3. Mice

MRL-Faslpr/J (MRL/MpJ-Faslpr/J; thereafter named MRL/lpr) and NSG (NOD.Cg-Prkdcscid Il2rgtm1Wjl/SzJ) mice were purchased from Jackson Laboratory and breed under specific pathogen free conditions at the animal house facility from Faculty of Medicine, University of Barcelona. MRL/lpr females were kept at the animal house facility until they reached 9 weeks old, when the experimental procedure ended. NSG mice were used between 8 and 12 weeks old for salivary gland, external lacrimal gland kidney, liver, and lung extraction, that were used for immunohistochemistry and immunofluorescence assays.

Mice experiments were performed according to the European Community Directive 2010/63/EU and Spanish legislation (Real Decreto 53/2013, BOE-A-2013- 101337) regulating the protection and usage of laboratory animals. Experimental procedures were approved by the Ethics Committee for Animal Experiments (CEEA) of the University of Barcelona.

3.1. Blood and plasma collection

Blood was obtained from MRL/lpr mouse facial vein using a 25G needle, or from mice heart at experimental procedure endpoint. It was collected in 1,5 mL microtubes (DDBiolab) with 20 µl of heparin (Rovi), gently mixed with the heparin, and then centrifuged 10 minutes at 2000 g at 4ºC. Plasma was transferred to new 1,5 mL microtube under sterile conditions, and samples were kept at -20ºC for subsequent analysis.

3.2. MRL/lpr mice MCMV infection

MCMV aliquots, stored at -80ºC, were thawed rapidly using a water bath at 37ºC, and then diluted in DMEM (Sigma) at the proper concentration to inject 10^4 PFU/mouse in a final volume of 200 µl. Thawed and aliquots preparation process was performed under sterile conditions using a laminar flow cabin. Finally, MCMV were intraperitoneally injected in 4 week-old MRL/lpr mice.

4. In vivo determination of polyreactive antibodies' role in SjS pathogenesis

4.1. Polyreactive antibodies half-life assay

Half-life assays with H2h4.7.50 and H2h4.7.94 antibodies were performed in order to determine the *in vivo* assay time-points, since polyreactive antibodies present a much shorter half-life in serum than mono-specific antibodies. 10 mg/ml of previously biotinylated antibodies were intraperitoneally injected in 4 week-old MRL/lpr females, while the equivalent volume of PBS 1X (Sigma) was injected in control mice; four mice were included in each group. Blood was collected at 24, 48 and 72 hours after antibody injection in order to obtained serum and quantify the biotinylated antibody by ELISA, and for H2h4.7.94 antibody the assay was repeated with blood collection shorter time points (12, 24 and 48h after injection).

96 well microplate for EIA/RIA (Corning®) was coated with 3 µg/ml of Goat anti-mouse IgG (Sigma) at 4ºC O/N. Then, plate was blocked and washed (as explained in **section 1.1**), 1/2 serial dilutions of mouse serum in PBS-BSA 2% with 1/50 initial dilution were plated (in duplicates) and incubated for 1h at RT. After PBS-Tween 0'001% washes, HRP-conjugated streptavidin (Roche) was incubated for 15 minutes at RT. After final washes, microplates were developed with TMB (BD Bioscience), and reaction was stopped with 2M H_2SO_4. Microplates were then read with an EPOCH Microplate Spectrophotometer (BioTek) at 450-570 nm. In order to quantify biotinylated antibodies, an aliquot of the previously biotinylated H2h4.7.50 antibody, with known concentration, was included as standard.

4.3. Polyreactive antibodies in vivo assay

Anti-Ro52 polyreactive monoclonal antibodies (mAbs) H2h4.7.50, H2h4.7.94 and B6.2.58 were used to test their capacity to induce or modify disease. MRL/lpr females were infected with a sublethal dose (10^4 PFU/mouse) of MCMV at the age of 4 weeks. During the first week after infection, mice were weighed every day in order to ensure they have been successfully infected, since weight loss is one of the most characteristic signs of the infection. At the age of 6 weeks (day 19 after infection), polyreactive mAbs injection started (10 mg/kg every 48h for 2 weeks); in control mice, PBS 1X (Sigma) was injected. At day 35 after MCMV infection (endpoint) mice were sacrificed, and salivary gland, external lacrimal gland, kidney, lung, and liver were obtained for immunohistopathological analysis. For tissue fixation, organs were placed in biopsy processing cassettes (Simport) and introduced in 4% formaldehyde solution O/N. Then, tissues were transferred to 30% ethanol solution and finally, organs were embedded in paraffin at the center histology facility. Besides, blood was obtained from infected MRL/lpr females at three time points: before infection (day 0), after the infection but before antibody injection (day 19) and endpoint (day 35). It is important to note that 4 days were left between the last mAbs injection and the experimental endpoint to ensure that these injected antibodies were not detected in the anti-Ro52 and anti-dsDNA autoantibodies detection ELISA.

4.4. Anti-Ro52 and anti-dsDNA determination in mouse sera

96-well microtiter ELISA plates (Costar) were coated with dsDNA (Thermo Fisher Scientific) or Ro52 (Sigma-Aldrich) at 3 µg/ml diluted in coating buffer and incubated O/N at 4ºC. Then, plates were blocked and washed, and triplicates of serum samples of each time point (days 0, 19 and 35) were diluted at 1/100 for dsDNA and 1/20 for Ro52 in PBS-BSA 2% and incubated for 1 hour at RT. After subsequent washes, HRP-conjugated goat anti-mouse IgG (Sigma) was incubated (100 µL/well) for 30 minutes at RT. ELISA plates were washed and finally, microplates were developed using TMB (BD Bioscience), and reaction was stopped with 2M H_2SO_4. Then, microplates were read with an EPOCH Microplate Spectrophotometer (BioTek) at 450-570 nm.

4.5. Flow cytometry

Lymphocytic subpopulations were analyzed in spleen, and plasma cells were analyzed in bone marrow. First, in order to eliminate red blood cells in cell suspensions, RBC lysis buffer 1X (Thermo Fisher Scientific) was used for 5 minutes at 4ºC. Then, cell lysis was stopped with PBS 1X, cell suspensions were centrifuged and resuspended in FACS staining buffer (see **table 2**). Cell suspensions from spleen and bone marrow were incubated with fluorophore-labeled antibodies for 45 minutes on ice. In spleen, the following antibodies were used: B220 PB (BD Pharmingen, RA3-6B2), CD138 PECy7 (Biolegend, 281-2)., CD19 A647 (Biolegend, 6D5), CD21 PECy7 (Invitrogen, eBio8D9), CD23 PE (BD Pharmingen), CD3 A488 (1/500), CD3 A647 (Biolegend, 145-2C11), CD4 PB (Biolegend, GK1.5), CD44 FITC (Biolegend, IM7), CD45RB PE (BD, C363.16A), CD5 PE (Biolegend, 53-7.3), CD8 PECy7 (Biolegend, 53-6.7), CD95 A647 (BD Biosciences, Jo2). , CXCR5 APC (Biolegend, L138D7), GL7 A488 (Invitrogen, GL-7), IgM FITC (Southern Biotech), PD1 PE (Tonbo biosciences, J43.1). For bone marrow, plasma cells were stained using B220 PB (BD Pharmingen, RA3-6B2), CD138 PECy7 (Biolegend, 281-2), IgD PE (Southern Biotech, 11-26), IgM FITC (Southern Biotech), Ly9 APC (Biolegend, Ly9ab3) antibodies. After incubation, cells were washed using FACS washing buffer (see **table 2**) and resuspended in FACS staining buffer. Finally, data were acquired with LSRII Fortessa flow cytometer (BD Biosciences) and analyzed with FlowJo vX.0.7 (Tree Star, Inc) software.

5. Immunohistopathological analysis

Immunohistopathologic analyses were performed using 2.5 µm sections of paraffin-embedded salivary gland, external lacrimal gland, and kidney, which were obtained using a microtome (Leica). Slides were incubated at 37ºC O/N, followed by deparaffinization and rehydration with xylene (PanReac AppliChem) and a series of decreasing concentrations of ethanol (Sigma). First, samples were immersed three times in xylene for 10 minutes each, and then, sections were immersed in different ethanol solutions for 5 minutes each: absolute ethanol, 96% (v/v), 70% (v/v) and 40% (v/v). Finally, samples were washed with distilled water (dH_2O).

5.1. Lymphocytic infiltrates number and area determination

For quantification of foci number and area measurement, rehydrated sections were stained with hematoxylin (Sigma) for 2 minutes and rinsed with tap water for 5 minutes. Subsequently, samples were immersed in acetic acid at 1% (v/v) three times, rinsed with dH_2O, and carefully dried. Next, slides were stained with eosin (Sigma) for 1 minute, washed, and dehydrated using increasing concentration of ethanol (40%, 70%, 96% and absolute ethanol for 5 minutes each) and xylene (three times, for 10 minutes each). Finally, slides were mounted with DPX (Sigma) and visualized at 10X, 20X and 40X magnifications using Olympus BX41 fluorescence microscope. Lymphocytic infiltrates were counted, and their respective area were measured using ImageJ software.

5.2. Immunofluorescence assay

For immunofluorescence characterization of lymphocytic populations infiltrating salivary glands, deparaffinized samples were subjected to heat-induced antigen retrieval in citrate buffer (pH 6,0) for 5 minutes using a pressure cooker. Following antigen retrieval and a 25-minute incubation period for allow samples to cool, slides were washed three times with PBS 1X for 5 minutes each. After carefully drying, non-specific binding was blocked using 100 µL/sample of PBS 1X - FBS 6%; samples were incubated for 30 min at RT in a humidified chamber. Once incubation was complete, blocking solution was removed, and primary antibodies were applied. These antibodies were diluted in the blocking solution and included CD45 (BD Pharmingen™, 553076), B220 (Thermo Fisher Scientific, 14-0452-82), CD3 (Cell Signaling, D7A6E), CD4 (Cell Signaling, D7D2Z) and CD8 (Cell Signaling, D8A8Y). After O/N incubation at 4ºC, slides were washed with PBS 1X for 5 minutes for three times, followed by 2 hours incubation at RT with secondary antibodies: anti-rat IgG-A488 (Jackson ImmunoResearch, 712-546-153) was used for CD45 and B220, while anti-rabbit IgG-Rhodamine (Jackson ImmunoResearch, 111-295-144) was used for CD3, CD4 and CD8 staining. Finally, tissue staining was revealed using DAB (Sigma, D7304). Double staining of B220 and CD3, B220 and CD4, and B220 and CD8 was performed in order to examine potential GC-like structures. Slides were finally mounted using aqueous mounting media (see **table 2**) and visualized at 10X, 20X and 40X magnifications using Olympus BX41 fluorescence microscope, and the area corresponding to each stain was quantified using ImageJ software.

5.3. Immunohistochemistry for Ro52 expression determination

Given that Ro52 overexpression has been described in patients' salivary gland tissue, Ro52 expression was analyzed by immunohistochemistry. After deparaffination, antigen retrieval and blockage, the monoclonal antibody anti-Ro52 (Thermo Fisher Scientific, PA5-106903) was incubated O/N at 4ºC. Following primary antibody incubation, samples were washed three times with PBS 1X. Then, endogenous peroxidase activity was blocked with H_2O_2 solution at 0,3% (diluted in dH_2O) for 10 minutes. Samples were washed and the secondary anti-rabbit IgG-HRP secondary (Thermo Fisher Scientific, 31460) was applied and incubated for 2h at RT. Samples revealing was performed with DAB (Sigma). Then, slices were washed and stained with hematoxylin for 2 minutes, followed by 5-minute wash with dH_2O and immersion in acetic acid at 1% (v/v) three times. Next, sections were washed in dH_2O and dehydrated using increasing concentration of ethanol (40%, 70%, 96% and absolute ethanol for 5 minutes each) and xylene (three times, for 10 minutes each). Finally, slides were mounted with DPX (Sigma) and visualized at 20X magnifications using Olympus BX41 fluorescence microscope. In order to quantify Ro52 expression levels, ImageJ software was employed.

6. Identification and characterization of autoantibodies against new autoantigens

6.1. Autoreactivity assay

To assess antibody autoreactivity, antibody supernatants were tested against L cells, a fibroblast cell line derived from mouse adipose tissue, by flow cytometry. L cells were trypsinized, trypsin was inactivated with FACS washing buffer (see **table 2**), and cells were fixed in PBS-formaldehyde (4%) at RT for 10 minutes. After rinsing and centrifugation, cell permeabilization was achieved using PBS-Triton X-100 (0.05%) for 20 minutes, followed by resuspension in FACS staining buffer (see **table 2**). Fixed and permeabilized L cells were stained with a 1/2 dilution of hybridoma supernatants for 45 minutes at RT. Cells were washed, and then PE $F(ab')_2$ Fragment Goat Anti-Mouse IgG was incubated as detection antibody for 30 minutes at RT. Finally, cells were washed and resuspended in FACS staining buffer. Flow cytometry data was collected using a

FACSCanto II flow cytometer from BD Biosciences, and analysis was conducted with FlowJo vX.0.7 software (Tree Star, Inc.).

6.2. Immunohistochemistry with paraffin-embedded tissue

Within the 168 hybridoma library generated in the B cell antibody repertoire analysis using NOD.H2^{h4} mice (Sáez et al., 2021), mAbs of IgG isotype that showed to be not autoreactive nor polyreactive were tested against salivary gland, kidney, liver, and lung paraffin-embedded tissue from NSG mice. 2.5 µm slices were deparaffinated, and after deparaffination, heat-induced antigen retrieval and blockage, supernatants were incubated overnight (ON) at 4ºC, and after wash, HRP-conjugated Goat anti-mouse IgG (Jackson ImmunoResearch, 115-035-072) secondary was incubated for 1h at RT. Finally, slices were stained with hematoxylin (Sigma) for 2 minutes and rinsed with tap water for 5 minutes. Subsequently, samples were immersed in acetic acid at 1% (v/v) three times, rinsed with dH_2O, carefully dried, and dehydrated using increasing concentration of ethanol (40%, 70%, 96% and absolute ethanol for 5 minutes each) and xylene (three times, for 10 minutes each). Finally, slides were mounted with DPX (Sigma) and visualized at 10X and 20X magnifications using Olympus BX41 fluorescence microscope.

6.3. Salivary gland lysate

Antibodies that were selected due to their specific pattern against salivary gland tissue by immunohistochemistry were analyzed by western blot. Hybridomas producing the selected antibodies were cultured as explained in **section 1.1** in order to collect their supernatants to be tested against salivary gland lysate. For salivary gland lysis, salivary glands were weighed in order to calculate the volume of lysis buffer (**table 2**), that was added in 1:5 proportion (w/v). Besides, for each ml of lysis buffer, 10 µl of the protease inhibitor Halt (Thermo Scientific) and 10 µl of EDTA 0,5M (Thermo Scientific) were added. Once immersed in the lysis buffer, salivary glands were mechanically disaggregated using a Tissue Homogenizer OMNI TH (OMNI International) and then incubated during 1h in gentle rotation at 4ºC. After incubation, samples were centrifuged at 12000 rpm at 4ºC for 20 minutes, and supernatants were collected and stored at -80ºC. Total protein was measured by BCA assay (Thermo Scientific).

6.4. Western blot

Hybridomas' supernatants were tested against salivary gland lysate by western blot. Salivary gland lysate (400 μg) was used in reducing conditions by adding β-mercaptoethanol at 1% (v/v), and electrophoresis in the polyacrylamide (BioRad) gel at 12% was performed, at 90 volts (V) at RT. For the determination of the molecular weights of each protein, a PageRuler Prestained Protein Ladder (Thermo Fisher Scientific) was used as a molecular weight marker. Following electrophoresis, proteins were transferred to a nitrocellulose membrane using the Mini Trans Blot Cassette system (BioRad, 170-3930). The nitrocellulose membrane was briefly hydrated in water for 5 minutes. The transfer cassette was prepared with the following components, in this order, on the black side: a sponge, Whatman paper, the hydrated nitrocellulose membrane, the acrylamide gel, Whatman paper, and another sponge, with all components pre-wetted in transfer buffer (see **table 2**). Subsequently, the cassette was sealed, ensuring no air bubbles were trapped between the membrane and the gel, placed in a container filled with 1x transfer buffer, and subjected to a voltage of 70V for 90 minutes at 4°C.

Following the transfer, the nitrocellulose membrane was retrieved, washed in TBS-T (prepared from TBS 10X; see **table 2**) under agitation for 5 minutes, and blocked with blocking buffer (see **table 2**) for 1 hour at RT. After blocking, the membrane was washed twice more in TBS-T for 5 minutes, and the membrane was cut into strips to incubate each of them with each supernatant. Anti-mouse actin antibody (R&D Systems, MAB8929), diluted in TBS-T with 5% BSA, was used as positive control. Membrane strips were incubated for 2 hours at RT. Subsequently, these were washed in TBS-T for 5 minutes and incubated with secondary antibody HRP-conjugated rabbit anti-IgG antibody, diluted in TBS-T with 5% powdered milk for 30 minutes at RT. Finally, membrane strips were washed twice in TBS-T for 5 minutes, followed by two additional washes in TBS for 5 minutes each. Protein visualization on the membrane was performed using the SuperSignal West Pico Chemiluminescent Substrate (Pierce, 34080F), following the manufacturer's instructions. ImageQuant^{TM} LAS4000 was used for visualization.

6.5. Antigenic microarray

Once the potential new autoantibodies were selected and in order to discard or confirm monospecificity, antigenic reactivity was analyzed by a specific microarray for systemic autoimmune diseases, which includes 120 autoantigens (GeneCopoeia™, PA001). Supernatants from H2h4.1.42, H2h4.2.3, H2h4.2.72, H2h4.2.341, H2h4.15.24.8, H2h4.15.47 and H2h4.16.128 hybridomas were included. Besides, supernatants from H2h4.7.50, H2h4.7.94 and B6.2.58 hybridomas were also included in order to deeper characterize their polyreactivity beyond the ELISA antigenic panel used in the previous B cell antibody repertoire analysis (Sáez et al., 2021).

The manufacturer's protocol is the following: "The array was incubated with supernatants, washed to remove unbound antibodies and other proteins, then co-incubated with Cy3- and Cy5-labeled secondary antibodies. The dual labeling strategy is intended to distinguish between immunoglobulin (Ig) subtypes present within samples. For example. a Cy3-labeled anti-IgG secondary antibody is used to detect IgG antibodies, and a Cy5-labeled anti-IgM secondary antibody is used to detect IgM antibodies. Fluorophore-labeled secondary antibodies are available for detecting IgA, IgD, IgE, IgG and IgM immunoglobulins, as well as IgG subclasses IgG1, IgG2, IgG3, and IgG4. After washing to remove unbound secondary antibodies, signals are detected using a GenePix® 4400A microarray scanner. The raw data is then analyzed using GenePix® 7.0 software".

7. Statistics

P-values for autoantibody levels in MRL/lpr sera, lymphocytic infiltration analyses in salivary glands, and flow cytometry results for lymphocytic subpopulations both in spleen and bone marrow were calculated by unpaired t test (Mann-Whitney) after confirming the non-parametric nature of the data using GraphPad Prism 10. Statistical difference was concluded if $p < 0.05$.

8. Cell Culture Medium and Buffers

Table 2. Cell culture, ELISA, antibody biotinylation, immunofluorescence and immunohistochemistry media and buffers.

Cell culture medium or Buffer	Composition
HAT+HFCS selective culture medium	RPMI containing: - 20% FBS - 1X Penicillin-Streptomycin - 1X L-Glutamine - 0,5% HFCS - 1X HAT
Coating buffer	For 1 liter: - 8,4 g NAHCO3 - 3,56 g NA2CO3
Biotinylation buffer	For 100 mL (adjust pH to 9.5): - 5,3 g Na2CO3 - 8,4 g NaHCO3
Aqueous mounting media	For 100 mL: - 90 mL Glycerol - 100 mL PBS 1X - 500 mg Propyl Gallate (Sigma)
Citrate buffer	For 2L (adjust to pH 6,0): - 5,88 g of sodium citrate tribasic dehydrate - 2 L dH2O
FACS washing buffer	PBS 1X containing: - 2% FBS - 0,01% NaN_3
FACS staining buffer	PBS 1X containing: - 2% FBS - 20% Rabbit serum - 0,01% NaN_3

Electrophoresis buffer	For 1 liter: - 14,41 g glycine - 3,03 g Tris base - 1 g SDS - 1L dH_2O
Transfer buffer	For 1 liter: - 8 g glycine - 3,56 g Tris base - 0,25 g SDS - 1L of methanol (20% in dH_2O)
TBS 10X	pH 7,4 - 0,2 M Tris base - 1,5 M NaCl
TBS - T	- 0,05% Tween-20 in TBS 1X
Blocking buffer (Western Blot)	- 5% of powdered milk in TBS 1X

V. RESULTS

1. Polyreactive antibodies reactivity

The polyreactive antibodies H2h4.7.50 and H2h4.7.94 were selected from the previous study of the B cell repertoire in the NOD.H-2^{h4} SjS mouse model. This study showed that the majority of polyreactive IgG antibodies were IgG2b, while in the non-autoimmune control strain, B6, the majority of polyreactive antibodies corresponded to IgG3. Besides, H2h4.7.8, H2h4.7.50 and H2h4.7.94 were identified as three clonally related antibodies in the 66 week-old NOD.H-2^{h4} mouse, and importantly it was observed that H2h4.7.94 has additional somatic mutations that increase its antigen reactivity strength when tested against the antigenic array by ELISA, and it also showed stronger cytoplasmic staining when tested against HEp-2 cells by immunofluorescence. Therefore, given the potential role of polyreactive antibodies in SjS pathogenesis, H2h4.7.50 and H2h4.7.94 antibodies were selected to test our hypothesis, expecting that the higher reactivity strength of H2h4.7.94 would induce more severe SjS symptoms than H2h4.7.50 when tested in the SjS mouse model. Importantly, these antibodies were also selected because of their IgG2b isotype, considering them as representative of the polyreactive antibodies that could be contributing to disease's pathogenesis. In addition, we decided to include a polyreactive antibody from the B6 non-autoimmune strain, so B6.2.58 antibody was selected since it presents an IgG3 subclass, the most frequent isotype in this mouse strain. Therefore, hybridomas producing the selected antibodies were cultured and antibodies were purified under endotoxin-free conditions.

B6.2.58, H2h4.7.50 and H2h4.7.94 polyreactivity was confirmed by ELISA using the antigenic panel including dsDNA, H1, Ro52, LPS, Insulin and OVA (**figure 12A**). Antibodies showed to maintain their polyreactivity, since all of them recognized three or more antigens. B6.2.58 showed to be reactive against dsDNA, insulin, OVA, and predominantly against Ro52. H2h4.7.50 showed to recognize with high affinity dsDNA, Ro52, LPS and OVA, and with moderate affinity H1 and insulin. H2h4.7.94 showed higher affinity against insulin and OVA than H2h4.7.50, while the affinity against dsDNA, H1, Ro52 and LPS was similar.

Furthermore, the reactivity patterns of antibodies were confirmed through immunohistochemistry analysis, employing paraffin-embedded tissue sections from salivary gland, lacrimal gland, and kidney. Additionally, immunofluorescence assays were conducted using Hep-2 cells, a commonly used test for ANA in clinic diagnostic (**Figure 12B**).

With respect to immunohistochemistry assays, H2h4.7.50 and H2h4.7.94 exhibited a consistent nuclear pattern across all tissues. Remarkably, in salivary glands, they demonstrated a predominant nuclear staining within the ductal epithelial cells. Meanwhile, B6.2.58 also displayed a nuclear staining pattern in all tissues, although the staining intensity appeared slightly lower compared to H2h4.7.50 and H2h4.7.94.

Regarding immunofluorescence assay using Hep-2 cells, B6.2.58 exhibited both nuclear and cytoplasmic patterns. H2h4.7.50 displayed a nuclear pattern with very faint cytoplasmic staining, while H2h4.7.94 exhibited a nuclear pattern and notably stronger cytoplasmic staining than H2h4.7.50. Intriguingly, a speckled pattern was observed in some cells for all three antibodies. This speckled pattern is a characteristic feature of ANAs associated with systemic autoimmune diseases, such as SLE and SjS, which, for instance, recognize Ro52.

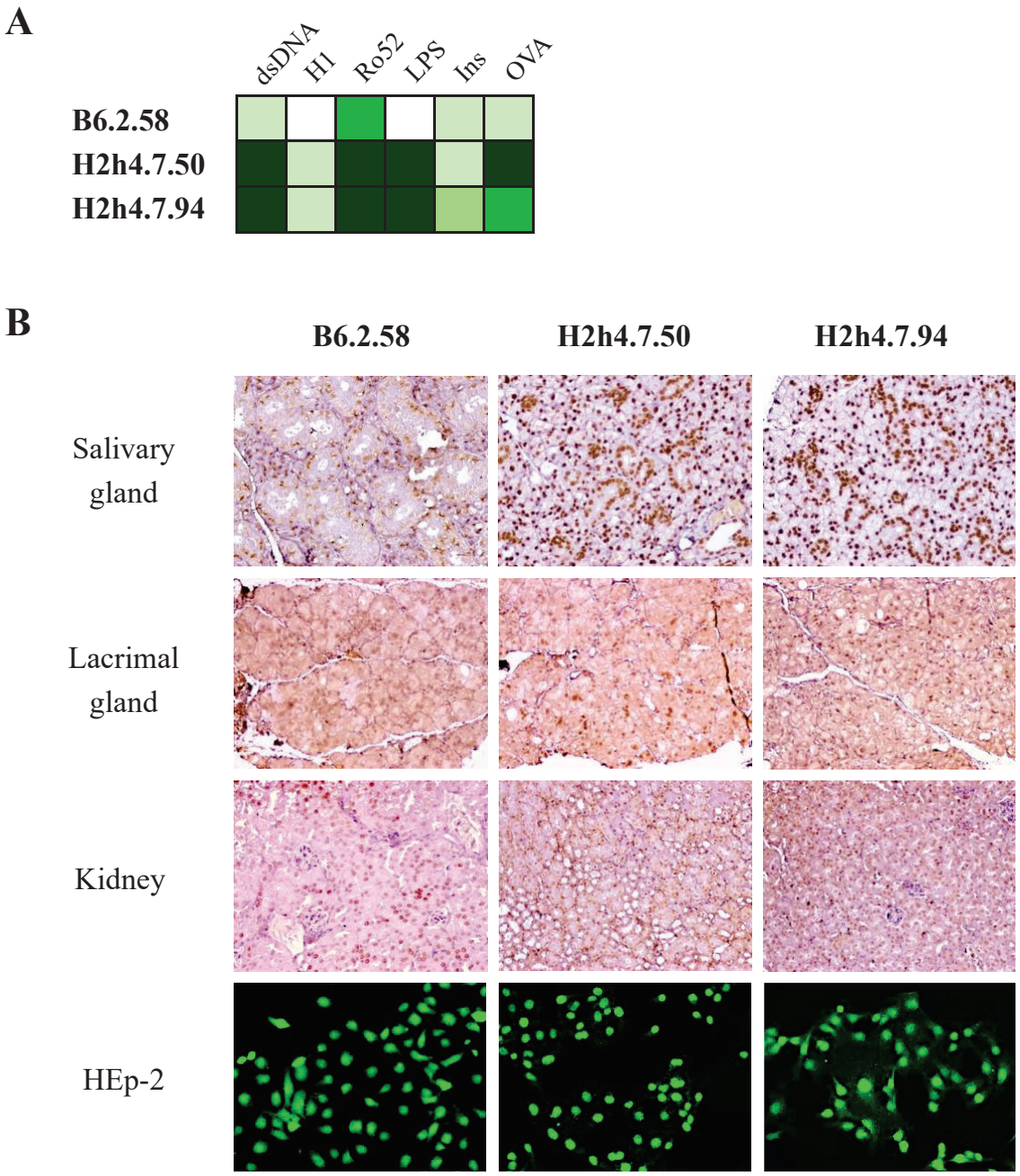

Figure 12. Reactivity confirmation of H2h4.7.50, H2h4.7.94 and B6.2.58 antibodies. (A) ELISA results against the antigenic array (dsDNA, H1, Ro52, LPS, Insulin and OVA). Color intensity correspond to the level of reactivity as measured by ELISA, with darker green indicating strong binding, moderate binding represented by lighter green, and low or no binding represented by white. **(B)** Immunohistochemistry results for salivary gland, lacrimal gland, and kidney paraffin-embedded tissue, and immunofluorescence assay results using HEp-2 cells for B6.2.58, H2h4.7.50 and H2h4.7.94 antibodies; 20X magnifications images.

2. Sjögren's syndrome MCMV infection model set up

MRL/lpr mouse strain was selected for testing the *in vivo* effects of the polyreactive antibodies B6.2.58, H2h4.7.50 and H24h.7.94. For testing these antibodies' pathogenicity *in vivo*, an acute SjS model was needed, so this strain was selected since the lack of Fas induces a severe autoimmunity that leads to lymphoproliferative syndrome which symptoms start at 9 weeks of age. However, since MRL/lpr mice do not spontaneously present anti-Ro52 autoantibodies in serum, it was needed to develop a more accurate model by infecting MRL/lpr females with a sublethal dose of MCMV (Li et al., 2018). MCMV target are mainly the epithelial cells of exocrine glands, driving there the immune response and inducing a SjS-like mouse model in which both anti-Ro52 and anti-dsDNA autoantibodies are present in mouse sera. Importantly, although these selected antibodies were obtained from the spontaneous SjS mouse model NOD.H-2^{h4}, this model was discarded to test the *in vivo* pathogenicity of those antibodies because of SjS-related symptoms start appearing after 14 weeks old, with a less acute disease development than MRL/lpr. Thus, in case of using NOD.H-2^{h4} model, we would have needed a longer treatment and then higher amount of each antibody to induce disease-related symptoms. Importantly, due to the lymphoproliferative syndrome in MRL/lpr mice, antibodies needed to be tested before symptoms started in order to ensure that the observed effects were due to the injected antibodies and no to the lymphoproliferative syndrome. Thus, it was decided to infect mice at 4 weeks old.

Firstly, the infection model was set up. In order to analyze the effects of the infection with sublethal dose of MCMV in 4 week-old MRL/lpr females, at the experimental endpoint (9 weeks old), SjS-related autoantibodies levels were measured in mouse sera by ELISA and salivary gland lymphocytic infiltration was analyzed in paraffin-embedded tissue by hematoxylin-eosin (H&E) staining.

Regarding SjS-related autoantibodies, both anti-dsDNA and anti-Ro52 were significantly increased in mouse sera after MCMV infection compared to control (**figure 13A).** Besides, salivary gland infiltration was also significantly increased, since no infiltrates were observed in the non-infected mice, but a significant increase in foci number was detected in the infected 9 week-old MRL/lpr females (**figure 13B**).

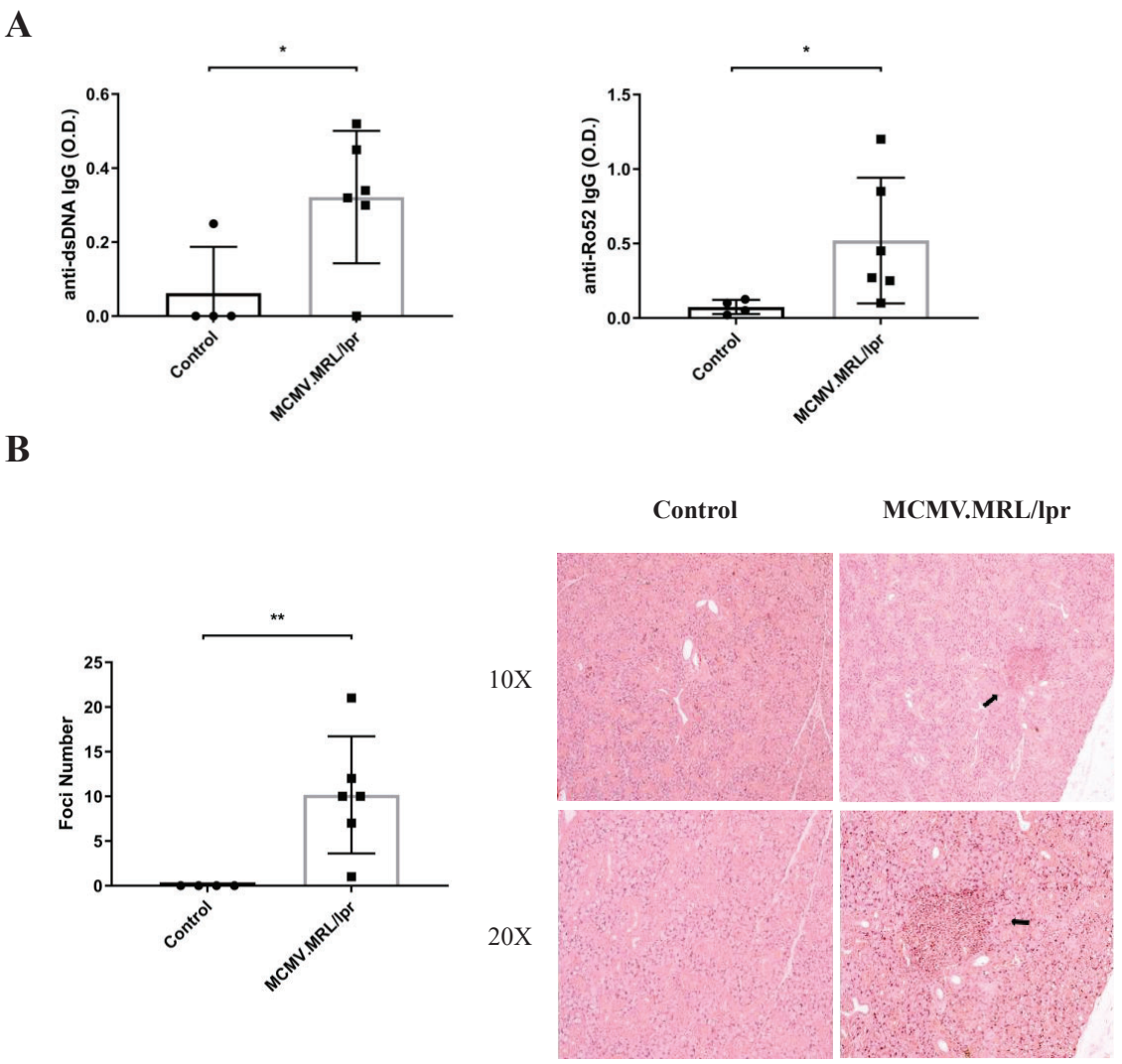

Figure 13. (A) Anti-dsDNA and anti-Ro52 autoantibody levels in mouse sera represented by optical density (O.D.) obtained by ELISA for control and infected (MCMV.MRL/lpr) mice **(B)** Foci number graph and representative images of H&E stained salivary gland tissue at 20X magnifications for control and infected (MCMV.MRL/lpr) mice. Infiltrates are indicated by a black arrow.

Besides, lymphocytic infiltration in the infected MRL/lpr mice was also confirmed by CD45 staining by immunofluorescence (**figure 14**). No infiltration was observed in the non-infected mice, while CD45 positive cells could be observed in the salivary gland samples from infected 9 weeks-old females (MCMV.MRL/lpr).

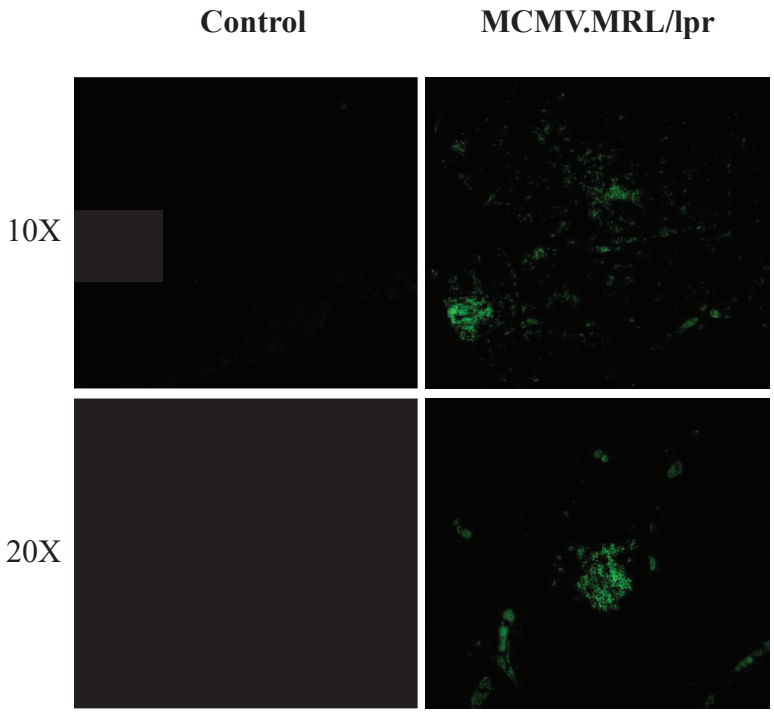

Figure 14. Representative images of CD45 staining (in green) by immunofluorescence in salivary gland tissue for control and infected (MCMV.MRL/lpr) mice at 10X and 20X magnifications.

3. Antibodies half-life assay

Since polyreactive antibodies present a much shorter half-life in serum than monospecific antibodies, half-life assays with H2h4.7.50 and H2h4.7.94 antibodies were performed in order to establish the time left between injections in the *in vivo* assay with MRL/lpr 4 week-old females in order to maintain the antibody concentration stable in blood during the treatment period. Thus, antibodies were biotinylated in order to detect them in mice sera by ELISA, and 160 μg/mouse was injected and detected at 24, 48 and 72 hours after the injection.

H2h4.7.50 showed to have an approximate half-life of 48 hours, while H2h4.7.94 half-life assay needed to be repeated since the antibody wasn't detected in mouse sera 24 hours after injection. Therefore, biotinylated H2h4.7.94 concentration was measured in mice sera at 6, 12 and 24 hours after injection, showing to have a half-life of approximately/lower than 6 hours (**figure 15**). This short half-life may be due to H2h4.7.94 high antigen binding strength. Thus, H2h4.7.94 antibody was excluded from the *in vivo* assay for various reasons: no comparable results if injection time-points were different, potentiated immunocomplexes formation and isotype-derived effects on disease development due to the repeated injection rather than the effects that depend on other antibody features beyond the isotype, and difficulties related to the production of such a high amount of antibody.

Therefore, these results lead to the establishment of the *in vivo* assay time points, infecting 4 week-old MRL/lpr females at day 0, start injecting B6.2.58 and H2h4.7.50 antibodies every 48 hours for two weeks (seven injections in total) at day 19 after MCMV infection. After the last injection, 4 days were left to ensure the injected polyreactive antibody was not present in mice sera and detected in the ELISA for anti-Ro52 and anti-dsDNA autoantibodies, so the experiment endpoint was established at day 35 after infection.

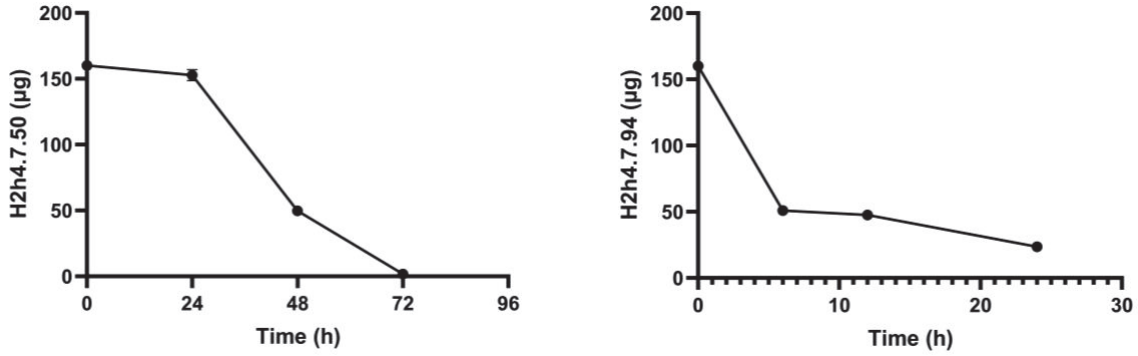

Figure 15. Half-life assay results for H2h4.7.50 (left) and H2h7.94 (right) represented as total micrograms (y axis) quantified by ELISA at each blood collection time point: 24, 28 and 72 hours for H2h4.7.50, and 6, 12 and 24 hours for H2h7.94.

4. H2h4.7.50 increases SjS-related autoantibodies in mouse sera

Autoantibody levels were analyzed in MRL/lpr females as a measure of disease development and progression in the mouse model, since the presence of autoantibodies that recognize Ro52 and dsDNA in serum is a hallmark of SjS. Autoantibody levels were measured by ELISA before MCMV infection (day 0), after the infection but before antibody injection (day 19), and at the *in vivo* assay endpoint (day 35). Importantly, at day 35, the injected antibodies which also recognize dsDNA could not be detected in the ELISA assay since 4 days were left after the last injection, and the polyreactive antibodies' half-life is 48 hours.

Results showed increased levels of both anti-dsDNA and anti-Ro52 antibodies at day 35 in the H2h4.7.50 group compared to control and B6.2.58 groups (**figure 16**). Importantly, the levels of both anti-dsDNA and anti-Ro52 autoantibodies were significantly increased between day 0 and day 19 in all experimental groups, indicating that MCMV infection similarly induced SjS-related autoantibodies increase in control, B6.2.58 and H2h4.7.50 mice.

Interestingly, only the H2h4.7.50 group showed a significant increase in autoantibody levels at day 35 compared to day 19, for both anti-dsDNA and anti-Ro52 autoantibodies. Therefore, it can be concluded that H2h4.7.50 induces an increase of both anti-dsDNA and anti-Ro52 autoantibodies, supporting the proposed hypothesis.

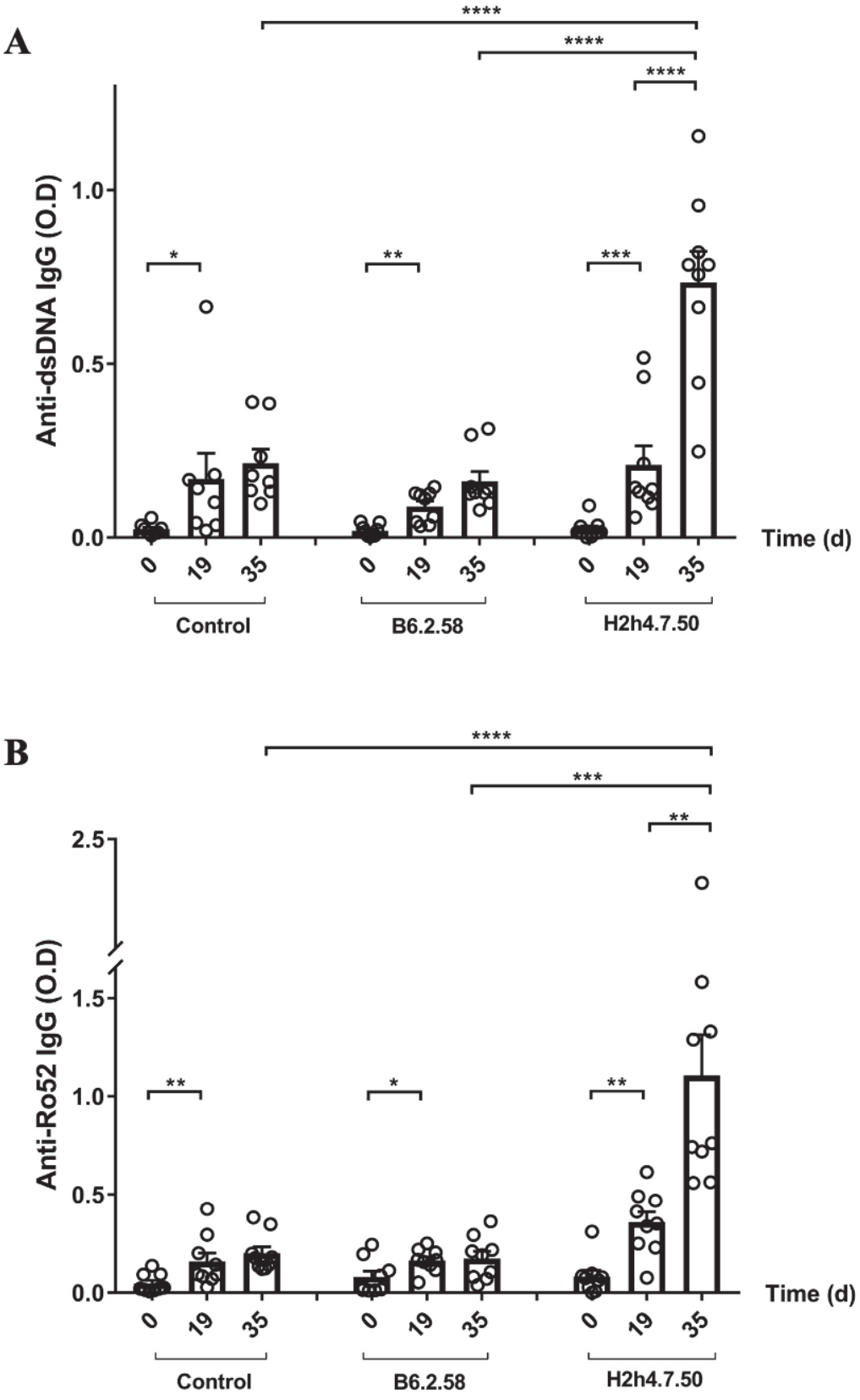

Figure 16. Anti-dsDNA and anti-Ro52 autoantibodies levels in mouse sera. Graphs showing optical density (O.D.) obtained by ELISA for each time point (days 0, 19 and 35) for control (N=7), B6.2.58 (N=9) and H2h4.7.50 (N=9).

5. H2h4.7.50 increases salivary gland infiltration

5.1. H2h4.7.50 increases foci number in salivary gland

Infiltrates were analyzed in salivary and lacrimal glands by H&E staining since lymphocytic infiltration in exocrine glands is one of the hallmarks of SjS. Besides, kidney sections were also analyzed in order to find extraglandular manifestations.

Importantly, histopathological analysis showed a significant increase in lymphocytic infiltration in H2h4.7.50 group salivary glands in terms of foci number, compared to control group. However, the mean area of these infiltrates was similar between groups (**figure 17**).

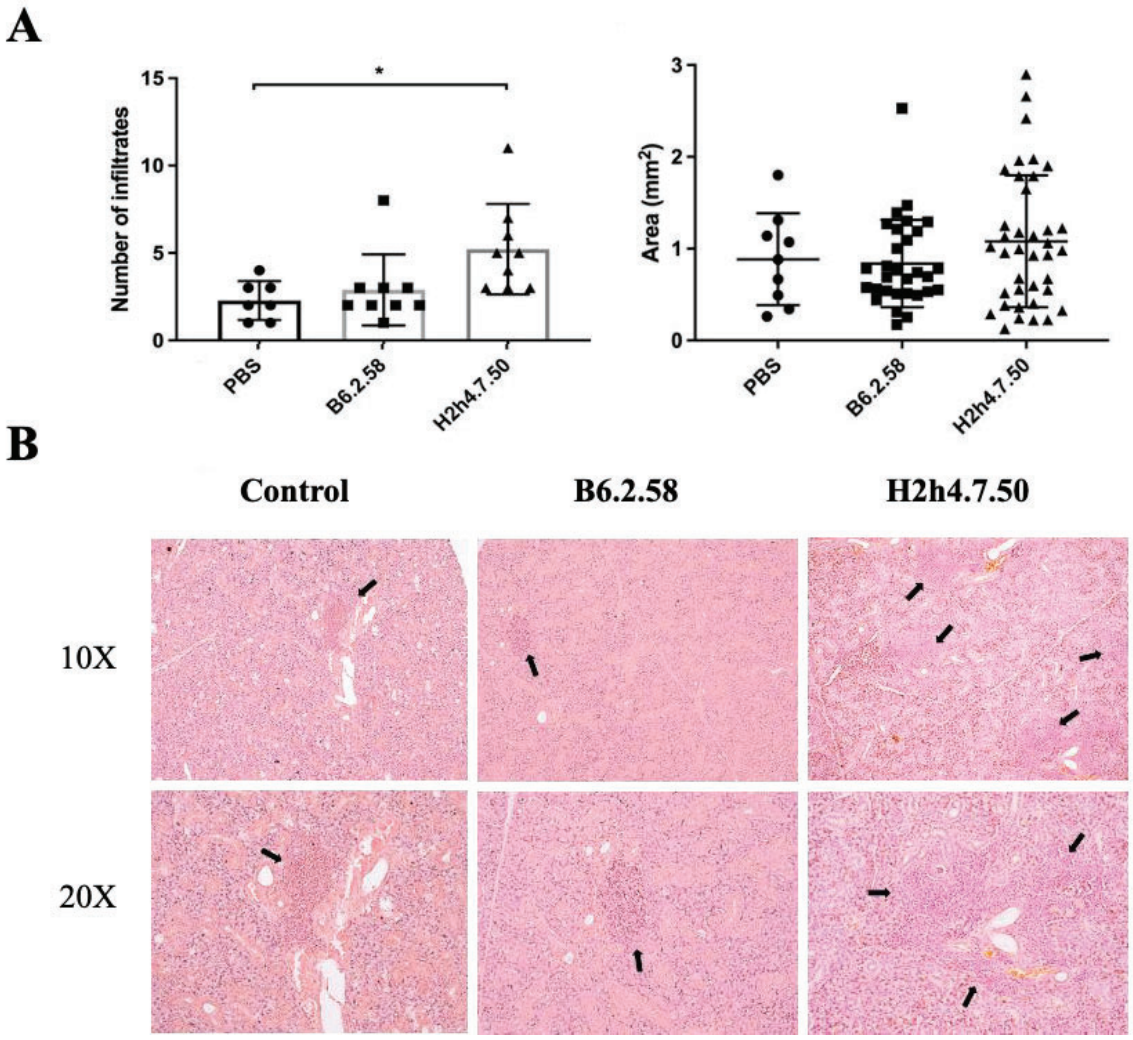

Figure 17. Salivary gland infiltration. (A) Number of infiltrates, and area of each infiltrate for control, B6.2.58 and H2h4.7.50 groups. **(B)** Representative H&E images of salivary glands for each experimental group at 10X and 20X magnifications. Infiltrates are indicated by black arrows.

Besides, no lymphocytic infiltration was observed in lacrimal gland tissue for any of the three experimental groups, and nor histopathological affectations were found in kidney sections (**figure 18**).

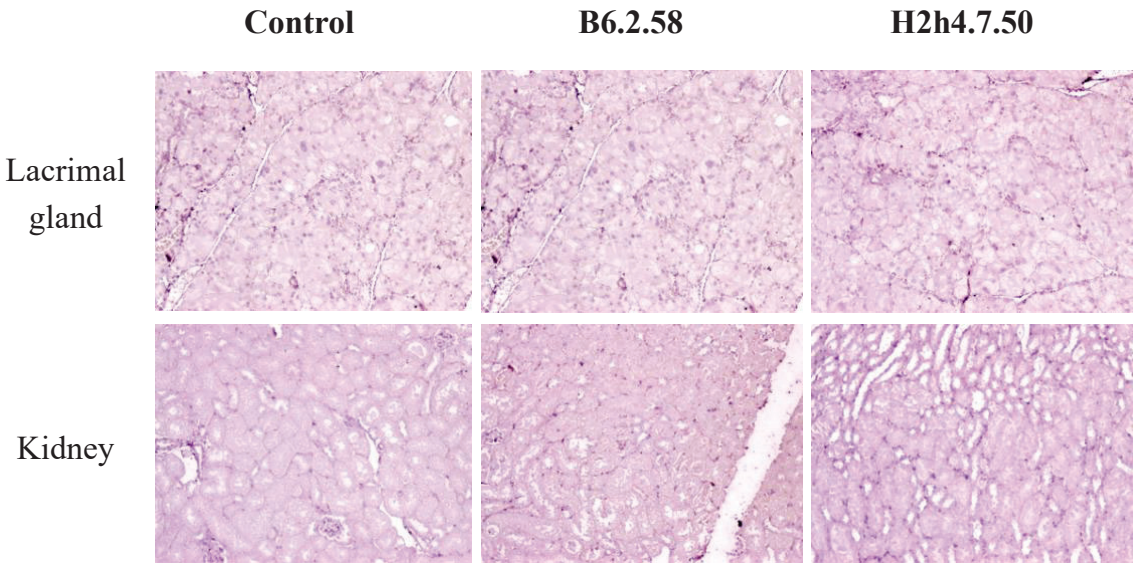

Figure 18. Lacrimal gland and kidney H&E images for control, B6.2.58 and H2h4.7.50 groups at 10X magnifications.

5.2. H2h4.7.50 induces lymphocytic infiltration in salivary gland

In order to determine total lymphocytic infiltration in salivary gland, CD45 staining was performed by immunofluorescence assay in paraffin-embedded tissue. Analysis showed a significant increase in CD45 cells infiltrated area in H2h4.7.50 group compared to B6.2.58 (**figure 19**).

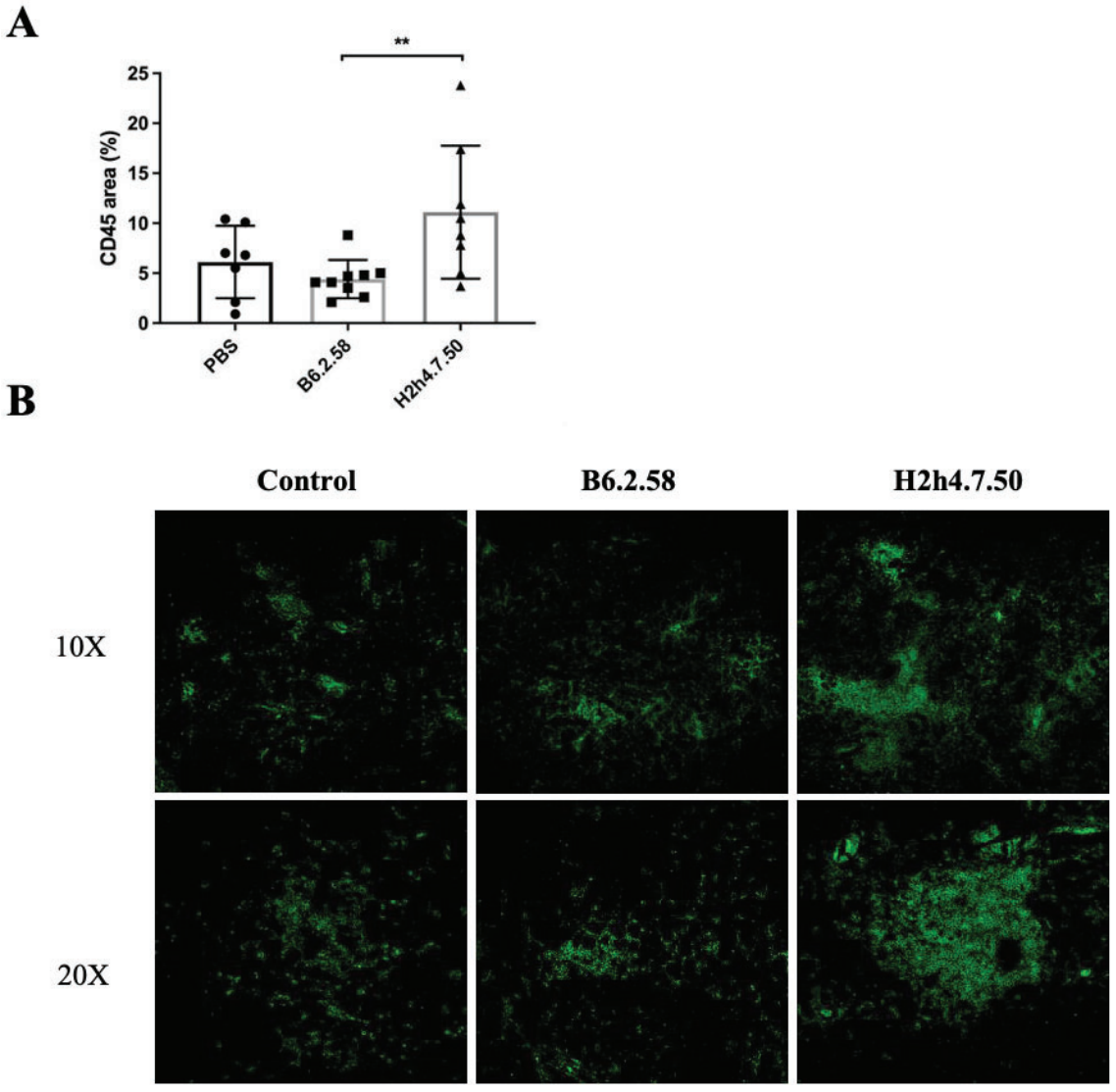

Figure 19. Salivary gland lymphocytic infiltration. (A) Infiltrated area (%) by CD45 cells for control (N=7), B6.2.58 (N=9) and H2h4.7.50 (N=9) groups. **(B)** Representative immunofluorescence images in salivary gland for each experimental group at 10X and 20X magnifications.

5.3. H2h4.7.50 induces infiltration by CD3 and CD8 cells in salivary gland

In order to better characterize the infiltrating lymphocytic populations, B and T cells staining was performed by immunofluorescence in salivary gland paraffin-embedded tissue. For B cells, B220 marker was used; for T cells, CD3, CD4 and CD8 markers were stained.

Importantly, an increase in CD3 positive area was found in H2h4.7.50 group compared to B6.2.58, and interestingly, a significantly higher CD8 positive area was observed in H2h4.7.50 compared to control group. However, no differences were found for B220 or CD4 infiltrated area, although a light increasing tendency could be observed for both markers. Therefore, immunofluorescence data showed that the increased infiltration rate in H2h4.7.50 group compared to control and B6.2.58 groups is mainly due to CD3 cells, and specifically to CD8 cells (**figure 20**).

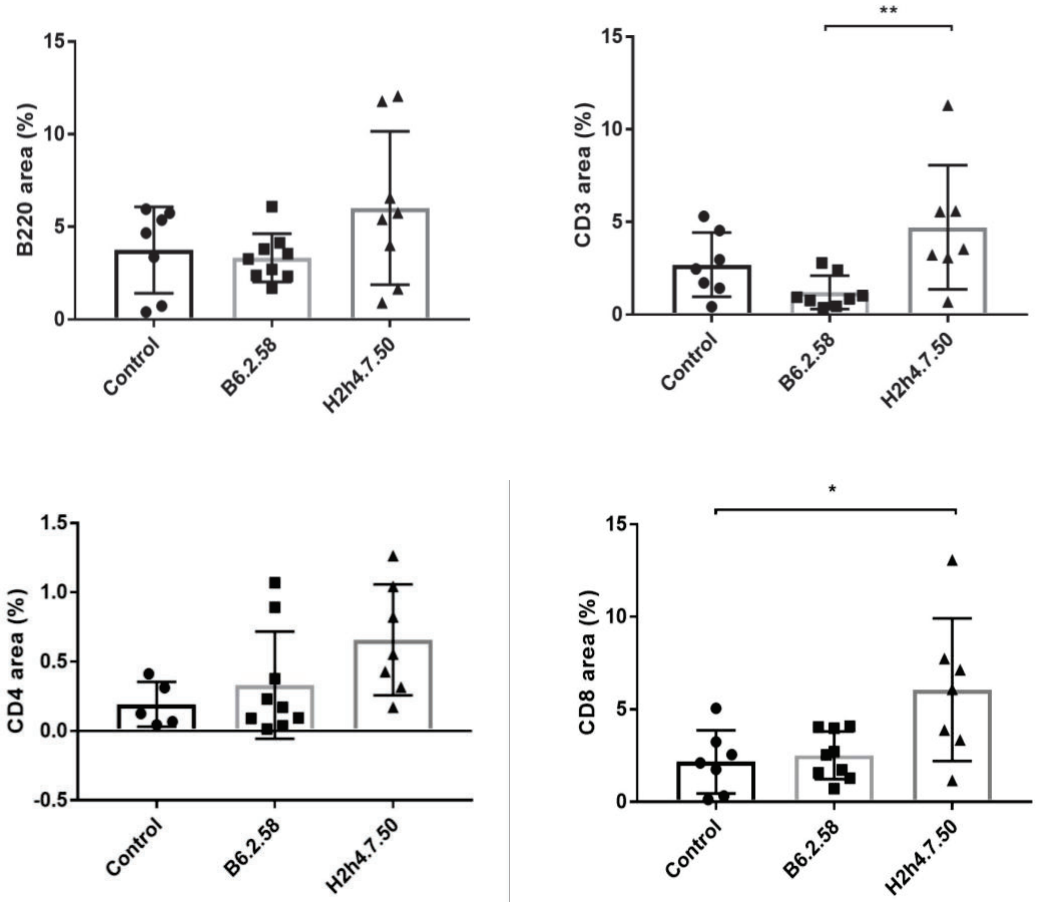

Figure 20. Infiltrating lymphocytic populations characterization by immunofluorescence assay. Positive area (%) for B220, CD3, CD4 and CD8 makers in mice salivary glands for control (N=7), B6.2.58 (N=9) and H2h4.7.50 (N=9) groups.

Besides, in order to determine the presence of GC-like structures in salivary glands, immunofluorescence images for B220-CD3, B220-CD4 and B220-CD8 were merged. It was observed that, although in all foci there were always different cell types (B and T cells), in each infiltrate one of the two cell types was predominant. Indeed, no organized structures were observed within these infiltrates, so it was determined that no ectopic GC-like structures existed in the salivary gland of either experimental group. Interestingly, it was also observed that CD8 cells were not only grouped in infiltrates, but these cells were also distributed over all the tissue section, mostly in the H2h4.7.50 group (**figure 21**).

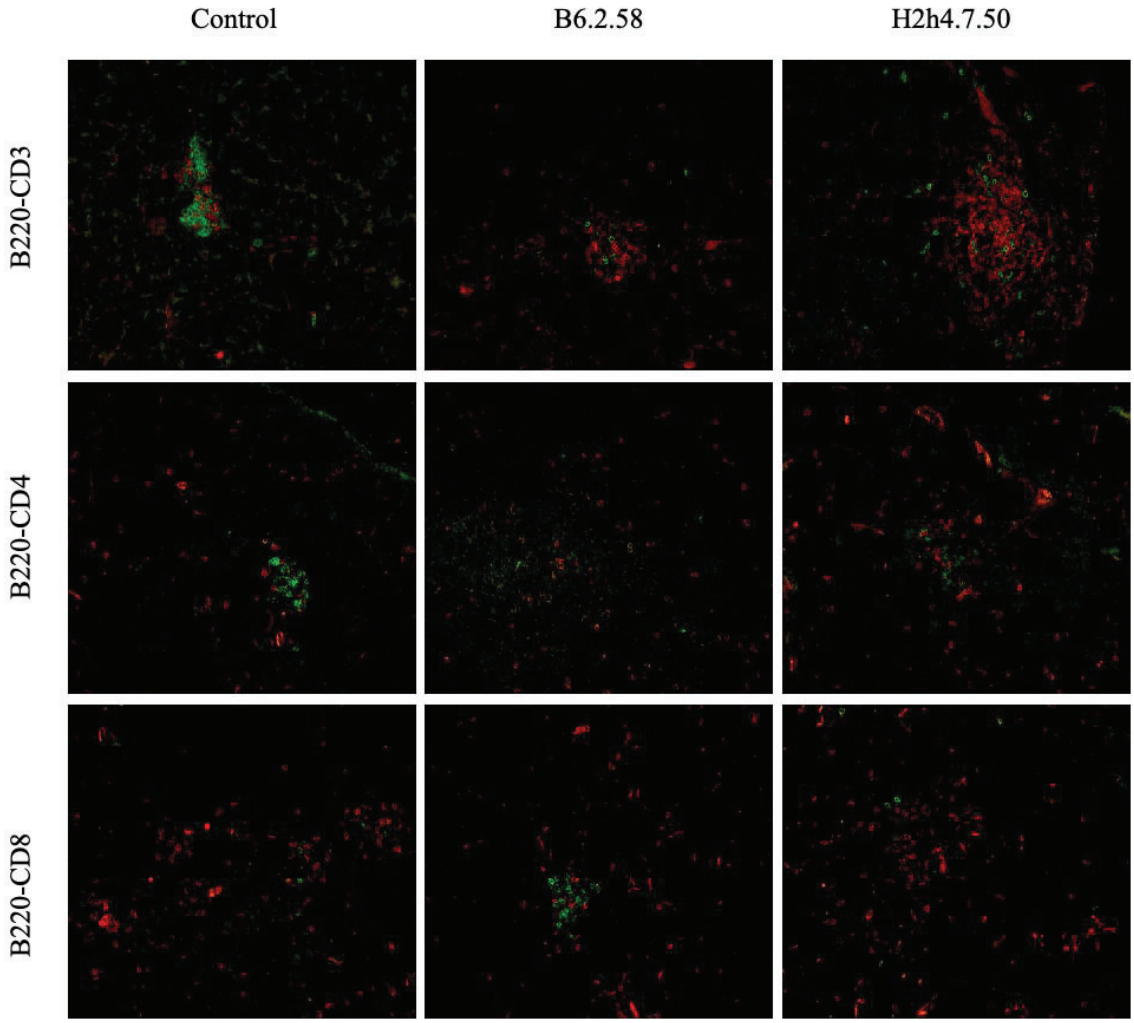

Figure 21. B220-CD3, B220-CD4 and B220-CD8 immunofluorescence assay in salivary gland. Representative merged images at 20X magnifications for control, B6.2.58 and H2h4.7.50 groups with B cells (B220) stained in green, and CD3, CD4 and CD8 T cells stained in red.

5.4. H2h4.7.50 induces Ro52 overexpression in salivary gland

Since Ro52 has been described to be overexpressed in patients' salivary glands, Ro52 staining was performed by IHC in mice salivary gland paraffin-embedded tissue. Results showed a significant increase for nuclear intensity mean in H2h4.7.50 group compared to both control and B6.2.58 groups (**figure 22**). Interestingly, this higher nuclear intensity mean was predominantly observed in the ductal epithelial cells' nuclei.

Thus, these data indicates that H2h4.7.50 polyreactive antibody induces a higher level of Ro52 expression in mice salivary gland.

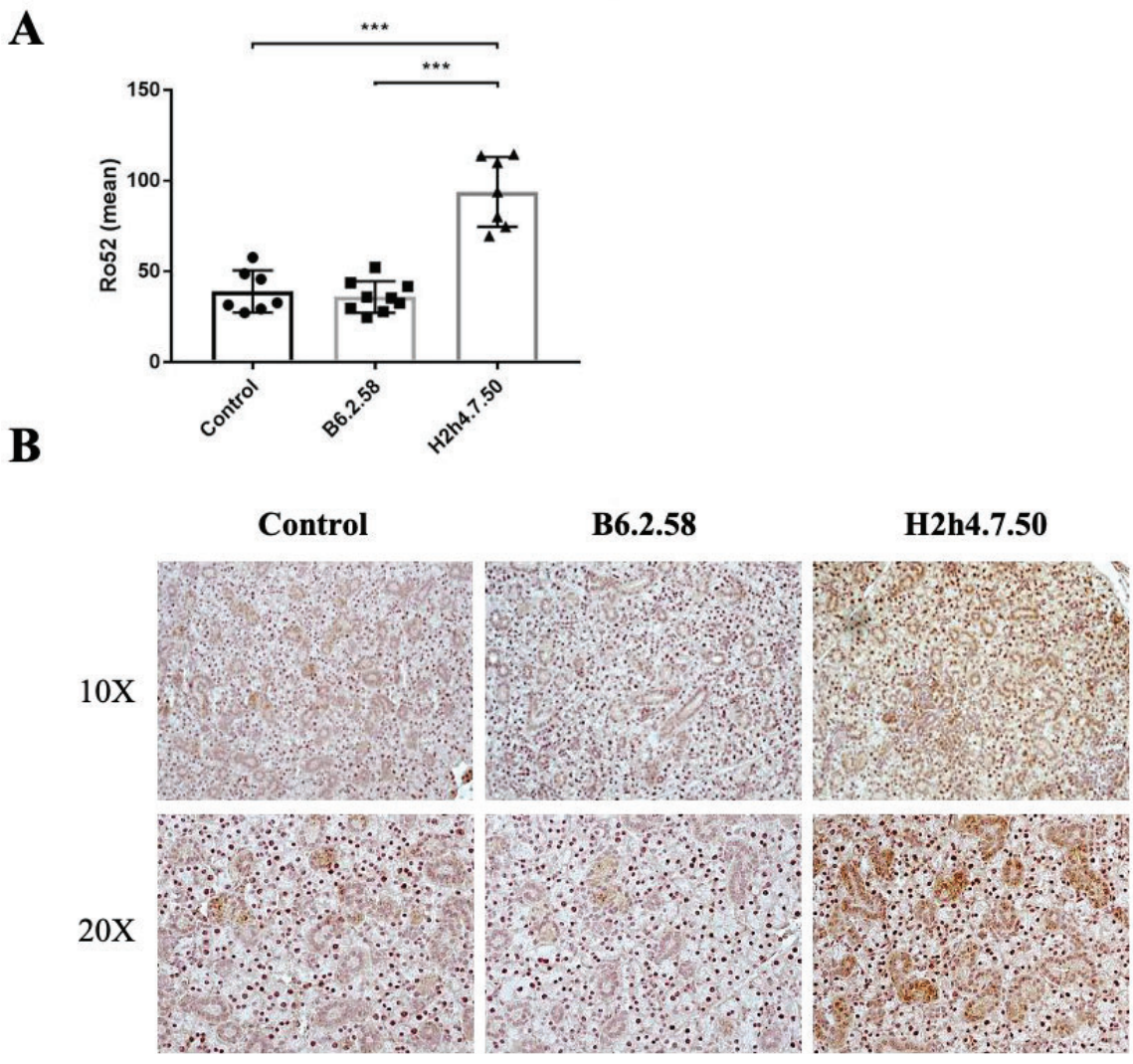

Figure 22. Ro52 staining by immunohistochemistry assay. (A) Ro52 nuclear intensity mean (y axis) for control (N=7), B6.2.58 (N=9) and H2h4.7.50 (N=9) groups. **(B)** Representative images (10X and 20X magnifications) for each group.

6. Lymphocytic population analysis by flow cytometry

In order to determine if polyreactive antibodies injection induced changes in lymphocytic populations in periphery, T and B cells were analyzed in spleen by flow cytometry. For T cells, CD3, T follicular helper (Tfh), CD4 and CD8 cells were measured. For B cells, MZ, follicular (FO), germinal center (GC), and B1 cells were analyzed. Besides, plasma cells (PC) were measured in bone marrow. All cell populations were graphed in percentages and absolute numbers.

Regarding T cells (**figure 23**), a significant increase was observed in the percentage of $CD3^+$ cells in H2h4.7.50 group compared to both control and B6.2.58, and to control group in terms of cell number. Besides, B6.2.58 group showed an increase of Tfh cells percentage compared to H2h4.7.50, while in terms of cells number, both B6.2.58 and H2h4.7.50 groups showed to be increased compared to control group. However, no differences between groups were observed for $CD4^+$ cells. Interestingly, the percentage of CD8 cells was increased in H2h4.7.50 group compared to B6.2.58, and the number of CD8 cells was increased compared to the control group.

With respect to B cells (**figure 24**), no differences between groups were found for B lymphocytes total number in spleen. A decrease in MZ B cells number was observed in H2h4.7.50 group compared to B6.2.58. No differences were found for FO B cells, while GC B cells number was decreased in H2h4.7.50 compared to B6.2.58 group. Besides, B1 cells were also decreased in H2h4.7.50 group compared to B6.2.58 group in both percentage and cells total number.

Finally, no differences for plasma cells were found between groups in the bone marrow (**figure 25**).

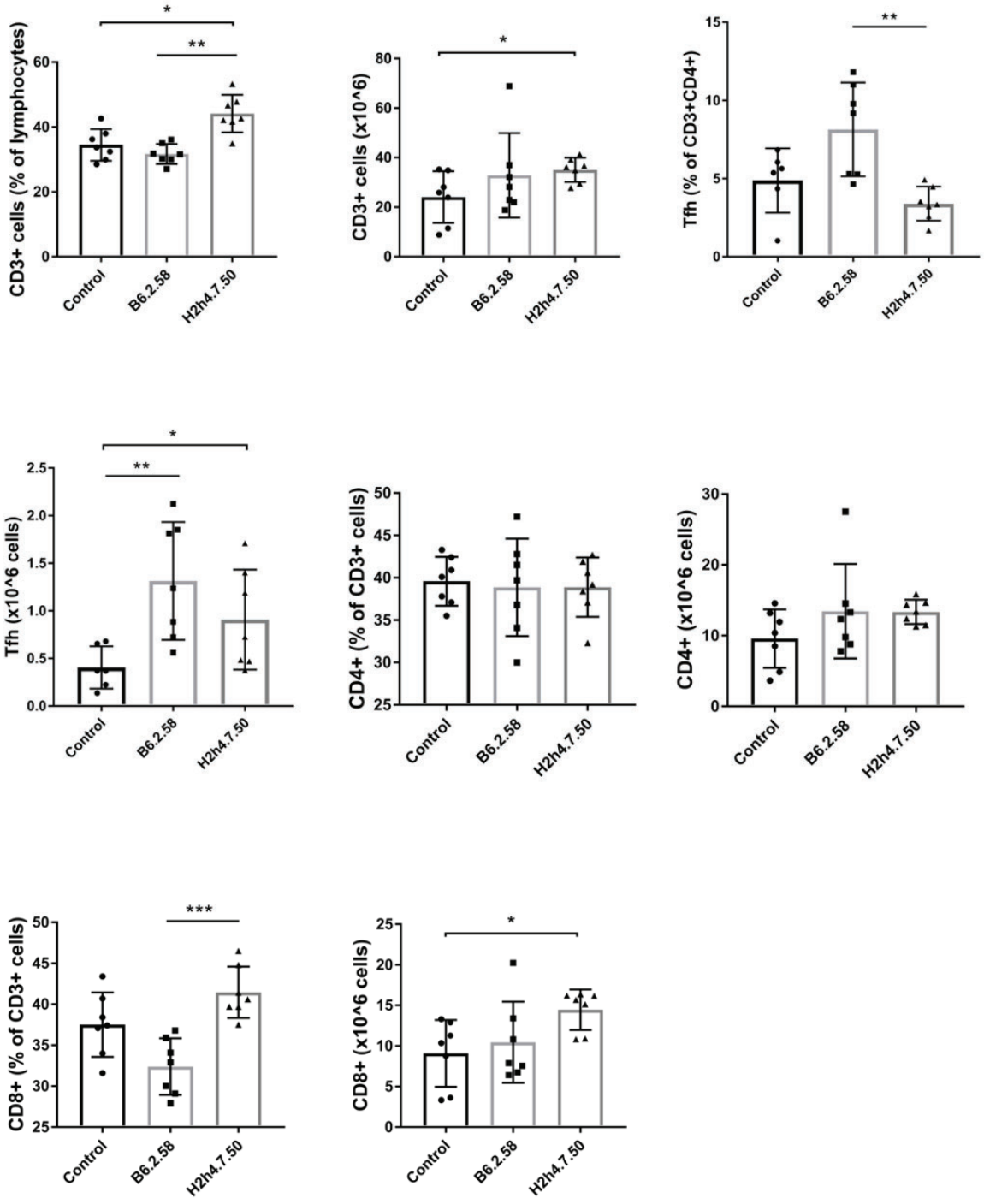

Figure 23. T cells population analysis by flow cytometry in spleen. CD3+ cells, Tfh cells, CD4+ and CD8+ cells percentages and total numbers in spleen for control (N=6), B6.2.58 (N=7) and H2h4.7.50 (N=7) groups.

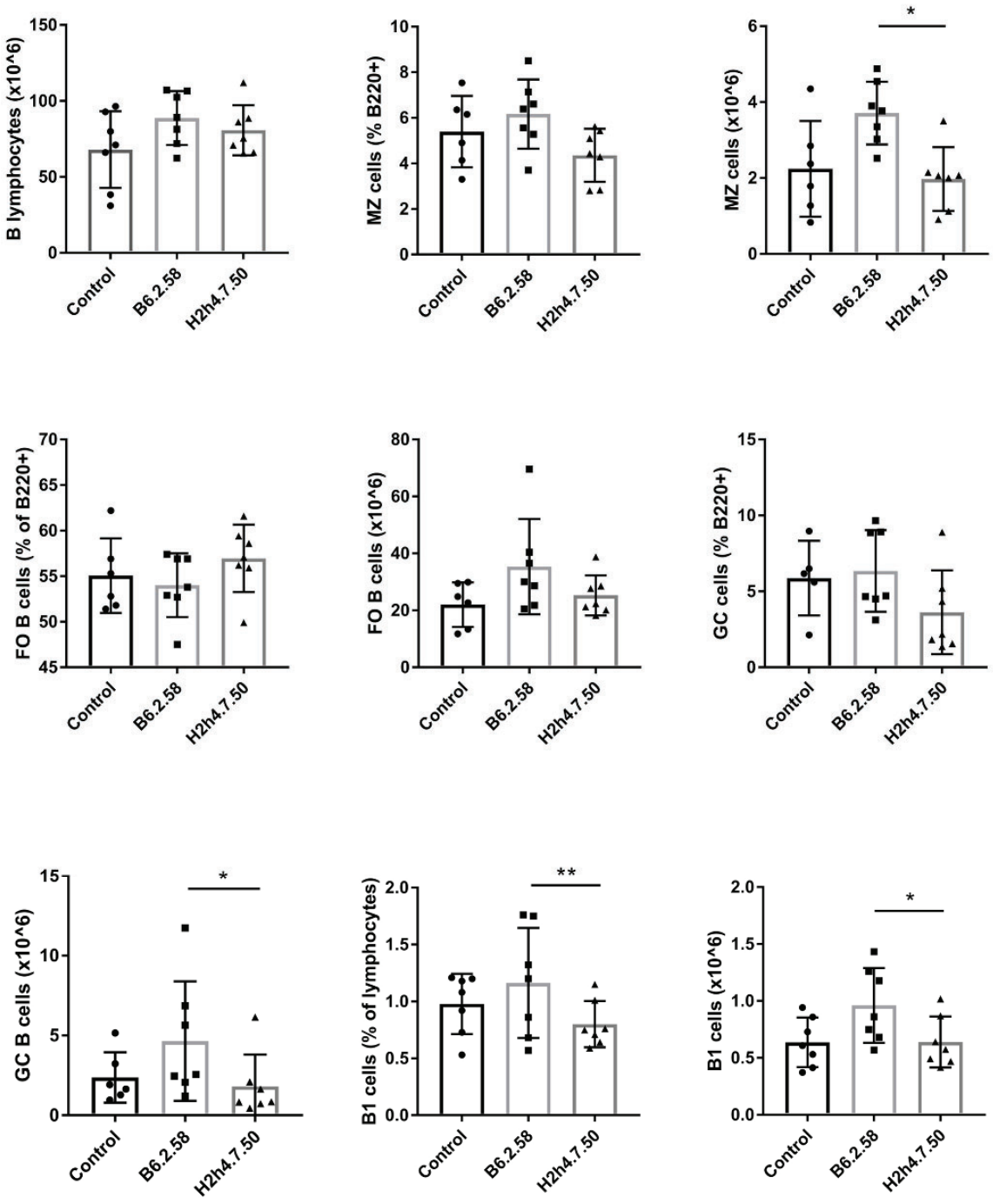

Figure 24. B cells population analysis by flow cytometry in spleen. B lymphocytes, MZ B cells, FO B cells, GC B cells and B1 cells percentages and total numbers in spleen for control (N=6), B6.2.58 (N=7) and H2h4.7.50 (N=7) groups.

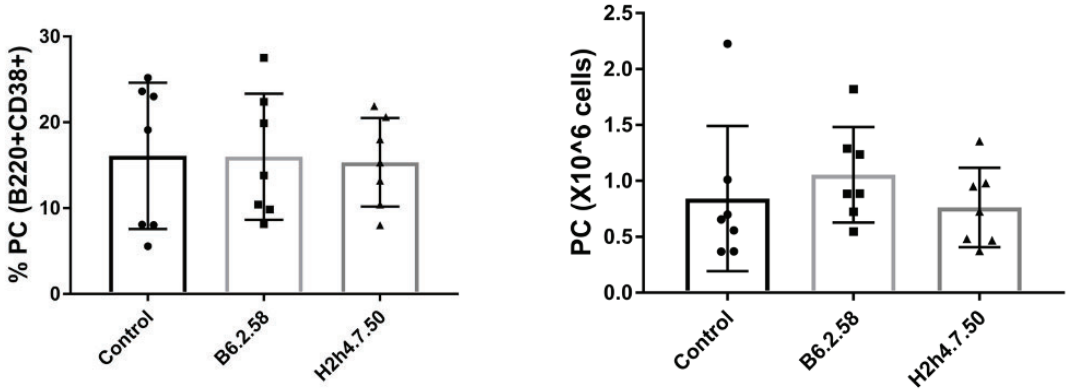

Figure 25. Plasma cells (PC) analysis by flow cytometry in bone marrow. Plasma cells (B220+ CD38+) percentage and total number for control (N=6), B6.2.58 (N=7) and H2h4.7.50 (N=7) groups.

7. Potential new autoantibodies showed to be polyreactive

In order to explore the presence of specific antibodies that could recognize novel autoantigens within the extensive B cell antibody repertoire analysis in NOD.H-2^{h4} SjS mouse model (Sáez et al., 2021), antibodies that were not polyreactive by the ELISA antigenic panel, and non-autoreactive by flow cytometry with L cells (mouse fibroblast cell line) were selected; examples of non-autoreactive and autoreactive antibodies by flow cytometry are shown in **figure 26**. After this screening, 26 antibodies were selected out of the total of 168 that were in the NOD.H-2^{h4} repertoire. The hybridomas producing these 26 monoclonal antibodies were cultured in order to obtain enriched supernatants, and these were tested by IHC against salivary gland, kidney, liver, and lung paraffin-embedded tissue from NSG mice. Tissues were obtained from the immunodeficient mouse strain due to the absence of IgG, so it was ensured that no endogenous IgG antibodies were detected by IHC.

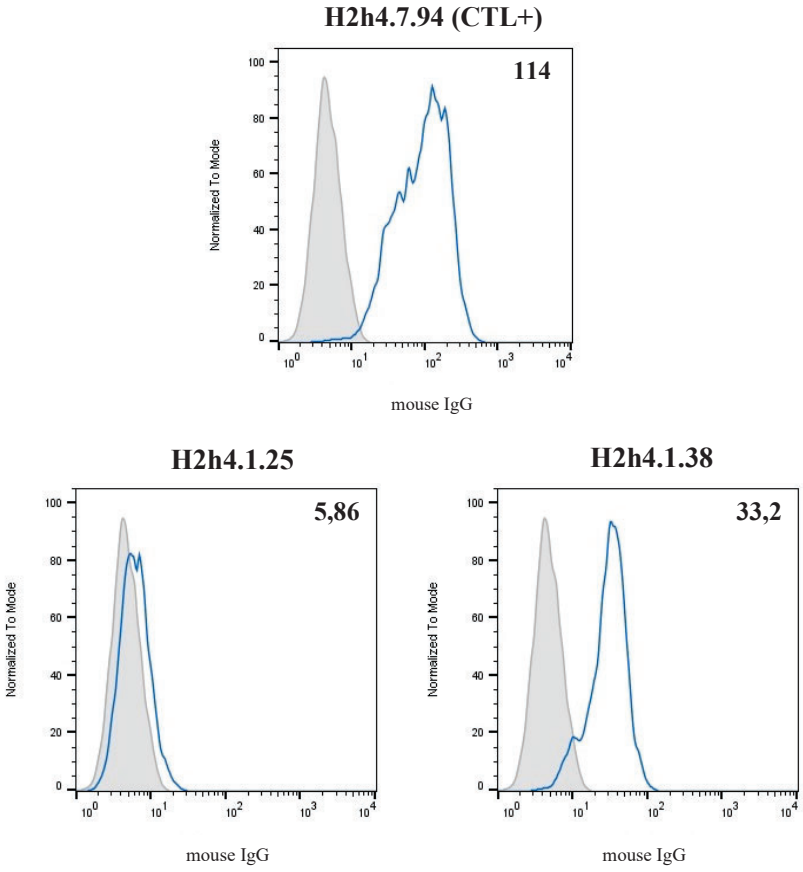

Figure 26. Autoreactivity analysis by flow cytometry with L cells. Antibodies within the B cell repertoire from NOD.H-2h4 were tested against L cells by flow cytometry in order to test their autoreactivity. The graphs show the positive control (upper histogram), an example of a non-autoreactive antibody, and on the right the histogram of an autoreactive antibody. In all three histograms the negative control is shown in light gray. Mean Fluorescence Intensity (MFI) for anti-mouse IgG is indicated in the upper right corner of each histogram.

Out of 26 antibodies, 7 IgGs were finally selected since they showed specific patterns against salivary gland tissue (**figure 27**). H2h4.2.3, H2h4.2.72, H2h4.2.341, H2h4.15.47 and H2h4.15.24.8 showed an intracellular staining pattern on the acinar epithelial cells. H2h4.1.42 antibody showed a homogenous cytoplasmic staining pattern over all the tissue section, and interestingly, H2h4.16.128 showed a nuclear pattern specific for ductal epithelial cells. Importantly, none of these antibodies showed to be reactive with the rest of tissues included in the screening (**figure 28**). Besides, the non-autoreactivity of the 7 selected antibodies, determined by flow cytometry using L cells, is shown in **figure 29**.

Next, in order to characterize antibodies' reactivity and specificity, supernatants were tested against salivary gland lysate from NSG mice by western blot. However, no specific band was identified for any of the selected antibodies, since they all showed numerous and smeared bands in the western blot membrane (**figure 30**). These results indicated that the selected antibodies might be polyreactive.

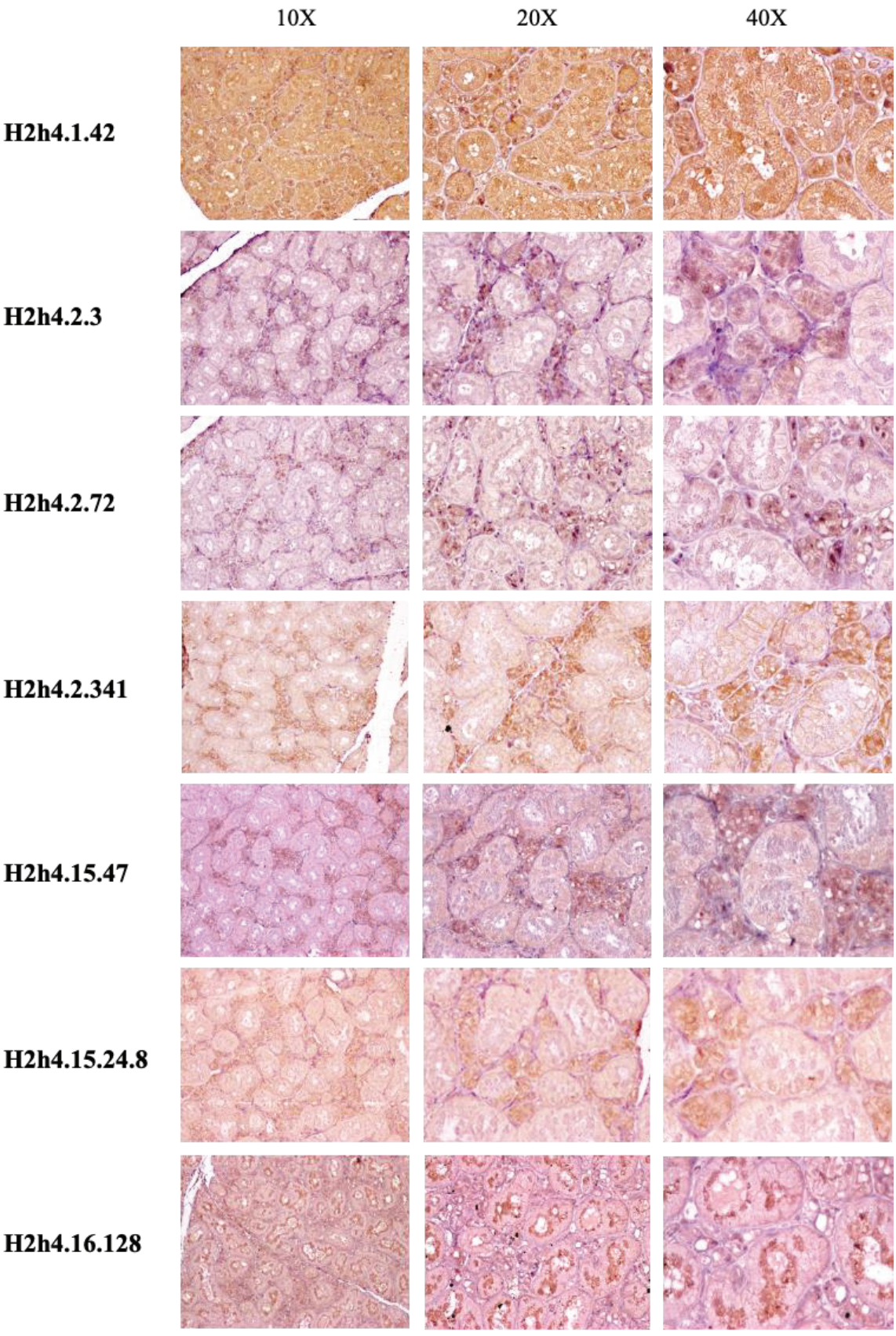

Figure 27. Immunohistochemistry images (10X, 20X and 40X magnifications) of salivary gland tissue sections stained with selected hybridomas supernatants and hematoxylin.

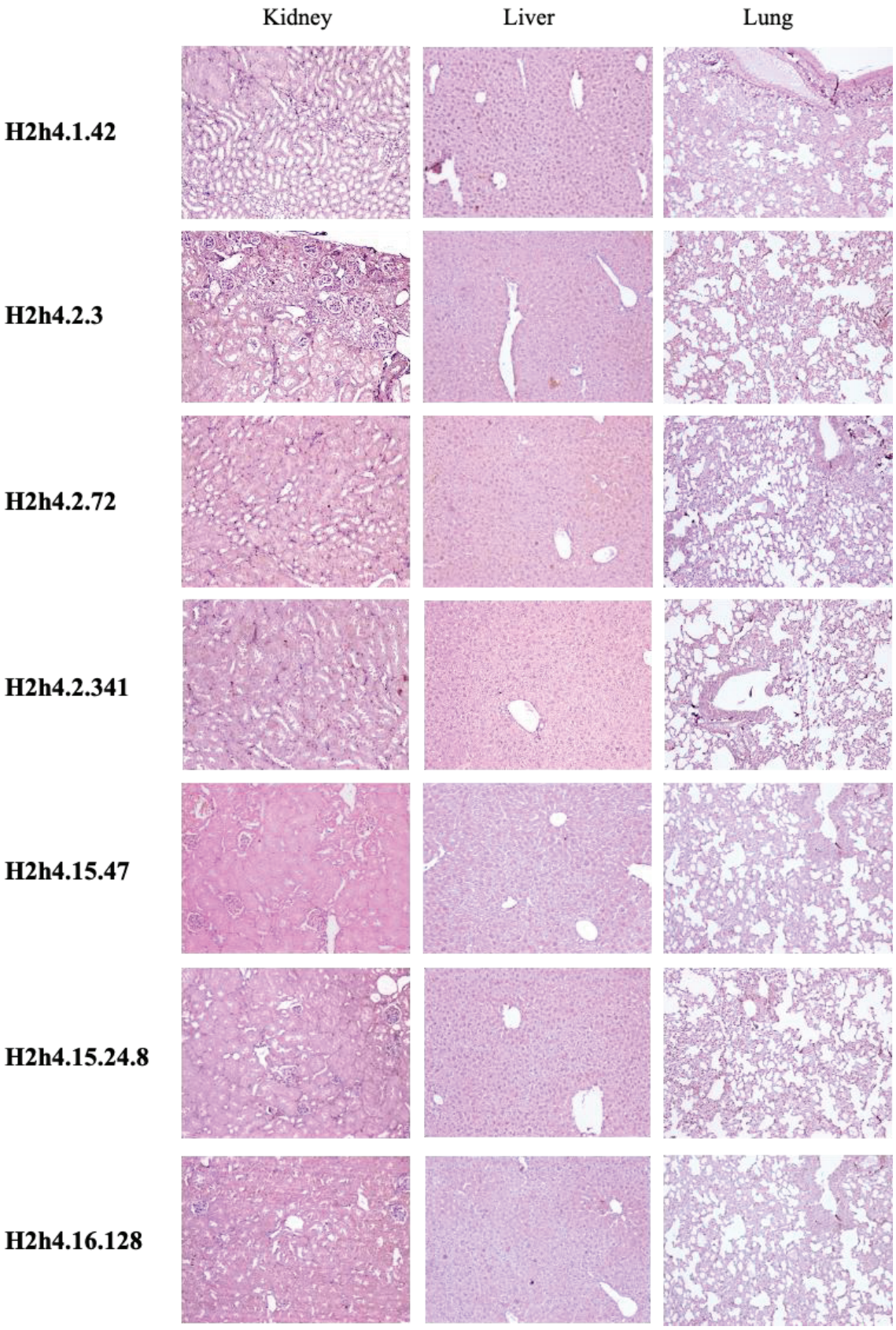

Figure 28. Immunohistochemistry images (10X magnifications) of kidney, liver and lung paraffin-embedded tissue sections stained with selected hybridomas supernatants and hematoxylin.

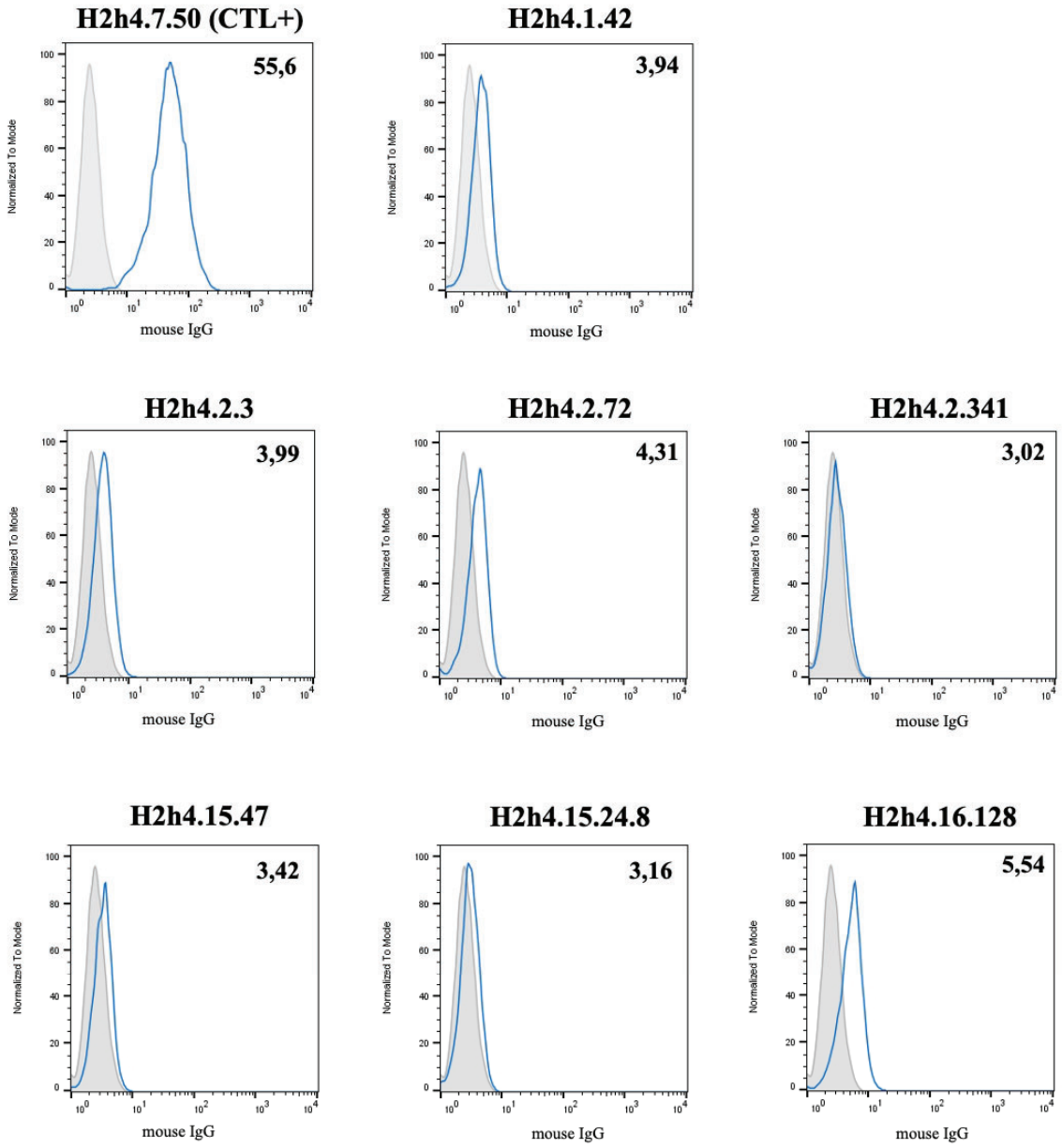

Figure 29. Non-autoreactivity confirmation of the 7 selected antibodies by flow cytometry using L cells. MFI for anti-mouse IgG is indicated in the upper right corner of each histogram.

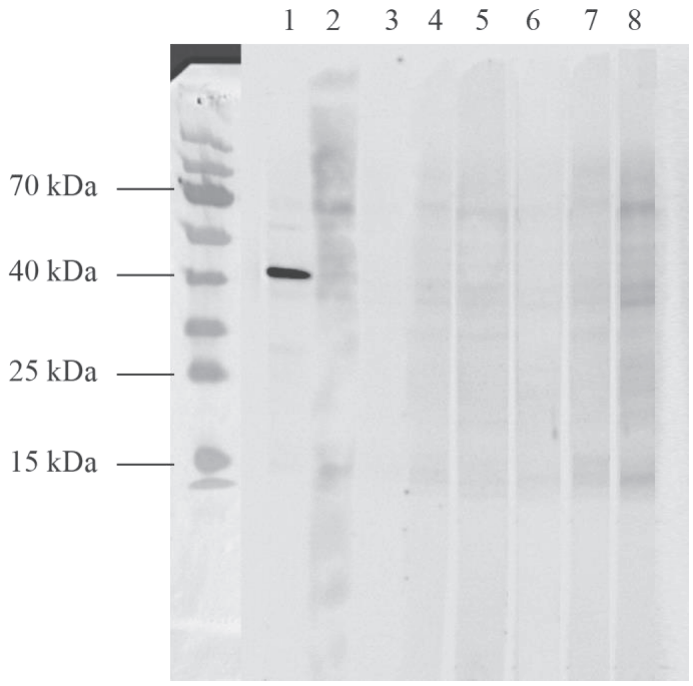

Figure 30. Western blot result. Anti-actin (1) antibody was used as positive control. H2h4.1.42 (2), H2h4.2.3 (3), H2h4.2.72 (4), H2h4.2.341 (5), H2h4.15.24.8 (6), H2h4.15.47 (7) and H2h4.16.128 (8) showed a smear effect in the membrane, with several bands against salivary gland lysate, indicating that these antibodies might be polyreactive.

In order to confirm and better characterize the polyreactivity pattern of the selected monoclonal antibodies, supernatants were tested in a specific microarray (GeneCopoeia^{TM}) used for autoantibodies profiling for systemic autoimmune diseases such as SLE and SjS. This array includes characteristic autoantigens such as Ro52, Ro60, La, Sm, and dsDNA among others. Importantly, B6.2.58, H2h4.7.50 and H2h4.7.94 antibodies were also included in the microarray analysis in order to deeper characterize their polyreactivity profile and thus better understand the role they might be playing *in vivo*.

As it was suspected from western blot results with the 7 selected IgGs, it was found that the selected antibodies were polyreactive (**figure 31**). H2h4.1.42 recognized with moderate affinity proteoglycan, Sn/RNP and ssRNA; H2h4.2.3 recognized with moderate affinity collagen I, fibrinogen IV and Ro52, while it recognized with high affinity sphingomyelin, cardiolipin and Nup 62 (nuclear pore glycoprotein p62); H2h4.2.72 recognized with moderate-high affinity collagen I, II, II, IV, V and VI, and other antigens such as β-actin, laminin and Nup 62; H2h4.2.341 recognized GM-CSF, mitochondrial antigen, ribo-phosphoprotein PO and PR3; H2h4.15.24.8 recognized collagen, CD8, core histone, β-actin, factor P, laminin, fibrinogen and neuropinin-1;

H2h4.15.47 bound collagen I, II, II, IV, V and VI, β-actin, TFG-β1 and Nup 62; H2h4.16.128 recognized CEN-P, proteoglycan, ssRNA and Sn/RNP. Among these antibodies, H2h4.2.3, H2h4.2.72, H2h4.15.24.8 and H2h4.15.47 showed the highest polyreactivity levels, while H2h4.1.42 and H2h4.2.341 showed lower levels of polyreactivity.

Interestingly, B6.2.58, H2h4.7.50 and H2.7.94 antibodies showed high levels of polyreactivity. These three antibodies recognized La and Ro60 with moderate affinity, and importantly they recognized Ro52 with higher affinity. These antibodies also recognized with high affinity β-actin, factor P, GDF-15, laminin, fibrinogen IV, TGF-β1, neuropilin-1, Scl-70, IFN-α1, IFN-r, IL-12, sphingomyelin, histone 4, nucleolin, IFN-λ2. Besides, B6.2.58 showed a high affinity against collagen IV, β2-microglobulin, IFN-ε, factor D, IFN-R, IL-15, β-actin and LPS. H2h4.7.50 showed a high affinity against collagen I and IV, Jo-1, ssDNA, core histone, dsDNA, cardiolipin, fibrinogen, histone 2, Scl100, Sm, mitochondrial antigen and ssRNA. Finally, H2h4.7.94 showed high affinity against IL-15, Mi-2 and also against ssDNA and dsDNA.

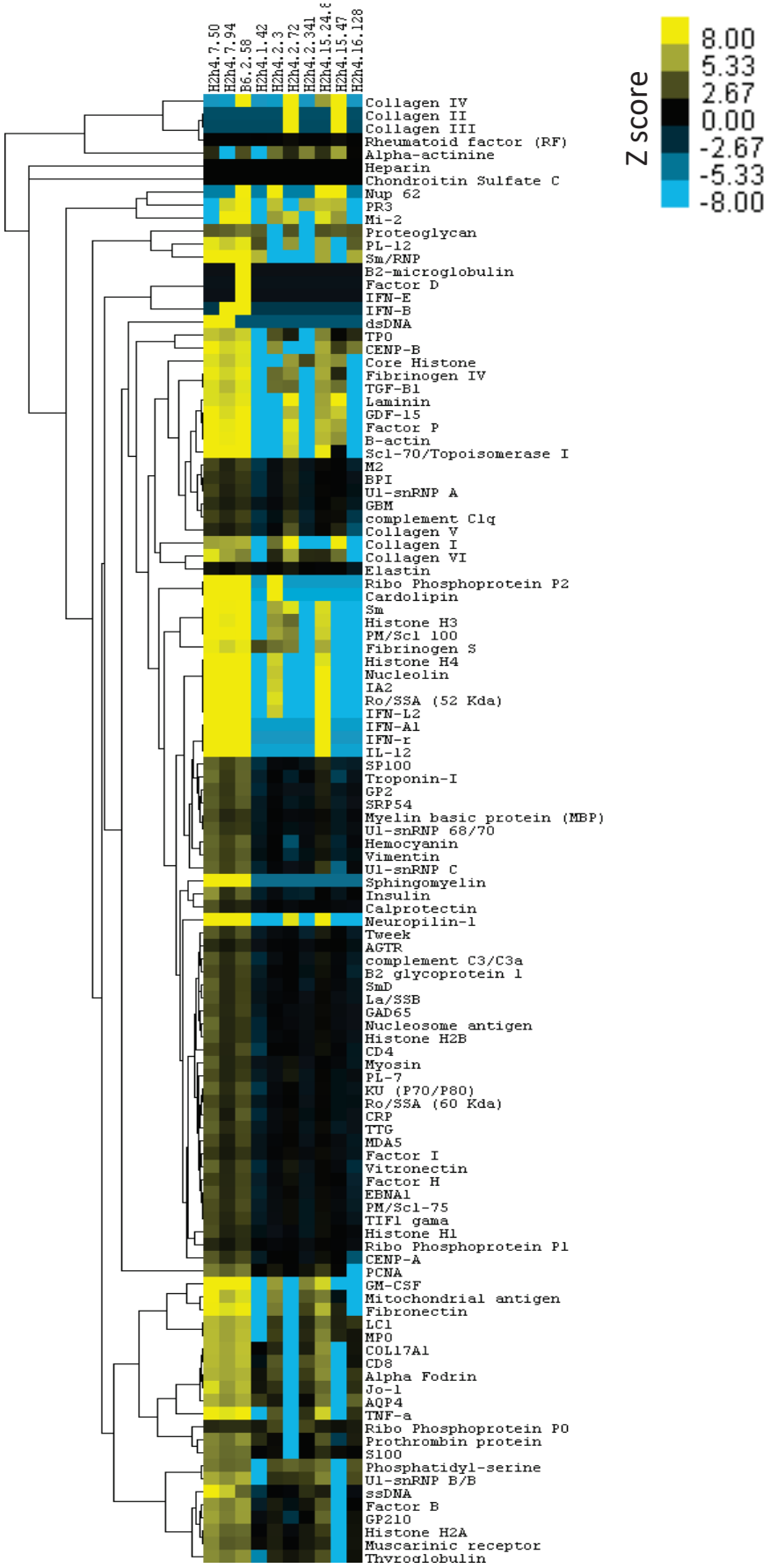

Figure 31. Heatmap graph: results from GeneCopoeia™ microarray. Yellow represents higher affinity and blue represents lower affinity for the antigen (Z score).

The antigen/s for which each antibody included in the array showed the highest affinity is shown in **table 3**.

Table 3. Table showing the preferential antigen/s for which antibody showed the highest affinity for on the GeneCopoeia™ microarray.

Antibody	Preferential antigen/s
H2h4.7.50	ssDNA
H2h4.7.94	ssDNA, Cardiolipin
B6.2.58	Cardiolipin, Insulin
H2h4.1.42	Sn/RNP
H2h4.2.3	Cardiolipin, Nup 62
H2h4.2.72	Collagen IV
H2h4.2.341	Sm, Mi-2
H2h4.15.24.8	Neurolipin, IFN-r
H2h4.15.47	Collagen IV
H2h4.16.128	Sn/RNP

VI. DISCUSSION

SjS is characterized by a complex immunological dysregulation that leads to B cells activation and the subsequent production of autoantibodies targeting a diverse array of self-antigens. This disruption of the immune tolerance mechanisms results in glandular dysfunction, systemic complications, and a diminished quality of life for affected individuals. In recent years, there has been an increasing awareness of the pivotal role played by B cells in the complexity of SjS pathogenesis. Dysregulated B cells emerge as crucial contributors to inflammation. They act as antigen-presenting cells, secrete pro-inflammatory cytokines, and, most notably, generate autoantibodies targeting a wide spectrum of autoantigens, including Ro52. Anti-Ro52 autoantibodies represent a hallmark of SjS and significantly contribute to its underlying immunopathology. Indeed, these anti-Ro52 antibodies have been found to be present before symptoms onset in both SjS patients. Moreover, since the accumulation of autoreactive naïve and memory B cells has been described in SjS patients, it is believed that there are sequential defects in both early and late immune tolerance mechanisms that lead to the accumulation of autoreactive B cells. (Aqrawi et al., 2014; Wright et al., 2021).

In our previous B cell repertoire analysis in the SjS mouse model NOD.H2h4, we observed that a significant part of autoantibodies corresponded to antibodies that recognized Ro52, and that these increased with mice age; strikingly, all of them showed to be polyreactive. This surprising results was consistent with the observation in humans, where it was described that anti-Ro52 antibodies from SjS patients presented high levels of polyreactivity (Glauzy et al., 2017). Indeed, B cells that recognize Ro52 have been detected within the lymphocytic infiltrated B cells in SjS patients' salivary glands (Szczerba et al., 2016). Interestingly, Corsiero et al. (2014) performed a single-cell sequencing study in order to determine autoreactivity and polyreactivity within the B cell peripheral repertoire in SjS patients. Beyond the increased levels of autoreactive naïve and memory B cells in the peripheral compartment, they proposed that the observed low number of polyreactive clones that recognized Ro52 in periphery might be due to their migration to the inflammation site, the salivary gland.

Consequently, unraveling the mechanisms responsible for the breakdown of B cell tolerance, elucidating the factors driving autoantibody production, and the potential pathogenic role of these frequent polyreactive autoantibodies that recognize Ro52 is essential to comprehend SjS pathogenesis.

Notably, upon the administration of H2h4.7.50 polyreactive antibody, we observed a significant increase in the levels of both anti-dsDNA and anti-Ro52 autoantibodies in MRL/lpr mice sera, while these results were not observed when B6.2.58 antibody was administered. These autoantibody levels can be considered as a measure of disease progression, so these results supported our hypothesis of the pathogenic role of anti-Ro52 polyreactive antibodies.

The pathogenicity of polyreactive antibodies that recognize dsDNA has been investigated in SLE. Anti-dsDNA antibodies are present in a high percentage of SjS patients, and they are also characteristic of other autoimmune diseases such as SLE. Although their pathogenicity is mostly related to their capacity to form ICs that induce inflammation and tissue damage, the link between their polyreactivity and their pathogenicity potential has been also investigated in SLE. It has been described that anti-dsDNA antibodies are able to cross-react with cardiolipin, phospholipids or other ribonucleoproteins such as Sm, suggesting that these antibodies are polyreactive (Ehlers et al., 2006). In fact, it was described that polyreactivity is a pathologic characteristic for lupus nephritis, since, whereas monospecific anti-dsDNA antibodies did not generate lupus nephritis, polyreactive anti-dsDNA antibodies did *in vivo*. Besides, these anti-dsDNA antibodies that showed to be polyreactive, also induced neurotoxicity and neuronal cell death compared to a control antibody when injected into C57BL/6 mice hippocampus, indicating the potential pathogenic role of these polyreactive antibodies in the development of neuropsychiatric manifestations in SLE patients when they penetrate the blood brain barrier. This neurotoxicity has been related to the cross-reaction of these anti-dsDNA antibodies with N-methyl-D-aspartate receptor (NMDAR), a receptor involved in neuronal cell death pathway (Madaio et al., 1987; Pankewycz et al., 1987; Zhang et al., 2009). These events in SLE due to polyreactive anti-dsDNA antibodies could be also relevant in SjS and be directly affecting exocrine glands.

With respect to anti-Ro52 autoantibodies, these are present in the majority of SjS patients, and they have been also found in other autoimmune diseases such as SLE and neonatal lupus syndrome (Harley & Scofield, 1991; Pourmand et al., 1999). Importantly, anti-Ro52 autoantibodies levels have been linked with a bad prognostic of disease progression (Lindop et al., 2012). Interestingly, neurological disorders have been also identified as a common extraglandular manifestation of SjS. Indeed,

intramedullary production of anti-Ro52 antibodies has been observed in SjS patients who present central nervous system (CNS) involvement. These patients showed to be positive for anti-Ro52 antibodies, but the majority were negative for anti-La autoantibodies in serum, and the majority showed cerebellar atrophy. Interestingly, the autopsy of one of these patients showed a selective loss of Purkinje cells in cerebellum, and high expression of Ro52 in these cells was also described. Therefore, it was proposed that anti-Ro52 antibodies were likely responsible for cerebellar degeneration in SjS patients. Thus, it has been proposed that the presence of anti-Ro52 autoantibodies in the cerebrospinal fluid (CSF) can be used as a biomarker for SjS-related CNS involvement (Mégevand et al., 2007; Tetsuka et al., 2021).

The pathogenicity of anti-Ro52 antibodies has been previously studied *in vivo* using mouse models. Szczerba et al. (2016) investigated the consequences of Ro52 immunization in NZM2758 mice, which do not spontaneously develop anti-Ro52 antibodies. However, they observed that innate immunity activation though the injection of an aluminum-containing adjuvant induced the development of a SjS-like disease. Therefore, they immunized these mice with recombinant Ro52 together with the adjuvant. They found that Ro52 immunization induced, beyond the consequent anti-Ro52 autoantibodies production, the deposition of these autoantibodies in mice salivary glands. Interestingly, they observed that this deposition was positively correlated with salivary gland dysfunction and poor saliva production. Moreover, they decided to perform passive transfer experiments with the anti-Ro52 positive sera of the previously immunized mice in non-immunized NZM2758 mice, but they didn't find any pathogenic consequence if innate immunity was not previously activated by adjuvant injection. Therefore, they also demonstrated the importance of innate immunity activation for the development of SjS disease. Notably, this corresponds with our model, since we needed to infect mice with MCMV before autoantibodies injection to induce an acuter model that allow us to evaluate the pathogenicity of these antibodies. Besides, in the case of CMV infection, it also drives the immune response to salivary glands. This innate immune responses activation induces pro-inflammatory cytokines production, that have been also reported in SjS patients, and indeed they have been related with the induction of Ro52 expression by ductal epithelial cells in salivary gland (Szczerba et al., 2016).

Importantly, this research group also studied the consequences of Ro52 immunization of NZM2758 mice in terms of salivary gland infiltration, IgG deposition and tear production. They observed that female mice positive for anti-Ro52 antibodies in sera had higher levels of IgG deposition in salivary gland tissue, and that the passive transfer of anti-Ro52 positive sera caused the reduction of tear production in these mice. Exocrine gland dysfunction investigation has been mostly focused on the study of autoantibodies targeting the cholinergic muscarinic receptor 3 (M3R), but these results indicate that anti-Ro52 autoantibodies could be also playing a role in exocrine gland dysfunction (Trzeciak et al., 2018). Therefore, this link between anti-Ro52 autoantibodies in exocrine gland dysfunction could be explain because of polyreactivity. Surprisingly, as will be discussed later, this link between anti-Ro52 antibodies and muscarinic receptors also coincides with the results of this project.

Regarding exocrine glands infiltration, we observed that H2h4.7.50 induced lymphocytic infiltration in salivary glands compared to control and B6.2.58 groups, whereas it didn't induce any histopathological effects on lacrimal glands neither extraglandular manifestations such as kidney tissue damage. Importantly, we observed increased levels of lymphocytic infiltration in salivary glands after H2h4.7.50 injection, mainly driven by $CD8^+$ T cells. Although in humans and various mouse models such as NOD.H-2^{h4} the major population driving exocrine glands infiltrations are T $CD4^+$ cells (Puñet-Ortiz et al., 2018; Yao et al., 2020), our results are also in consistence with other mouse models in which an increased frequency of $CD8^+$ T cells has been observed in submandibular salivary glands. Indeed, in Lgals1 KO mice, besides the increase in $CD8^+$ T cells, no differences for $B220^+$ B cells and $CD4^+$ T cells were found, in a manner consistent with our model (Martínez-Allo et al., 2020).

Interestingly, $CD8^+$ T cells infiltrating salivary glands have been shown to express high levels of IFN gamma, and it was demonstrated that the adoptive transfer of $CD8^+$ T cells with cytotoxic phenotype induced lacrimal gland inflammation in NOD-SCID mice. Besides, the specific depletion of these $CD8^+$ T cells abrogates SjS development and blocking IFN-γ production decreased T cells infiltration (Barr et al., 2017; Gao et al., 2019; Ríos-Ríos et al., 2020). Thus, our results together with those obtained using other mouse models support the crucial role of $CD8^+$ T cells in SjS pathogenesis. In fact, it has been demonstrated that these $CD8^+$ lymphocytes can alter tight junction integrity

and function in parotid epithelial cells though they cytotoxic function, leading to cell death and gland dysfunction damage (Matsumura et al., 2000; Baker et al., 2008).

Besides, although no differences were observed for B cells within MRL/lpr mice after anti-Ro52 polyreactive antibodies injection, it may be of interest to explore the presence and potential alteration in MZ B cells within MRL/lpr salivary glands, since MZ B cells have been described to infiltrate this target tissue, participating in the GC-like structures and the production of autoantibodies, including polyreactive antibodies. Importantly, previous research in our group evidenced that depleting MZ B cells using an anti-CD229 (Ly9) monoclonal antibody can ameliorate disease symptoms (Puñet-Ortiz et al., 2018). It is also important to note that we did not observe GC-like structures within mice salivary glands. Interestingly, these ectopic structures have been described in NOD.H-2^{h4} mouse model, but not in MRL/lpr mice (Van Blokland et al., 2000). Besides, to explore the lymphocytic populations that are infiltrating the salivary glands of MRL/lpr within our three experimental groups more deeply may be considered worthwhile, for instance including GC markers.

Furthermore, it has been also described that plasmacytoid dendritic cells (pDCs) play an important role when infiltrate the salivary glands, since they are considered professional produced of IFN-I cytokines, which induce monocytes to produce BAFF, leading to B cell differentiation to plasma cell, leading to autoreactive antibodies production, for instance against Ro52, and salivary gland tissue inflammation (Bodewes et al., 2021). Therefore, these cells could be crucial in the SjS pathogenesis, and it may be worth looking into their presence in MRL/lpr salivary glands by immunofluorescence assays.

Additionally, our research unveiled a notable increase in Ro52 expression within mice treated with the H2h4.7.50 antibody, but not in those receiving B6.2.58. This Ro52 overexpression was mainly observed in ductal epithelial cells within the salivary gland, and it highlights the potential significance of Ro52 in SjS immunopathology. Although anti-Ro52 autoantibodies are considered a hallmark of SjS, the extent of this autoantigen's expression within autoimmune target organs remains poorly understood. Importantly, Aqrawi et al. (2014) demonstrated that Ro52 expression is induced by pro-inflammatory stimuli, as a viral infection. In consistence with our results, they also showed that Ro52 was overexpressed in ductal epithelial cells, and that this overexpression was positively correlated with salivary gland inflammation in SjS

patients. They propose that a high expression of Ro52 might induce the breakage of tolerance and generation of Ro52 autoantibodies in genetically susceptible individuals, and that the up-regulation of Ro52 in ductal epithelium might trigger SjS disease progression. Interestingly, the over-expression of Ro52 has been associated with apoptosis induction and decreased cell proliferation, and this could explain the tissue degeneration and impairment of exocrine glands function.

Ro52, a multifunctional protein, assumes a pivotal role not only as an autoantigen but also as a regulator of immune responses, since it participates in a downregulation loop of type I interferon (IFN-I) signaling, a fundamental component of the innate immune response. Perturbations in this regulatory pathway may culminate in excessive innate immune activation, uncontrolled inflammation, and the potential induction of autoimmunity (Jones et al., 2021). Ro52 multifaceted role adds complexity to our understanding of how intracellular molecules like Ro52 can orchestrate intricate autoantibody responses. Besides, this IFN-I signaling cascade and innate immune response can also be induced by infections, such as viral infections by CMV, that in our model is the trigger to inflammation in salivary glands.

How Ro52 can be driving the autoimmune response if it is an intracellular molecule has been a subject of debate for years. However, the fact that it can be also being expressed in the membrane of SGECs, apoptotic cells or even to be found in exosomes, help to elucidate how these anti-Ro52 autoantibodies can be generated in individuals with genetic predisposition in which a tolerance breakdown has occur. Interestingly, it has been proposed that exosomes containing Ro52 could be taken by DCs, that have been described to be accumulated in salivary glands of SjS patients, and therefore these cells would be continuously presenting Ro52 peptides to autoreactive T cells infiltrating the salivary gland, inducing inflammation, and perpetuating disease progression, salivary gland infiltration and autoantibodies production (Bodewes et al., 2019).

Besides, the expression of Ro52 has been also evaluated in biopsies from cutaneous lupus erythematosus (CLE), normal skin biopsies from healthy donors, or in lesions induced experimentally by artificial sources of UV-radiation (UVR). They found that Ro52 was upregulated in CLE lesions, while in non-affected skin, both from donors and patients, Ro52 was not overexpressed. This Ro52 overexpression was observed in keratinocytes and dermal cell infiltrates, and they could also induce this Ro52

upregulation in keratinocytes by UVR in vitro (Oke et al., 2009). Therefore, Ro52 is overexpressed not only in salivary gland tissue of SjS patients, but also in skin lesions of CLE patients, and it can be induced by environmental factors that induce pro-inflammatory signals, such as UVR or viral infections.

On the other hand, alterations in lymphocytic population percentages and absolute counts in spleen were observed by flow cytometry analysis. Regarding T cell compartment, we observed an increased in $CD3^+$ and specifically in $CD8^+$ T cells in H2h4.7.50 group compared to control and B6.2.58. Importantly, this results corresponds to the observed effects in salivary gland infiltration, where we observed an increase in $CD8^+$ T cells infiltrating the target organ. Besides, it is important to note that this higher number of $CD8^+$ T cells has been also reported in SjS patients compared to healthy controls. However, in SjS patients it has been reported a decrease in peripheral $CD4^+$ cells, while we didn't observe any alteration for this subpopulation after anti-Ro52 polyreactive antibodies injection (Barcelos et al., 2023). Besides, we also observed and increase absolute counts for T follicular helper cells (Tfh) in mice that received B6.2.58 and H2h4.7.50 antibodies compared to control. This increase pf Tfh cells has been described in SjS patients, and it has been positively correlated with autoantibody levels. Interestingly, Tfh cells can promote B cells maturation and differentiation into plasma cells which can produce anti-Ro52 and anti-La autoantibodies, thus participating in disease pathogenesis. These cells have been also described to be involved in GC-like structures formation though IL-21 production (Barcelos et al., 2021; Wei and Niu, 2023). In fact, it has been demonstrated that the deficiency of Tfh cells attenuates autoantibody production and disease progression in an *in vivo* model of experimental SjS (Xiao et al., 2018).

Regarding B cells, no alterations were observed for the levels of total B cells between groups, and the same result was observed for SjS patients compared to healthy controls (Barcelos et al., 2021). Surprisingly, H2h4.7.50 group showed lower levels of MZ B cells, GC B cells and B1 cells compared to B6.2.58, but no differences were found compared to control. With respect to MZ B cells and B1 cells, both responsible for autoantibody production, including polyreactive antibodies, does not correspond to autoantibody levels of this group, since autoantibody levels were higher in H2h4.7.50 compared to both control and B6.2.58 groups. Besides, no differences were observed

between groups regarding plasma cells in the bone marrow, which could be attributed to the need for a more extended treatment to observe such alterations.

Additionally, when we analyzed the antibodies reactivity against several systemic autoimmune diseases characteristic antigens using the microarray, we observed that H2h4.7.50 and H2h4.94, and B6.2.58, showed reactivity against autoimmune systemic diseases characteristic antigens such as Sm or cardiolipin. Importantly, the microarray showed that these antibodies recognize Ro52, Ro60 and La, the three most characteristic autoantigens in SjS. However, polyreactive antibodies showed to have higher affinity against Ro52 than for Ro60 and La.

As it was mentioned before, anti-dsDNA autoantibodies in SLE have been shown to cause lupus nephritis and to be cross-reactive with cardiolipin. Cardiolipin is a hallmark of antiphospholipid syndrome (APS), characterized by thrombosis and recurrent miscarriages. This finding raises questions about potential shared epitopes or pathways between Sjögren's syndrome and SLE. Furthermore, the heightened reactivity of antibodies against Sm antigens is noteworthy. The Sm antigen complex is a well-characterized target in SLE. This finding emphasizes the intricate and interconnected nature of autoimmune responses.

On the other hand, H2h4.7.50 and H2h4.7.94 also showed to be reactive against muscarinic receptors. These receptors play a crucial role in regulating salivary gland secretion, and their dysfunction can lead to impaired saliva production and tear, a hallmark of Sjögren's syndrome. The reactivity of these antibodies against muscarinic receptors suggests a potential direct link between autoantibodies and the disruption of exocrine glands function, and it could explain the tear production suppression when anti-Ro52 positive serum was passively transferred in NZM2758 mice (Trzeciak et al., 2018). In order to evaluate the effect of these antibodies in salivary gland dysfunction, further experiments would be needed, and the analysis of salivary gland production should be performed in MRL/lpr infected mice during or after treatment with the anti-Ro52 polyreactive antibodies. Further investigation into the functional consequences of this reactivity is warranted, as it may provide insights into the pathogenesis of dry mouth in Sjögren's syndrome.

Moreover, we also found that these antibodies showed to be reactive against IFN-I related cytokines such as IFN-α, so they could be participating in IFN-I signaling cascade and inducing alterations in this pathway, what in addition to their reactivity against Ro52, could be altering the pathway upstream and downstream. It has been demonstrated the importance of type-I IFN signaling and Ro52 in SjS pathogenesis, so these autoantibodies could contribute to disease progression altering this pathway at different levels, altering the functions of Ro52, IFN receptors, or related cytokines (Bodewes et al., 2019).

In summary, the reactivity patterns of these antibodies against a diverse array of antigens provide insights into the multifaceted nature of autoimmune responses in Sjögren's syndrome. These findings open possibilities for further exploration and may ultimately contribute to better understand SjS pathogenesis. Besides, the other 7 IgG antibodies that were included in the microarray, which were first thought to be potentially monospecific, also showed to be polyreactive. This result was consistent with the result we obtained from the previous B cell repertoire in NOD.H-2^{h4} mice, in which a high proportion of autoantibodies corresponded to polyreactive antibodies (Sáez et al., 2021).

Regarding H2h4.7.94, we anticipated promising outcomes due to its heightened relative affinity for antigens resulting from its mutations. However, it displayed a short half-life, which led to its exclusion from the *in vivo* assay. One possible future approach could be prolonging H2h4.7.94 half-life through Fc modifications. Indeed, in the context of HIV infection therapy, substantial efforts are underway to optimize the half-life and pharmacokinetics of bNAbs, with the aim of utilizing them in passive transfer-based therapies featuring these engineered polyreactive antibodies (Kwon et al., 2021; Kwon et al., 2023). The potential therapeutic utility of polyreactive antibodies is also under consideration in the context of various infections, including bacterial and fungal infections. In fact, studies have demonstrated the efficacy of Igs preparations with enhanced polyreactivity (Djoumerska-Alexieva et al., 2015) as well as the administration of the H2h4.7.50 polyreactive antibody (Català et al., 2022) in conferring robust protection against septic shock in *in vivo* experimental sepsis models. Therefore, enhancing the pharmacokinetics of these polyreactive antibodies could hold significant promise for the development of therapeutic interventions against diverse types of infections.

In the context of Fc modifications, we also contemplate whether the observed differences between B6.2.58 and H2h4.7.50 antibodies can be attributed to their respective origins, non-autoimmune and autoimmune strains, or simply to their distinct isotypes, IgG3 and IgG2b, respectively. To address these uncertainties, an ongoing approach of this research project involves the generation of a recombinant antibody for B6.2.58 with an IgG2b subclass. Subsequently, both *in vivo* assays and subsequent analyses will be replicated. Antibody isotypes play a pivotal role in modulating the biological functions of antibodies. They significantly influence antibody interactions with immune cells, effector functions, and pro- or anti-inflammatory properties. IgG2 antibodies, characterized by their robust complement activation and effector functions, stand in stark contrast to IgG3 antibodies, which often exhibit a more subdued effector profile, tending towards regulatory or anti-inflammatory roles. Therefore, this approach aims to conclusively establish whether the pathogenic or non-pathogenic attributes of the anti-Ro52 polyreactive antibodies are indeed contingent upon the autoimmune background of the antibodies.

Therefore, polyreactive antibodies recognizing Ro52 appear to play a pathogenic role in both the initiation and perpetuation of the disease. H2h4.7.50 antibody injection has induced the emergence of characteristic SjS-related symptoms and manifestations, including elevated serum autoantibodies, infiltration of the salivary gland primarily by CD8 cells, and an increase in peripheral CD8 cells. Furthermore, it is noteworthy to emphasize the upregulation of Ro52 expression, especially within the ductal epithelial cells of the salivary gland, mirroring patterns observed in patients. All of these findings collectively support our hypothesis regarding the pathogenic role of anti-Ro52 antibodies in Sjögren's syndrome. This underscores the importance of prior activation of innate immunity, in our case through CMV infection, which directs the immune response to the salivary gland. This, together with anti-Ro52 IgG2b antibody injection, leads to Ro52 overexpression, increased salivary gland infiltration and heightened autoantibody production. Thus, it is evident that this is a multifaceted process with various contributing factors.

VII. CONCLUSIONS

1. MRL/lpr infection with sublethal dose of murine cytomegalovirus induces Sjögren's syndrome-related autoantibodies increase in mouse sera, as well as salivary gland leukocyte infiltration, indicating that a useful Sjögren's syndrome mouse model was established.
2. H2h4.7.50 polyreactive antibody induces a significant increase of anti-dsDNA and anti-Ro52 autoantibodies levels in mouse sera compared to control and B6.2.58 groups.
3. H2h4.7.50 polyreactive antibody induces salivary gland infiltration, increasing infiltrates number compared to control and B6.2.58 groups.
4. H2h4.7.50 treated mice showed a significantly higher percentage of CD45 positive area within the salivary gland, indicating increased levels of lymphocytic infiltration.
5. H2h4.7.50 group showed significantly higher CD3 positive area in salivary gland tissue. Specifically, H2h4.7.50 induces higher infiltration by CD8 cells compared to control and B6.2.58 groups.
6. IgG2 polyreactive antibody against Ro52 induces pathogenic phenomena in genetically susceptible mice, indicating a role of these antibodies in the pathogenesis of SjS disease.
7. H2h4.7.50 treated mice showed significantly higher number of CD3, CD8 and T follicular helper T cells in spleen when analyzed by flow cytometry.
8. All the IgG antibodies that were selected due to their specific patterns to salivary gland tissue by immunohistochemistry showed to be highly polyreactive in the antigenic microarray.
9. The observed pathogenic effects of anti-Ro52 autoantibodies indicate a role of these polyreactive antibodies in the pathogenesis of SjS.

IX. REFERENCES

Abughanam G, Maria OM, Tran SD. Studying Sjögren's syndrome in mice: What is the best available model? J Oral Biol Craniofac Res. 2021 Apr-Jun;11(2):245-255.

Ambrosi A, Dzikaite V, Park J, Strandberg L, Kuchroo VK, Herlenius E, Wahren-Herlenius M. Anti-Ro52 monoclonal antibodies specific for amino acid 200-239, but not other Ro52 epitopes, induce congenital heart block in a rat model. Ann Rheum Dis. 2012 Mar;71(3):448-54.

An Q, Zhao J, Zhu X, Yang B, Wu Z, Su Y, Zhang L, Xu K, Ma D. Exploiting the role of T cells in the pathogenesis of Sjögren's syndrome for therapeutic treatment. Front Immunol. 2022 Oct 28;13:995895.

Aqrawi LA, Kvarnström M, Brokstad KA, Jonsson R, Skarstein K, Wahren-Herlenius M. Ductal epithelial expression of Ro52 correlates with inflammation in salivary glands of patients with primary Sjögren's syndrome. Clin Exp Immunol. 2014 Jul;177(1):244-52.

Aqrawi LA, Kvarnström M, Brokstad KA, Jonsson R, Skarstein K, Wahren-Herlenius M. Ductal epithelial expression of Ro52 correlates with inflammation in salivary glands of patients with primary Sjögren's syndrome. Clin Exp Immunol. 2014 Jul;177(1):244-52.

Aqrawi LA, Kvarnström M, Brokstad KA, Jonsson R, Skarstein K, Wahren-Herlenius M. Ductal epithelial expression of Ro52 correlates with inflammation in salivary glands of patients with primary Sjögren's syndrome. Clin Exp Immunol. 2014 Jul;177(1):244-52.

Arstila TP, Jarva H. Human APECED; a Sick Thymus Syndrome? Front Immunol. 2013 Oct 7;4:313.

Avrameas S, Alexopoulos H, Moutsopoulos HM. Natural Autoantibodies: An Undersugn Hero of the Immune System and Autoimmune Disorders-A Point of View. Front Immunol. 2018 Jun 12;9:1320.

Avrameas S, Selmi C. Natural autoantibodies in the physiology and pathophysiology of the immune system. J Autoimmun. 2013 Mar;41:46-9.

References

Avrameas S, Ternynck T, Tsonis IA, Lymberi P. Naturally occurring B-cell autoreactivity: a critical overview. J Autoimmun. 2007 Dec;29(4):213-8.

Avrameas S. Autopolyreactivity Confers a Holistic Role in the Immune System. Scand J Immunol. 2016 Apr;83(4):227-34.

Baker OJ, Camden JM, Redman RS, Jones JE, Seye CI, Erb L, Weisman GA. Proinflammatory cytokines tumor necrosis factor-alpha and interferon-gamma alter tight junction structure and function in the rat parotid gland Par-C10 cell line. Am J Physiol Cell Physiol. 2008 Nov;295(5):C1191-201.

Barcelos F, Brás-Geraldes C, Martins C, Papoila AL, Monteiro R, Cardigos J, Madeira N, Alves N, Vaz-Patto J, Cunha-Branco J, Borrego LM. Added value of lymphocyte subpopulations in the classification of Sjögren's syndrome. Sci Rep. 2023 Apr 27;13(1):6872.

Barcelos F, Brás-Geraldes C, Martins C, Papoila AL, Monteiro R, Cardigos J, Madeira N, Alves N, Vaz-Patto J, Cunha-Branco J, Borrego LM. Added value of lymphocyte subpopulations in the classification of Sjögren's syndrome. Sci Rep. 2023 Apr 27;13(1):6872.

Barr JY, Wang X, Meyerholz DK, Lieberman SM. CD8 T cells contribute to lacrimal gland pathology in the nonobese diabetic mouse model of Sjögren syndrome. Immunol Cell Biol. 2017 Sep;95(8):684-694.

Barr JY, Wang X, Meyerholz DK, Lieberman SM. CD8 T cells contribute to lacrimal gland pathology in the nonobese diabetic mouse model of Sjögren syndrome. Immunol Cell Biol. 2017 Sep;95(8):684-694.

Baxter AG, Hodgkin PD. Activation rules: the two-signal theories of immune activation. Nat Rev Immunol. 2002 Jun;2(6):439-46.

Besnard M, Padonou F, Provin N, Giraud M, Guillonneau C. AIRE deficiency, from preclinical models to human APECED disease. Dis Model Mech. 2021 Feb 5;14(2):dmm046359.

Blinova VG, Vasilyev VI, Rodionova EB, Zhdanov DD. The Role of Regulatory T Cells in the Onset and Progression of Primary Sjögren's Syndrome. Cells. 2023 May 10;12(10):1359.

Bodewes ILA, Björk A, Versnel MA, Wahren-Herlenius M. Innate immunity and interferons in the pathogenesis of Sjögren's syndrome. Rheumatology (Oxford). 2021 Jun 18;60(6):2561-2573.

Bogdanos DP, Smyk DS, Rigopoulou EI, Mytilinaiou MG, Heneghan MA, Selmi C, Gershwin ME. Twin studies in autoimmune disease: genetics, gender and environment. J Autoimmun. 2012 May;38(2-3):J156-69.

Bona CA. Postulates defining pathogenic autoantibodies and T cells. Autoimmunity. 1991;10(3):169-72

Bonasia CG, Abdulahad WH, Rutgers A, Heeringa P, Bos NA. B Cell Activation and Escape of Tolerance Checkpoints: Recent Insights from Studying Autoreactive B Cells. Cells. 2021 May 13;10(5):1190.

Borodina E, Katz I, Antonelli A, Gzgzyan AM, Dzhemlikhanova LK, Ostrinski Y, Niauri D, Khizroeva J, Bitsadze V, Makatsariya A, Tincani A, Nalli C, Churilov LP, Shovman O, Halpert G, Blank M, Shoenfeld Y, Amital H. The pathogenic role of circulating Hashimoto's Thyroiditis-derived TPO-positive IgG on fetal loss in naïve mice. Am J Reprod Immunol. 2021 Jan;85(1):e13331.

Bossuyt X, De Langhe E, Borghi MO, Meroni PL. Understanding and interpreting antinuclear antibody tests in systemic rheumatic diseases. Nat Rev Rheumatol. 2020 Dec;16(12):715-726.

Boughter CT, Borowska MT, Guthmiller JJ, Bendelac A, Wilson PC, Roux B, Adams EJ. Biochemical patterns of antibody polyreactivity revealed through a bioinformatics-based analysis of CDR loops. Elife. 2020 Nov 10;9:e61393.

Braley-Mullen H, Yu S. NOD.H-2h4 mice: an important and underutilized animal model of autoimmune thyroiditis and Sjogren's syndrome. Adv Immunol. 2015;126:1-43.

References

Brink R, Phan TG. Self-Reactive B Cells in the Germinal Center Reaction. Annu Rev Immunol. 2018 Apr 26;36:339-357.

Brink R, Phan TG. Self-Reactive B Cells in the Germinal Center Reaction. Annu Rev Immunol. 2018 Apr 26;36:339-357.

Brito-Zerón P, Baldini C, Bootsma H, Bowman SJ, Jonsson R, Mariette X, Sivils K, Theander E, Tzioufas A, Ramos-Casals M. Sjögren syndrome. Nat Rev Dis Primers. 2016 Jul 7;2:16047.

Brito-Zerón P, Baldini C, Bootsma H, Bowman SJ, Jonsson R, Mariette X, Sivils K, Theander E, Tzioufas A, Ramos-Casals M. Sjögren syndrome. Nat Rev Dis Primers. 2016 Jul 7;2:16047.

Brown CC, Rudensky AY. Spatiotemporal regulation of peripheral T cell tolerance. Science. 2023 May 5;380(6644):472-478.

Brown GJ, Cañete PF, Wang H, Medhavy A, Bones J, Roco JA, He Y, Qin Y, Cappello J, Ellyard JI, Bassett K, Shen Q, Burgio G, Zhang Y, Turnbull C, Meng X, Wu P, Cho E, Miosge LA, Andrews TD, Field MA, Tvorogov D, Lopez AF, Babon JJ, López CA, Gónzalez-Murillo Á, Garulo DC, Pascual V, Levy T, Mallack EJ, Calame DG, Lotze T, Lupski JR, Ding H, Ullah TR, Walters GD, Koina ME, Cook MC, Shen N, de Lucas Collantes C, Corry B, Gantier MP, Athanasopoulos V, Vinuesa CG. TLR7 gain-of-function genetic variation causes human lupus. Nature. 2022 May;605(7909):349-356.

Caddy SL, Vaysburd M, Papa G, Wing M, O'Connell K, Stoycheva D, Foss S, Terje Andersen J, Oxenius A, James LC. Viral nucleoprotein antibodies activate TRIM21 and induce T cell immunity. EMBO J. 2021 Mar 1;40(5):e106228.

Català C, Velasco-de Andrés M, Leyton-Pereira A, Casadó-Llombart S, Sáez Moya M, Gutiérrez-Cózar R, García-Luna J, Consuegra-Fernández M, Isamat M, Aranda F, Martínez-Florensa M, Engel P, Mourglia-Ettlin G, Lozano F. CD6 deficiency impairs early immune response to bacterial sepsis. iScience. 2022 Sep 5;25(10):105078.

Chaplin DD. Overview of the immune response. J Allergy Clin Immunol. 2010 Feb;125(2 Suppl 2):S3-23.

Corsiero E, Sutcliffe N, Pitzalis C, Bombardieri M. Accumulation of self-reactive naïve and memory B cell reveals sequential defects in B cell tolerance checkpoints in Sjögren's syndrome. PLoS One. 2014 Dec 23;9(12):e114575.

D'Ippolito S, Ticconi C, Tersigni C, Garofalo S, Martino C, Lanzone A, Scambia G, Di Simone N. The pathogenic role of autoantibodies in recurrent pregnancy loss. Am J Reprod Immunol. 2020 Jan;83(1):e13200.

Daridon C, Pers JO, Devauchelle V, Martins-Carvalho C, Hutin P, Pennec YL, Saraux A, Youinou P. Identification of transitional type II B cells in the salivary glands of patients with Sjögren's syndrome. Arthritis Rheum. 2006 Jul;54(7):2280-8.

David T, Ling SF, Barton A. Genetics of immune-mediated inflammatory diseases. Clin Exp Immunol. 2018 Jul;193(1):3-12.

Demaria L, Henry J, Seror R, Frenzel L, Hermine O, Mariette X, Nocturne G. Rituximab-Bendamustine (R-Benda) in MALT lymphoma complicating primary Sjögren syndrome (pSS). Br J Haematol. 2019 Feb;184(3):472-475.

Dendrou CA, Petersen J, Rossjohn J, Fugger L. HLA variation and disease. Nat Rev Immunol. 2018 May;18(5):325-339.

Dimitrov JD, Planchais C, Roumenina LT, Vassilev TL, Kaveri SV, Lacroix-Desmazes S. Antibody polyreactivity in health and disease: statu variabilis. J Immunol. 2013 Aug 1;191(3):993-9.

Dimitrov JD. Harnessing the Therapeutic Potential of 'Rogue' Antibodies. Trends Pharmacol Sci. 2020 Jun;41(6):409-417.

Djoumerska-Alexieva I, Roumenina L, Pashov A, Dimitrov J, Hadzhieva M, Lindig S, Voynova E, Dimitrova P, Ivanovska N, Bockmeyer C, Stefanova Z, Fitting C, Bläss M, Claus R, von Gunten S, Kaveri S, Cavaillon JM, Bauer M, Vassilev T. Intravenous Immunoglobulin with Enhanced Polyspecificity Improves Survival in Experimental Sepsis and Aseptic Systemic Inflammatory Response Syndromes. Mol Med. 2016 Apr;21(1):1002-1010.

References

Doria-Rose NA, Landais E. Coevolution of HIV-1 and broadly neutralizing antibodies. Curr Opin HIV AIDS. 2019 Jul;14(4):286-293.

Du W, Han M, Zhu X, Xiao F, Huang E, Che N, Tang X, Zou H, Jiang Q, Lu L. The Multiple Roles of B Cells in the Pathogenesis of Sjögren's Syndrome. Front Immunol. 2021 Jun 8;12:684999.

ElTanbouly MA, Noelle RJ. Rethinking peripheral T cell tolerance: checkpoints across a T cell's journey. Nat Rev Immunol. 2021 Apr;21(4):257-267.

English J, Patrick S, Stewart LD. The potential role of molecular mimicry by the anaerobic microbiota in the aetiology of autoimmune disease. Anaerobe. 2023 Apr;80:102721.

Espinosa A, Zhou W, Ek M, Hedlund M, Brauner S, Popovic K, Horvath L, Wallerskog T, Oukka M, Nyberg F, Kuchroo VK, Wahren-Herlenius M. The Sjogren's syndrome-associated autoantigen Ro52 is an E3 ligase that regulates proliferation and cell death. J Immunol. 2006 May 15;176(10):6277-85.

Fasano S, Mauro D, Macaluso F, Xiao F, Zhao Y, Lu L, Guggino G, Ciccia F. Pathogenesis of primary Sjögren's syndrome beyond B lymphocytes. Clin Exp Rheumatol. 2020 Jul-Aug;38 Suppl 126(4):315-323. Epub 2020 Oct 23.

Finney J, Kelsoe G. Poly- and autoreactivity of HIV-1 bNAbs: implications for vaccine design. Retrovirology. 2018 Jul 28;15(1):53.

Fleck M, Kern ER, Zhou T, Lang B, Mountz JD. Murine cytomegalovirus induces a Sjögren's syndrome-like disease in C57Bl/6-lpr/lpr mice. Arthritis Rheum. 1998 Dec;41(12):2175-84.

Fox RI, Fox CM, Gottenberg JE, Dörner T. Treatment of Sjögren's syndrome: current therapy and future directions. Rheumatology (Oxford). 2021 May 14;60(5):2066-2074.

Fröhlich E, Wahl R. Thyroid Autoimmunity: Role of Anti-thyroid Antibodies in Thyroid and Extra-Thyroidal Diseases. Front Immunol. 2017 May 9;8:521.

Gandolfo S, De Vita S. Emerging drugs for primary Sjögren's syndrome. Expert Opin Emerg Drugs. 2019 Jun;24(2):121-132.

Gao CY, Yao Y, Li L, Yang SH, Chu H, Tsuneyama K, Li XM, Gershwin ME, Lian ZX. Tissue-Resident Memory CD8+ T Cells Acting as Mediators of Salivary Gland Damage in a Murine Model of Sjögren's Syndrome. Arthritis Rheumatol. 2019 Jan;71(1):121-132.

Gao CY, Yao Y, Li L, Yang SH, Chu H, Tsuneyama K, Li XM, Gershwin ME, Lian ZX. Tissue-Resident Memory CD8+ T Cells Acting as Mediators of Salivary Gland Damage in a Murine Model of Sjögren's Syndrome. Arthritis Rheumatol. 2019 Jan;71(1):121-132.

Gao Y, Chen Y, Zhang Z, Yu X, Zheng J. Recent Advances in Mouse Models of Sjögren's Syndrome. Front Immunol. 2020 Jun 30;11:1158.

Getahun A. Role of inhibitory signaling in peripheral B cell tolerance. Immunol Rev. 2022 May;307(1):27-42.

Glauzy S, Sng J, Bannock JM, Gottenberg JE, Korganow AS, Cacoub P, Saadoun D, Meffre E. Defective Early B Cell Tolerance Checkpoints in Sjögren's Syndrome Patients. Arthritis Rheumatol. 2017 Nov;69(11):2203-2208.

Goodnow CC, Sprent J, Fazekas de St Groth B, Vinuesa CG. Cellular and genetic mechanisms of self tolerance and autoimmunity. Nature. 2005 Jun 2;435(7042):590-7.

Goules AV, Tzioufas AG. Lymphomagenesis in Sjögren's syndrome: Predictive biomarkers towards precision medicine. Autoimmun Rev. 2019 Feb;18(2):137-143.

Gregersen PK, Behrens TW. Genetics of autoimmune diseases--disorders of immune homeostasis. Nat Rev Genet. 2006 Dec;7(12):917-28.

Griffith TS, Ferguson TA. Cell death in the maintenance and abrogation of tolerance: the five Ws of dying cells. Immunity. 2011 Oct 28;35(4):456-66.

Groom J, Kalled SL, Cutler AH, Olson C, Woodcock SA, Schneider P, Tschopp J, Cachero TG, Batten M, Wheway J, Mauri D, Cavill D, Gordon TP, Mackay CR, Mackay F. Association of BAFF/BLyS overexpression and altered B cell differentiation

with Sjögren's syndrome. J Clin Invest. 2002 Jan;109(1):59-68. doi: 10.1172/JCI14121. PMID: 11781351; PMCID: PMC150825.

Gryka-Marton M, Szukiewicz D, Teliga-Czajkowska J, Olesinska M. An Overview of Neonatal Lupus with Anti-Ro Characteristics. Int J Mol Sci. 2021 Aug 27;22(17):9281.

Halverson R, Torres RM, Pelanda R. Receptor editing is the main mechanism of B cell tolerance toward membrane antigens. Nat Immunol. 2004 Jun;5(6):645-50.

Harroud A, Hafler DA. Common genetic factors among autoimmune diseases. Science. 2023 May 5;380(6644):485-490.

Herzog S, Jumaa H. Self-recognition and clonal selection: autoreactivity drives the generation of B cells. Curr Opin Immunol. 2012 Apr;24(2):166-72.

Hillen MR, Urso K, Koppe E, Lopes AP, Blokland SLM, Pandit A, Slocombe T, van Maurik A, van Roon JAG, Radstake TRDJ. Autoantigen *TRIM21*/Ro52 is expressed on the surface of antigen-presenting cells and its enhanced expression in Sjögren's syndrome is associated with B cell hyperactivity and type I interferon activity. RMD Open. 2020 Jun;6(2):e001184.

Holodick NE, Rodríguez-Zhurbenko N, Hernández AM. Defining Natural Antibodies. Front Immunol. 2017 Jul 26;8:872.

Imgenberg-Kreuz J, Rasmussen A, Sivils K, Nordmark G. Genetics and epigenetics in primary Sjögren's syndrome. Rheumatology (Oxford). 2021 May 14;60(5):2085-2098.

Jones EL, Laidlaw SM, Dustin LB. TRIM21/Ro52 - Roles in Innate Immunity and Autoimmune Disease. Front Immunol. 2021 Sep 6;12:738473.

Kapsogeorgou EK, Tzioufas AG. Interaction of Human Salivary Gland Epithelial Cells with B Lymphocytes: Implications in the Pathogenesis of Sjögren's Syndrome. Mediterr J Rheumatol. 2020 Dec 28;31(4):424-426.

Karnell JL, Mahmoud TI, Herbst R, Ettinger R. Discerning the kinetics of autoimmune manifestations in a model of Sjögren's syndrome. Mol Immunol. 2014 Dec;62(2):277-82.

Kashiwakura J, Okayama Y, Furue M, Kabashima K, Shimada S, Ra C, Siraganian RP, Kawakami Y, Kawakami T. Most Highly Cytokinergic IgEs Have Polyreactivity to Autoantigens. Allergy Asthma Immunol Res. 2012 Nov;4(6):332-40.

Klein F, Diskin R, Scheid JF, Gaebler C, Mouquet H, Georgiev IS, Pancera M, Zhou T, Incesu RB, Fu BZ, Gnanapragasam PN, Oliveira TY, Seaman MS, Kwong PD, Bjorkman PJ, Nussenzweig MC. Somatic mutations of the immunoglobulin framework are generally required for broad and potent HIV-1 neutralization. Cell. 2013 Mar 28;153(1):126-38.

Köhler F, Hug E, Eschbach C, Meixlsperger S, Hobeika E, Kofer J, Wardemann H, Jumaa H. Autoreactive B cell receptors mimic autonomous pre-B cell receptor signaling and induce proliferation of early B cells. Immunity. 2008 Dec 19;29(6):912-21.

Krammer PH. CD95's deadly mission in the immune system. Nature. 2000 Oct 12;407(6805):789-95.

Kwon YD, Asokan M, Gorman J, Zhang B, Liu Q, Louder MK, Lin BC, McKee K, Pegu A, Verardi R, Yang ES, Program VP, Carlton K, Doria-Rose NA, Lusso P, Mascola JR, Kwong PD. A matrix of structure-based designs yields improved VRC01-class antibodies for HIV-1 therapy and prevention. MAbs. 2021 Jan-Dec;13(1):1946918.

Kwon YD, Pegu A, Yang ES, Zhang B, Bender MF, Asokan M, Liu Q, McKee K, Lin BC, Liu T, Louder MK, Rawi R, Reveiz M, Schaub AJ, Shen CH, Doria-Rose NA, Lusso P, Mascola JR, Kwong PD. Improved pharmacokinetics of HIV-neutralizing VRC01-class antibodies achieved by reduction of net positive charge on variable domain. MAbs. 2023 Jan-Dec;15(1):2223350.

Kyriakidis NC, Kapsogeorgou EK, Tzioufas AG. A comprehensive review of autoantibodies in primary Sjögren's syndrome: clinical phenotypes and regulatory mechanisms. J Autoimmun. 2014 Jun;51:67-74.

Kyriakidis NC, Kapsogeorgou EK, Tzioufas AG. A comprehensive review of autoantibodies in primary Sjögren's syndrome: clinical phenotypes and regulatory mechanisms. J Autoimmun. 2014 Jun;51:67-74.

References

Lee AYS. A review of the role and clinical utility of anti-Ro52/TRIM21 in systemic autoimmunity. Rheumatol Int. 2017 Aug;37(8):1323-1333.

Li B, Wang F, Schall N, Muller S. Rescue of autophagy and lysosome defects in salivary glands of MRL/lpr mice by a therapeutic phosphopeptide. J Autoimmun. 2018 Jun;90:132-145.

Li H, Zhou Y, Wang P, Wang Y, Feng Y, Zhang Y, Wu Z. Alterations of $CD8^+$ T cells in the blood and salivary glands of patients with primary Sjögren's syndrome. Clin Rheumatol. 2023 May;42(5):1327-1338.

Lima CM, Santos S, Dourado A, Carvalho NB, Bittencourt V, Lessa MM, Siqueira I, Carvalho EM. Association of Sicca Syndrome with Proviral Load and Proinflammatory Cytokines in HTLV-1 Infection. J Immunol Res. 2016;2016:8402059.

Liu Z, Chu A. Sjögren's Syndrome and Viral Infections. Rheumatol Ther. 2021 Sep;8(3):1051-1059.

Liu Z, Chu A. Sjögren's Syndrome and Viral Infections. Rheumatol Ther. 2021 Sep;8(3):1051-1059.

Lleo A, Invernizzi P, Gao B, Podda M, Gershwin ME. Definition of human autoimmunity--autoantibodies versus autoimmune disease. Autoimmun Rev. 2010 Mar;9(5):A259-66.

Lobo PI. Role of Natural Autoantibodies and Natural IgM Anti-Leucocyte Autoantibodies in Health and Disease. Front Immunol. 2016 Jun 6;7:198.

Ludwig RJ, Vanhoorelbeke K, Leypoldt F, Kaya Z, Bieber K, McLachlan SM, Komorowski L, Luo J, Cabral-Marques O, Hammers CM, Lindstrom JM, Lamprecht P, Fischer A, Riemekasten G, Tersteeg C, Sondermann P, Rapoport B, Wandinger KP, Probst C, El Beidaq A, Schmidt E, Verkman A, Manz RA, Nimmerjahn F. Mechanisms of Autoantibody-Induced Pathology. Front Immunol. 2017 May 31;8:603.

Lutz HU, Binder CJ, Kaveri S. Naturally occurring auto-antibodies in homeostasis and disease. Trends Immunol. 2009 Jan;30(1):43-51.

Madaio MP, Carlson J, Cataldo J, Ucci A, Migliorini P, Pankewycz O. Murine monoclonal anti-DNA antibodies bind directly to glomerular antigens and form immune deposits. J Immunol. 1987 May 1;138(9):2883-9. PMID: 3553329.

Martín-Nares E, Hernández-Molina G. Novel autoantibodies in Sjögren's syndrome: A comprehensive review. Autoimmun Rev. 2019 Feb;18(2):192-198.

Martínez-Allo VC, Hauk V, Sarbia N, Pinto NA, Croci DO, Dalotto-Moreno T, Morales RM, Gatto SG, Manselle Cocco MN, Stupirski JC, Deladoey Á, Maronna E, Marcaida P, Durigan V, Secco A, Mamani M, Dos Santos A, Catalán Pellet A, Pérez Leiros C, Rabinovich GA, Toscano MA. Suppression of age-related salivary gland autoimmunity by glycosylation-dependent galectin-1-driven immune inhibitory circuits. Proc Natl Acad Sci U S A. 2020 Mar 24;117(12):6630-6639.

Matson DR, Yang DT. Autoimmune Lymphoproliferative Syndrome: An Overview. Arch Pathol Lab Med. 2020 Feb;144(2):245-251.

Matsumura R, Umemiya K, Goto T, Nakazawa T, Ochiai K, Kagami M, Tomioka H, Tanabe E, Sugiyama T, Sueishi M. Interferon gamma and tumor necrosis factor alpha induce Fas expression and anti-Fas mediated apoptosis in a salivary ductal cell line. Clin Exp Rheumatol. 2000 May-Jun;18(3):311-8.

Mavragani CP, Moutsopoulos HM. Sjögren's syndrome: Old and new therapeutic targets. J Autoimmun. 2020 Jun;110:102364.

Mazel JA, El-Sherif N, Buyon J, Boutjdir M. Electrocardiographic abnormalities in a murine model injected with IgG from mothers of children with congenital heart block. Circulation. 1999 Apr 13;99(14):1914-8.

Mégevand P, Chizzolini C, Chofflon M, Roux-Lombard P, Lalive PH, Picard F. Cerebrospinal fluid anti-SSA autoantibodies in primary Sjogren's syndrome with central nervous system involvement. Eur Neurol. 2007;57(3):166-71.

Mielle J, Tison A, Cornec D, Le Pottier L, Daien C, Pers JO. B cells in Sjögren's syndrome: from pathophysiology to therapeutic target. Rheumatology (Oxford). 2021 Jun 18;60(6):2545-2560.

References

Miller FW. The increasing prevalence of autoimmunity and autoimmune diseases: an urgent call to action for improved understanding, diagnosis, treatment, and prevention. Curr Opin Immunol. 2023 Feb;80:102266.

Molinos-Albert LM, Clotet B, Blanco J, Carrillo J. Immunologic Insights on the Membrane Proximal External Region: A Major Human Immunodeficiency Virus Type-1 Vaccine Target. Front Immunol. 2017 Sep 19;8:1154.

Moutsopoulos HM. Sjögren's syndrome: a forty-year scientific journey. J Autoimmun. 2014 Jun;51:1-9.

Mueller DL. Mechanisms maintaining peripheral tolerance. Nat Immunol. 2010 Jan;11(1):21-7.

Nakazawa D, Masuda S, Tomaru U, Ishizu A. Pathogenesis and therapeutic interventions for ANCA-associated vasculitis. Nat Rev Rheumatol. 2019 Feb;15(2):91-101.

Nemazee D, Hogquist KA. Antigen receptor selection by editing or downregulation of V(D)J recombination. Curr Opin Immunol. 2003 Apr;15(2):182-9.

Nemazee D. Mechanisms of central tolerance for B cells. Nat Rev Immunol. 2017 May;17(5):281-294.

Nguyen TT, Elsner RA, Baumgarth N. Natural IgM prevents autoimmunity by enforcing B cell central tolerance induction. J Immunol. 2015 Feb 15;194(4):1489-502.

Nishihata SY, Shimizu T, Umeda M, Furukawa K, Ohyama K, Kawakami A, Nakamura H. The Toll-like Receptor 7-Mediated Ro52 Antigen-Presenting Pathway in the Salivary Gland Epithelial Cells of Sjögren's Syndrome. J Clin Med. 2023 Jun 30;12(13):4423.

Nocturne G, Mariette X. B cells in the pathogenesis of primary Sjögren syndrome. Nat Rev Rheumatol. 2018 Mar;14(3):133-145. doi: 10.1038/nrrheum.2018.1. Epub 2018 Feb 8.

Ohyama Y, Carroll VA, Deshmukh U, Gaskin F, Brown MG, Fu SM. Severe focal sialadenitis and dacryoadenitis in NZM2328 mice induced by MCMV: a novel model for human Sjögren's syndrome. J Immunol. 2006 Nov 15;177(10):7391-7.

Oke V, Vassilaki I, Espinosa A, Strandberg L, Kuchroo VK, Nyberg F, Wahren-Herlenius M. High Ro52 expression in spontaneous and UV-induced cutaneous inflammation. J Invest Dermatol. 2009 Aug;129(8):2000-10.

Oke V, Wahren-Herlenius M. The immunobiology of Ro52 (TRIM21) in autoimmunity: a critical review. J Autoimmun. 2012 Aug;39(1-2):77-82.

Oke V, Wahren-Herlenius M. The immunobiology of Ro52 (TRIM21) in autoimmunity: a critical review. J Autoimmun. 2012 Aug;39(1-2):77-82.

Pacheco Y, Acosta-Ampudia Y, Monsalve DM, Chang C, Gershwin ME, Anaya JM. Bystander activation and autoimmunity. J Autoimmun. 2019 Sep;103:102301.

Panda S, Ding JL. Natural antibodies bridge innate and adaptive immunity. J Immunol. 2015 Jan 1;194(1):13-20.

Pankewycz OG, Migliorini P, Madaio MP. Polyreactive autoantibodies are nephritogenic in murine lupus nephritis. J Immunol. 1987 Nov 15;139(10):3287-94. PMID: 3500215.

Pauls SD, Marshall AJ. Regulation of immune cell signaling by SHIP1: A phosphatase, scaffold protein, and potential therapeutic target. Eur J Immunol. 2017 Jun;47(6):932-945.

Pelanda R, Greaves SA, Alves da Costa T, Cedrone LM, Campbell ML, Torres RM. B-cell intrinsic and extrinsic signals that regulate central tolerance of mouse and human B cells. Immunol Rev. 2022 May;307(1):12-26.

Prigent J, Jarossay A, Planchais C, Eden C, Dufloo J, Kök A, Lorin V, Vratskikh O, Couderc T, Bruel T, Schwartz O, Seaman MS, Ohlenschläger O, Dimitrov JD, Mouquet H. Conformational Plasticity in Broadly Neutralizing HIV-1 Antibodies Triggers Polyreactivity. Cell Rep. 2018 May 29;23(9):2568-2581.

Puñet-Ortiz J, Sáez Moya M, Cuenca M, Caleiras E, Lazaro A, Engel P. Ly9 (CD229) Antibody Targeting Depletes Marginal Zone and Germinal Center B Cells in Lymphoid Tissues and Reduces Salivary Gland Inflammation in a Mouse Model of Sjögren's Syndrome. Front Immunol. 2018 Nov 16;9:2661.

Reed JH. Transforming mutations in the development of pathogenic B cell clones and autoantibodies. Immunol Rev. 2022 May;307(1):101-115.

Ríos-Ríos WJ, Sosa-Luis SA, Torres-Aguilar H. T Cells Subsets in the Immunopathology and Treatment of Sjogren's Syndrome. Biomolecules. 2020 Nov 11;10(11):1539.

Ríos-Ríos WJ, Sosa-Luis SA, Torres-Aguilar H. T Cells Subsets in the Immunopathology and Treatment of Sjogren's Syndrome. Biomolecules. 2020 Nov 11;10(11):1539.

Roberts ME, Kaminski D, Jenks SA, Maguire C, Ching K, Burbelo PD, Iadarola MJ, Rosenberg A, Coca A, Anolik J, Sanz I. Primary Sjögren's syndrome is characterized by distinct phenotypic and transcriptional profiles of IgD+ unswitched memory B cells. Arthritis Rheumatol. 2014 Sep;66(9):2558-69.

Rojas M, Restrepo-Jiménez P, Monsalve DM, Pacheco Y, Acosta-Ampudia Y, Ramírez-Santana C, Leung PSC, Ansari AA, Gershwin ME, Anaya JM. Molecular mimicry and autoimmunity. J Autoimmun. 2018 Dec;95:100-123

Rönnelid J, Turesson C, Kastbom A. Autoantibodies in Rheumatoid Arthritis - Laboratory and Clinical Perspectives. Front Immunol. 2021 May 14;12:685312.

Sáez Moya M, Gutiérrez-Cózar R, Puñet-Ortiz J, Rodríguez de la Concepción ML, Blanco J, Carrillo J, Engel P. Autoimmune B Cell Repertoire in a Mouse Model of Sjögren's Syndrome. Front Immunol. 2021 Apr 23;12:666545.

Sakaguchi S, Yamaguchi T, Nomura T, Ono M. Regulatory T cells and immune tolerance. Cell. 2008 May 30;133(5):775-87.

Salomonsson S, Dzikaite V, Zeffer E, Eliasson H, Ambrosi A, Bergman G, Fernlund E, Theander E, Ohman A, Rydberg A, Skogh T, Wållberg-Jonsson S, Elfving A, Fored M,

Ekbom A, Lundström U, Mellander M, Winqvist O, Sonesson SE, Gadler F, Jonzon A, Wahren-Herlenius M. A population-based investigation of the autoantibody profile in mothers of children with atrioventricular block. Scand J Immunol. 2011 Nov;74(5):511-7.

Samuels H, Malov M, Saha Detroja T, Ben Zaken K, Bloch N, Gal-Tanamy M, Avni O, Polis B, Samson AO. Autoimmune Disease Classification Based on PubMed Text Mining. J Clin Med. 2022 Jul 26;11(15):4345.

Sandel PC, Monroe JG. Negative selection of immature B cells by receptor editing or deletion is determined by site of antigen encounter. Immunity. 1999 Mar;10(3):289-99.

Sandhya P, Kurien BT, Danda D, Scofield RH. Update on Pathogenesis of Sjogren's Syndrome. Curr Rheumatol Rev. 2017;13(1):5-22.

Schreiber K, Sciascia S, de Groot PG, Devreese K, Jacobsen S, Ruiz-Irastorza G, Salmon JE, Shoenfeld Y, Shovman O, Hunt BJ. Antiphospholipid syndrome. Nat Rev Dis Primers. 2018 Jan 11;4:17103.

Scofield RH, Asfa S, Obeso D, Jonsson R, Kurien BT. Immunization with short peptides from the 60-kDa Ro antigen recapitulates the serological and pathological findings as well as the salivary gland dysfunction of Sjogren's syndrome. J Immunol. 2005 Dec 15;175(12):8409-14.

Sène D, Ismael S, Forien M, Charlotte F, Kaci R, Cacoub P, Diallo A, Dieudé P, Lioté F. Ectopic Germinal Center-Like Structures in Minor Salivary Gland Biopsy Tissue Predict Lymphoma Occurrence in Patients With Primary Sjögren's Syndrome. Arthritis Rheumatol. 2018 Sep;70(9):1481-1488.

Sethi DK, Agarwal A, Manivel V, Rao KV, Salunke DM. Differential epitope positioning within the germline antibody paratope enhances promiscuity in the primary immune response. Immunity. 2006 Apr;24(4):429-38.

Shen L, Gao C, Suresh L, Xian Z, Song N, Chaves LD, Yu M, Ambrus JL Jr. Central role for marginal zone B cells in an animal model of Sjogren's syndrome. Clin Immunol. 2016 Jul;168:30-36.

Shiboski CH, Shiboski SC, Seror R, Criswell LA, Labetoulle M, Lietman TM, Rasmussen A, Scofield H, Vitali C, Bowman SJ, Mariette X; International Sjögren's Syndrome Criteria Working Group. 2016 American College of Rheumatology/European League Against Rheumatism Classification Criteria for Primary Sjögren's Syndrome: A Consensus and Data-Driven Methodology Involving Three International Patient Cohorts. Arthritis Rheumatol. 2017 Jan;69(1):35-45.

Shlomchik MJ. Sites and stages of autoreactive B cell activation and regulation. Immunity. 2008 Jan;28(1):18-28.

Sidiq T, Yoshihama S, Downs I, Kobayashi KS. Nod2: A Critical Regulator of Ileal Microbiota and Crohn's Disease. Front Immunol. 2016 Sep 20;7:367.

Singer GG, Carrera AC, Marshak-Rothstein A, Martínez C, Abbas AK. Apoptosis, Fas and systemic autoimmunity: the MRL-lpr/lpr model. Curr Opin Immunol. 1994 Dec;6(6):913-20.

Soldan SS, Lieberman PM. Epstein-Barr virus and multiple sclerosis. Nat Rev Microbiol. 2023 Jan;21(1):51-64.

Staels F, Collignon T, Betrains A, Gerbaux M, Willemsen M, Humblet-Baron S, Liston A, Vanderschueren S, Schrijvers R. Monogenic Adult-Onset Inborn Errors of Immunity. Front Immunol. 2021 Nov 17;12:753978.

Subramaniam KS, Datta K, Quintero E, Manix C, Marks MS, Pirofski LA. The absence of serum IgM enhances the susceptibility of mice to pulmonary challenge with Cryptococcus neoformans. J Immunol. 2010 May 15;184(10):5755-67.

Szczerba BM, Kaplonek P, Wolska N, Podsiadlowska A, Rybakowska PD, Dey P, Rasmussen A, Grundahl K, Hefner KS, Stone DU, Young S, Lewis DM, Radfar L, Scofield RH, Sivils KL, Bagavant H, Deshmukh US. Interaction between innate immunity and Ro52-induced antibody causes Sjögren's syndrome-like disorder in mice. Ann Rheum Dis. 2016 Mar;75(3):617-22.

Szczerba BM, Kaplonek P, Wolska N, Podsiadlowska A, Rybakowska PD, Dey P, Rasmussen A, Grundahl K, Hefner KS, Stone DU, Young S, Lewis DM, Radfar L, Scofield RH, Sivils KL, Bagavant H, Deshmukh US. Interaction between innate

immunity and Ro52-induced antibody causes Sjögren's syndrome-like disorder in mice. Ann Rheum Dis. 2016 Mar;75(3):617-22.

Szyszko EA, Brokstad KA, Oijordsbakken G, Jonsson MV, Jonsson R, Skarstein K. Salivary glands of primary Sjögren's syndrome patients express factors vital for plasma cell survival. Arthritis Res Ther. 2011 Jan 7;13(1):R2.

Tetsuka S, Suzuki T, Ogawa T, Hashimoto R, Kato H. Anti-Ro/SSA Antibodies May Be Responsible for Cerebellar Degeneration in Sjogren's Syndrome. J Clin Med Res. 2021 Feb;13(2):113-120.

Thorlacius GE, Björk A, Wahren-Herlenius M. Genetics and epigenetics of primary Sjögren syndrome: implications for future therapies. Nat Rev Rheumatol. 2023 May;19(5):288-306.

Thornton AM, Shevach EM. CD4+CD25+ immunoregulatory T cells suppress polyclonal T cell activation in vitro by inhibiting interleukin 2 production. J Exp Med. 1998 Jul 20;188(2):287-96.

Tian Y, Yang H, Liu N, Li Y, Chen J. Advances in Pathogenesis of Sjögren's Syndrome. J Immunol Res. 2021 Oct 7;2021:5928232.

Tiegs SL, Russell DM, Nemazee D. Receptor editing in self-reactive bone marrow B cells. The Journal of Experimental Medicine. 1993. 177: 1009-1020. J Immunol. 2011 Feb 1;186(3):1313-24.

Torres M, Casadevall A. The immunoglobulin constant region contributes to affinity and specificity. Trends Immunol. 2008 Feb;29(2):91-7.

Trzeciak M, Bagavant H, Papinska J, Deshmukh US. Immune Response Targeting Sjögren's Syndrome Antigen Ro52 Suppresses Tear Production in Female Mice. Int J Mol Sci. 2018 Sep 27;19(10):2935.

Übelhart R, Jumaa H. Autoreactivity and the positive selection of B cells. Eur J Immunol. 2015 Nov;45(11):2971-7.

Van Blokland SC, van Helden-Meeuwsen CG, Wierenga-Wolf AF, Drexhage HA, Hooijkaas H, van de Merwe JP, Versnel MA. Two different types of sialoadenitis in the

NOD- and MRL/lpr mouse models for Sjögren's syndrome: a differential role for dendritic cells in the initiation of sialoadenitis? Lab Invest. 2000 Apr;80(4):575-85.

Vang T, Nielsen J, Burn GL. A switch-variant model integrates the functions of an autoimmune variant of the phosphatase PTPN22. Sci Signal. 2018 Apr 17;11(526):eaat0936.

Vaysburd M, Watkinson RE, Cooper H, Reed M, O'Connell K, Smith J, Cruickshanks J, James LC. Intracellular antibody receptor TRIM21 prevents fatal viral infection. Proc Natl Acad Sci U S A. 2013 Jul 23;110(30):12397-401.

Verbeek JS, Hirose S, Nishimura H. The Complex Association of FcγRIIb With Autoimmune Susceptibility. Front Immunol. 2019 Oct 15;10:2061.

Verbeek JS, Hirose S, Nishimura H. The Complex Association of FcγRIIb With Autoimmune Susceptibility. Front Immunol. 2019 Oct 15;10:2061

Verstappen GM, Kroese FGM, Bootsma H. T cells in primary Sjögren's syndrome: targets for early intervention. Rheumatology (Oxford). 2021 Jul 1;60(7):3088-3098.

Vinuesa CG, Grenov A, Kassiotis G. Innate virus-sensing pathways in B cell systemic autoimmunity. Science. 2023 May 5;380(6644):478-484.

Vivino FB. Sjogren's syndrome: Clinical aspects. Clin Immunol. 2017 Sep;182:48-54.

Voight BF, Cotsapas C. Human genetics offers an emerging picture of common pathways and mechanisms in autoimmunity. Curr Opin Immunol. 2012 Oct;24(5):552-7.

Wang Y, Liu J, Burrows PD, Wang JY. B Cell Development and Maturation. Adv Exp Med Biol. 2020;1254:1-22.

Wang Zq, Horowitz HW, Orlikowsky T, Hahn BI, Trejo V, Bapat AS, Mittler RS, Rayanade RJ, Yang SY, Hoffmann MK. Polyspecific self-reactive antibodies in individuals infected with human immunodeficiency virus facilitate T cell deletion and inhibit costimulatory accessory cell function. J Infect Dis. 1999 Oct;180(4):1072-9.

Wardemann H, Yurasov S, Schaefer A, Young JW, Meffre E, Nussenzweig MC. Predominant autoantibody production by early human B cell precursors. Science. 2003 Sep 5;301(5638):1374-7.

Warter L, Appanna R, Fink K. Human poly- and cross-reactive anti-viral antibodies and their impact on protection and pathology. Immunol Res. 2012 Sep;53(1-3):148-61.

Wei X, Niu X. T follicular helper cells in autoimmune diseases. J Autoimmun. 2023 Jan;134:102976.

Wilkinson NM, Chen HC, Lechner MG, Su MA. Sex Differences in Immunity. Annu Rev Immunol. 2022 Apr 26;40:75-94.

Wright JA, Bazile C, Clark ES, Carlesso G, Boucher J, Kleiman E, Mahmoud T, Cheng LI, López-Rodríguez DM, Satterthwaite AB, Altman NH, Greidinger EL, Khan WN. Impaired B Cell Apoptosis Results in Autoimmunity That Is Alleviated by Ablation of Btk. Front Immunol. 2021 Aug 26;12:705307. doi: 10.3389/fimmu.2021.705307.

Xiao F, Han M, Rui K, Ai X, Tian J, Zhang W, Zhao F, Zhao Y, Jiang Q, Lu L. New insights into follicular helper T cell response and regulation in autoimmune pathogenesis. Cell Mol Immunol. 2021 Jun;18(6):1610-1612.

Xiao ZX, Miller JS, Zheng SG. An updated advance of autoantibodies in autoimmune diseases. Autoimmun Rev. 2021 Feb;20(2):102743.

Yamada A, Arakaki R, Saito M, Kudo Y, Ishimaru N. Dual Role of Fas/FasL-Mediated Signal in Peripheral Immune Tolerance. Front Immunol. 2017 Apr 5;8:403.

Yao Y, Ma JF, Chang C, Xu T, Gao CY, Gershwin ME, Lian ZX. Immunobiology of T Cells in Sjögren's Syndrome. Clin Rev Allergy Immunol. 2021 Feb;60(1):111-131.

Yao Y, Ma JF, Chang C, Xu T, Gao CY, Gershwin ME, Lian ZX. Immunobiology of T Cells in Sjögren's Syndrome. Clin Rev Allergy Immunol. 2021 Feb;60(1):111-131.

Zhang J, Jacobi AM, Wang T, Berlin R, Volpe BT, Diamond B. Polyreactive autoantibodies in systemic lupus erythematosus have pathogenic potential. J Autoimmun. 2009 Nov-Dec;33(3-4):270-4.

References

Zhang S, Qu J, Wang L, Li M, Xu D, Zhao Y, Zhang F, Zeng X. Activation of Toll-Like Receptor 7 Signaling Pathway in Primary Sjögren's Syndrome-Associated Thrombocytopenia. Front Immunol. 2021 Mar 9;12:637659.

Zheng J, Huang Q, Huang R, Deng F, Yue X, Yin J, Zhao W, Chen Y, Wen L, Zhou J, Huang R, Riemekasten G, Liu Z, Petersen F, Yu X. B Cells Are Indispensable for a Novel Mouse Model of Primary Sjögren's Syndrome. Front Immunol. 2017 Oct 24;8:1384.

Zhou H, Yang J, Tian J, Wang S. $CD8^+$ T Lymphocytes: Crucial Players in Sjögren's Syndrome. Front Immunol. 2021 Jan 28;11:602823.

Zhou ZH, Notkins AL. Polyreactive antigen-binding B (PAB-) cells are widely distributed and the PAB population consists of both B-1+ and B-1- phenotypes. Clin Exp Immunol. 2004 Jul;137(1):88-100.

Zintzaras E, Voulgarelis M, Moutsopoulos HM. The risk of lymphoma development in autoimmune diseases: a meta-analysis. Arch Intern Med. 2005 Nov 14;165(20):2337-44.

X. ACKNOWLEDGMENTS

Acknowledgments